Universitat Autònoma de Barcelona

Discovery of synthetic lethal or viable interactions between DNA repair pathways

Daniela Steigerwald

Universitat Autònoma de Barcelona

Faculty of Biosciences

Department of Genetics and Microbiology

Genome Instability and DNA repair group

Discovery of synthetic lethal or viable interactions between DNA repair pathways

Doctoral Dissertation

Daniela Steigerwald

February 2022

Universitat Autònoma de Barcelona

Faculty of Biosciences

Department of Genetics and Microbiology

Genome Instability and DNA repair group

Discovery of synthetic lethal or viable interactions between DNA repair pathways

Dissertation respectfully submitted by

Daniela Steigerwald

February 2022

To Universitat Autónoma de Barcelona in partial fulfilment of the requirements for the degree of Doctor of Philosophy, as per the Doctorate Program in Genetics

Thesis Director and Tutor,	Thesis Director,	Author,
Prof. Dr. Jordi Surrallés,	Dr. Massimo Bogliolo	Daniela Steigerwald

Acknowledgements

First of all I would like to thank Dr. Jordi Surrallés for giving me this great opportunity to work in his laboratory and his group and I would like to thank Dr. Massimo Bogliolo for his supervision, support and input in my work. Thank you both for everything that you have done for me and my journey.

A laboratory can never work without its irreplaceable Lab Technician, I am really thankful for Montse Peíro's help and insight for any problem or question that I had. A Thank you, also to our secretary for making miracles happen and to the rest of the research group for always having an open ear for questions and advice. A special thank you to my fellow PhD students in the lab, I am so fortunate that I could always count on you. Marta Soler and Manuela Costa would teach and help me with a lot of time and patience all my Cytometer knowledge, thank you.

I want to thank my parents, sister and all my friends that supported me during hard times, when frustration was bigger than curiosity and motivation. I am very thankful to my husband who is always standing by my side, thank you, that you believe in me.

I would like to thank the pre-doctoral program of the Spanish ministry of Science and Innovation that they granted me this fellowship (FPI) as a part of the RETOS project SAF2015-64152-R without it, it would not have been possible.

I want to thank all dedicated people in the UAB and of the research facility in the Hospital de la Santa Creu I Sant Pau for giving me the opportunity to research there.

And finally I would like to thank all FA patients and families that were sharing their story or giving us their trust and allowing me to be part of their community, I hope that in the future FA research can be pushed further.

Abbreviations

6-4PP	**6-4 photoproducts**
AA	**Amino acid**
ADP	**Adenine diphosphate**
AP	**Abasic site**
APEX1	**DNA-(apurinic or apyrimidinic site) endonuclease 1**
AT	**Ataxia Telangiectasia**
ATM	**Ataxia Telangiectasia Mutated**
ATR	**ATM and Rad3 related**
BER	**Base-excision repair**
BLM	**Bloom syndrome protein**
bp	**Base pairs**
BRAD1	**BRCA1-associated RING domain protein 1**
BRCA1	**Breast cancer type 1 susceptibility protein**
BRCA1	**Breast cancer susceptibility gene 1**
BRCA2	**Breast cancer type 2 susceptibility protein**
BRCA2	**Breast cancer susceptibility gene 2**
C	**Degree Celsius**
Cas9	**CRISPR-associated protein 9**
Cas9	**CRISPR-associated endonuclease**
CCA	**Colour competition assay**
CDK	**Cyclin dependent Kinase**
CETN2	**Centrin-2**
CFA	**Colony forming assay**
CHK1	**Serine/threonine-protein kinase Chk1**
cm	**Centimetre**
CPDs	**Cyclopyrimidine dimers**
CRISPR	**Clustered interspaced short palindromic repeats**
crRNA	**CRISPR RNA**
CS	**Cockayne syndrome**
CSA	**Cockayne syndrome WD repeat proteins A**
CSB	**Cockayne syndrome WD repeat proteins B**
CtIP	**DNA endonuclease RBBP8**
d	**Day**
DAPI	**4′,6-diamidino-2-phenylindole**
DDR	**DNA damage response**
DEB	**Diepoxybutane**
DMEM	**Dulbeco's Modified Eagle medium**
DNA	**Desoxiribonucleic acid**
DNA2	**DNA replication ATP-dependent helicase/nuclease DNA2**
DNA-PK	**DNA protein kinase**
DNA-PKcs	**DNA-dependent protein kinase catalytic subunit**
DSB	**Double strand break**
dsDNA	**Double strand DNA**

DSS1	**Deleted In Split-Hand/Split-Foot 1**
E.coli	**Echerischia coli**
EMA	**Ethidium monoazide bromide**
EME1	**Crossover junction endonuclease EME1**
ERCC1	**DNA excision repair protein ERCC-1**
EXO1	**Exonuclease 1**
FA	**Fanconi anaemia**
FAAP100	**Fanconi anaemia associated protein 100**
FAAP20	**Fanconi anaemia associated protein 20**
FANCA	**Fanconi anaemia group A protein**
FANCA	**Fanconi anaemia group A protein**
FANCB	**Fanconi anaemia group B protein**
FANCC	**Fanconi anaemia group C protein**
FANCD1	**Fanconi anaemia group D1 protein**
FANCD2	**Fanconi anaemia group D2 protein**
FANCD2	**Fanconi anaemia group D2 protein**
FANCE	**Fanconi anaemia group E protein**
FANCF	**Fanconi anaemia group F protein**
FANCG	**Fanconi anaemia group G protein**
FANCI	**Fanconi anaemia group I protein**
FANCJ	**Fanconi anaemia group J protein**
FANCL	**Fanconi anaemia group L protein**
FANCM	**Fanconi anaemia group M protein**
FANCN	**Fanconi anaemia group N protein**
FANCO	**Fanconi anaemia group O protein**
FANCP	**Fanconi anaemia group P protein**
FANCQ	**Fanconi anaemia group Q protein**
FANCR	**Fanconi anaemia group R protein**
FANCS	**Fanconi anaemia group S protein**
FANCT	**Fanconi anaemia group T protein**
FANCU	**Fanconi anaemia group U protein**
FANCV	**Fanconi anaemia group V protein**
FANCW	**Fanconi anaemia group W protein**
FBS	**Fetal bovine serum**
FEN1	**Flap endonuclease 1**
FeS	**Iron-sulfor cluster**
GAPDH	**Glyceraldehyde-3-phosphate dehydrogenase**
gDNA	**Genomic DNA**
GFP	**Green fluorescent protein**
GGR	**Global genome repair**
GPD Motif	**Gly/Pro rich domain**
Gua	**Guanine**
h	**Hour**
HA2X	**Histone H2A.X**

HBS	**Histidin buffered solution**
HEK	**Human embryonic kindey fibroblast**
HJ	**Holliday Junction**
HMGN1	**High mobility group nucleosome-binding domain-containing Protein 1**
HNSCC	**Head and Neck squamous cell carcinoma**
HR	**Homologous Recombination**
HR	**Homologous Recombination**
ICL	**Interstrand cross-link**
ICLR	**Interstrand cross-link repair**
InDels	**Insertion and Deletion mutation**
IQR	**Interquarantil range**
KO	**Knock-down**
Ku70	**X-ray repair cross-complementing protein 6**
Ku80	**ATP-dependent DNA helicase 2 subunit KU80**
LB	**Luria broth**
LIG1	**Ligase 1**
LIG4	**Ligase 4**
MBD4	**Methyl-CpG Binding Domain 4, DNA Glycosylase**
mg	**Milligramm**
MHMR	**Microhomology-mediated repair**
min	**Minutes**
ml	**Milliliter**
MLH1	**MutL homolog 1, DNA Mismatch Repair Protein**
mM	**Millimolar**
MMC	**Mitomycin C**
MMR	**Mismatch repair**
MMS	**Methyl methansulfonate**
MPG	**DNA-3-methyladenine glycosylase**
MRE11	**Double-strand break repair protein MRE11**
MSH2	**MutS homolog 2**
MSH3	**MutS homolog 3**
MSH6	**MutS homolog 6**
MUS81	**Crossover junction endonuclease MUS81**
MutL	**Salmonella LT7 Mutator**
MutS	**Sigel Mutator**
MUTYH	**MutY DNA Glycosylase**
NAD	**Nicotine amide**
NBS1	**Nibrin**
NEB	**New England Biolabs**
NEIL1	**Nei Like DNA Glycosylase 1**
NEIL2	**Nei Like DNA Glycosylase 2**
NEIL3	**Nei Like DNA Glycosylase 3**
NER	**Nucleotid Excision Repair**
NHEJ	**Non-homologous End Joining**

nm	**Nanometre**
nM	**Nanomolar**
nt	**Nucleotides**
NT	**Non treated**
NTC	**Non-template control**
NTHL1	**Endonuclease III-like protein 1**
OGG1	**8-Oxoguanine DNA Glycosylase**
PALB2	**Partner and localizer of BRCA2**
PAM	**Protospacer adjacent motif**
PARP1	**Poly [ADP-ribose] polymerase 1**
PARylation	**Poly-(ADP-)ribosylation**
PCNA	**Proliferating cell nuclear antigen**
PCR	**Polymerase chain reaction**
pH	**Potential of Hydrogen**
pmol	**Picomol**
PMS2	**Postmeiotic Segregation Increased 2, Mismatch repair endonuclease**
PNKP	**Bifunctional polynucleotide phosphatase/kinase**
Pol	**Polymerase**
qPCR	**Quantitative PCR**
RAD23B	**UV excision repair protein RAD23 homolog B**
RAD50	**RAD50 Double Strand Break Repair Protein**
RAD51	**DNA repair protein RAD51 homolog 1**
RAD52	**DNA repair protein RAD51 homolog**
RIPA	**Radioimmunoprecipitation assay**
RNA	**Ribonucleic acid**
ROS	**Reactive oxygen species**
RPA	**Replication protein A**
RPE1	**Retinal pigmented epithelium cell line 1**
rpm	**Rounds per minutes**
RT	**Room temperature**
SCC	**Squamous cell carcinoma**
SDSA	**Synthesis dependent strand annealing**
sec	**Seconds**
sgRNA	**Small guide RNA**
shRNA	**Short hairpin RNA**
siRNA	**Small interfering RNA**
SL	**Synthetic lethality**
SLX1	**Structure-specific endonuclease subunit SLX1**
SLX4	**Structure-specific endonuclease subunit SLX4**
SMN1	**DNA cross-link repair 1A protein**
SMN1B	**5' exonuclease Apollo**
SMUG1	**Single-strand selective monofunctional uracil DNA glycosylase**
SOC medium	**Super Optimal broth with Catabolite repression**
SRB	**Sulforhodamie B survival**

SSA	**Single strand annealing**
SSB	**Single strand break**
SSBR	**Single strand break repair**
ssDNA	**Single strand DNA**
TCA	**Trichloro acid**
TCR	**Transcription coupled repair**
TDG	**G/T mismatch-specific thymine DNA glycosylase**
Thy	**Thymidine**
TLS	**Translesion synthesis**
tracrRNA	**Transactivating RNA**
tRFP	**Red fluorescent protein**
TRIS	**Tris(hydroxymethyl)aminomethane**
UAF1	**USP1 associated factor 1**
UDS	**Unscheduled DNA synthesis**
ug	**Micro gramm**
ul	**Microliter**
uM	**Micromolar**
UNG	**Uracil N-glycosylase**
Ura	**Uracil**
USP1	**Ubiquiting-specific protease 1**
USP7	**Ubiquiting-specific-processing protease 7**
UV	**Ultraviolet radiation**
UVC	**Ultraviolet radiation sperctrum (100-280 nm)**
UVSSA	**UV-stimulated scaffold protein A**
V	**Volt**
vol	**Volume**
Wee1	**Wee1-like protein kinase**
wt	**Weight**
Wt	**Wildtype**
XAB2	**XPA-binding proteins 2**
XFE	**Progeroid syndrome**
XLF	**Non-homologous end-joining factor 1**
XP	**Xenoderma pigmentosum**
XPA	**Xenoderma pigmentosum protein A**
XPB	**DNA repair protein complementing XP-B cells**
XPC	**Xeroderma pigmentosum group C**
XPD	**DNA repair protein complementing XP-D cells**
XPE	**Xeroderma pigmentosum group E**
XPF	**Xenoderma pigmentosum protein F**
XPG	**DNA repair protein complementing XP-G cells**
XPV	**DNA repair protein complementing XP-V cells**
XRCC1	**X-ray repair cross-complementing protein 1**
XRCC4	**X-ray repair cross-complementing protein 4**

Abstract

Mammalian cells have developed a set of DNA repair pathways to protect the genomic information from mutations that could lead to cancer or cell death. Each DNA repair pathway responds to a specific kind of DNA damage. The Fanconi/BRCA pathway is one of these specialized and highly important DNA repair networks correcting interstrand cross-links that would lead to highly toxic double strand breaks if left unrepaired. Mutations in the Fanconi/BRCA pathway cause a rare blood and cancer susceptibility disease called Fanconi Anaemia. The concept of synthetic lethality is used in cancer treatment to kill specifically cancer cells. Synthetic lethality refers to the inhibition/deficiency of two gene products that leads to cell death while inhibition of either one alone does not affect viability. The treatment of BRCA-deficient breast and ovarian cancers with PARP inhibitors is an application of this concept, which proved successful in clinical trials. Fanconi genes are found regularly mutated in cancer and so far, there are a few described synthetic lethal interactions in the Fanconi pathway, which opens the possibility of exploiting this synthetic lethality for cancer treatment. The term "synthetic viability" instead, refers to a genetic interaction in which a cell that is non-viable, sensitive to a specific drug, or altered due to the presence of a genetic mutation, becomes viable with a second mutation in a different gene. The objective of the thesis was to find novel synthetic lethal or viable interactions between the Fanconi proteins FANCA and FANCD2 and other DNA repair pathways. For this a method was developed, the colour competition assay that detects synthetic lethality or viability by cytometer measurement. With the CRISPR/Cas9 method knock-out clones for FANCA and FANCD2 were generated and used with shRNA for silencing a second gene in a DNA repair pathway. Additionally, commercial or patient cell lines with known knock-outs in genes of other DNA repair pathways were employed and treated with shRNA to test for synthetic lethality or viability with FANCA or FANCD2. The colour competition assay could not discover any novel synthetic lethal interaction, it revealed a synthetic viability interaction between FANCA and FEN1 that and a second synthetic viability between FANCA and two proteins of the NER pathway, XPA and XPF. This discovery could lead to potential therapeutic applications in Fanconi anaemia treatment.

Table of Contents

1 Introduction

1.1 Genomic instability and DNA repair

1.1.1 DNA Damage and Genome Instability

Desoxyribonucleic acid (DNA) is the molecule that stores, preserves, and passes on all information relevant for the function of cells. The entire genetic information of a cell is encoded in DNA and is called the genome. As the genome is necessary for the function of the cell, it is essential to maintain the genome free of damage and lesions [1][2]. This leads to the necessity of mechanisms to preserve the genetic information and to repair DNA. If lesions cannot be repaired and the damage change the genetic information, this is referred to as mutation (figure 1).

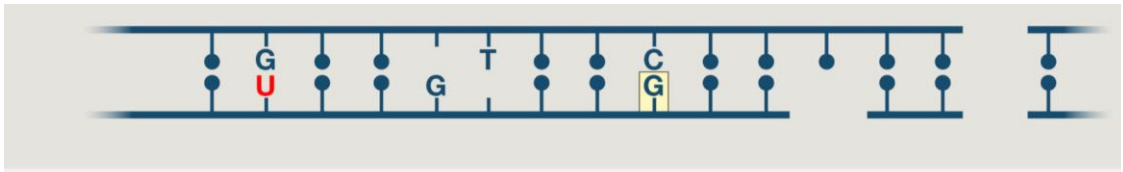

Damage	Cytosine deamination	Depurination/ depyrimidination	8-oxoG	SSB	DSB
Estimated frequency (per cell per day)	192	12,000/600	2,800	55,000	25
Predominant mutation	C>T	Substitutions	G>T	Substitutions, DBSs	Chromosome rearrangements

Figure 1: Types of DNA damage and their frequency, adapted from [6]

DNA damage can lead to the accumulation of mutations, which can cause functional changes in the encoded proteins. In extreme cases, this can result in either cell death or dysregulation of cell growth. One way to protect an organism from aberrant cell growth is aging. Depending on the damage, aging means either cell death or senescence which prohibits cells from enteringfurther cell cycles [3]. This prevents cells form accumulating more damage over cell cycles and become eventually immortal cancer cells [4][5].

1.1.2 DNA Repair pathways

DNA damage can be caused by many endogenous sources side product of metabolism such as reactive oxygen species (ROS) or aldehydes or from exogenous origins like ultraviolet (UV) and ionizing radiation, or toxic chemicals [6]. With this amount of assault, the potential of cells to divide would soon be exhausted if senescence was the only way of protection. Thus, cells evolved highly specialised multi protein pathways to detect and repair DNA damage (Figure 1). For the purpose of this thesis, the focus will be on the major DNA repair pathways.

1.1.2.1 Base excision repair

Base excision repair (BER) is specialised in repairing non-bulky lesions mainly caused by deamination, oxidation, or methylation of bases [7]. This repair pathway, as all following ones, mainly take place in the nucleus of the cell where the gDNA is stored. The first step of BER is the incision of the damaged base by one of at least eleven DNA glycosylases which hydrolyse the N-glycosyl bond of the damaged base and create an abasic site (AP) [7]. This initial incision is followed by end processing, repair synthesis and ligation.

The glycosylase removing the altered base depends on the type of base damage. Also, the following steps are mediated by different proteins depending on the glycosylase involved. In humans there are four classes of DNA glycosylases that can initiate the first step of BER repair and they are grouped by conserved folds and motives. One is the Uracil (Ura)-DNA glycosylase superfamily that specifically excises Ura form DNA single or double strands while it shows no activity to Ura in RNA [8]. In humans, three Uracil-DNA glycosylases are known: UNG, TDG that exclusively excises Ura or Thymidine (Thy) from mismatched Guanine (Gua) (Figure 1), and SMUG1, which is only found in eukaryotes and has an affinity for Ura abducts [8][9].

Some members of the Nth superfamily of glycosylases have a FeS cluster like NTHL1, MUTYH and MBD4 while the others only keep the Helix-turn-Helix and GPD motif. They are the most diverse group of glycosylases which can work on oxidized purines and 8-oxoguanine-DNA (Figure 1). To this family belong the NLTH1, OGG1, MUTYH and MBD4 glycosylases[8][9].

The fpg/Nei superfamily of glycosylases are bifunctional. NEIL1, NEIL2 and NEIL3 are the human members of this group which removes oxidized pyrimidines and formamido-

pyrimidines. NEIL2 is associated with transcription-coupled repair. MPG is a DNA-glycosylase that does not fit in with the other enzymes, as it is a methylpurine-DNA glycosylase [8][9]. All DNA-glycosylases favour specific kinds of damage but have also overlapping functions.

After the removal of the base the next step is end processing, the removal of the deoxyribose phosphate by nicking the strand 5' to the AP site which is done by APEX1 or in specific cases by PNKP. Following this step BER can either continue through the short-patch or the long-patch repair. For the short-patch repair only one single nucleotide is exchanged by Pol β and the strand is ligated by either DNA ligase 1 or DNA ligase 3 [7]. For the long patch repair the strand with the nicked AP site is extended by Pol δ/ε and the created flap is trimmed by FEN1 or proliferating cell nuclear antigen (PCNA) before it is ligated through DNA ligase 1 [7]. X-ray cross-complementation group 1 protein (XRCC1) interacts with pol β and Ligase 3 to activate them [10][11].

The Poly-(ADP-ribosyl)polymerase 1 (PARP1) is an enzyme most known for its therapeutic inhibition in triple negative breast and ovarian cancer. Its therapeutic effect is thought to be over synthetic lethality (SL), which will be discussed in more detail in chapter 1.2, through an impairment of the BER pathway. PARP1 deficient cells that are sensitive to methyl methansulfonate (MMS), which causes DNA damage that is repaired over BER [7][9][12][13] and PARP1 localises to sites of BER repair [12]. Even if PARP1 has been recognized as part of BER, its actual function in the pathway is not understood and there are conflicting evidence regarding its participation in the pathway [14][15][16][17]. Nonetheless PARP1 is an important enzyme in DNA damage response (DDR) and what is known is its participation in single strand break repair (SSBR) [18]. PARP1 is a Poly-(ADP-ribosyl)transferase, which PARylates itself, histones and non-histone proteins. PARylation is the polymerisation of ADP-ribose residues coming from NAD+ onto target substrates by PARPs. PAR itself is a highly negatively charged, branch-structured posttranslational modification. PARP1 senses single strand breaks (SSBs) which are formed after a glycosylase cut or after a nuclease. Binding of PARP1 to DNA triggers a conformational change that activates its auto-PARylation [19] to which, DDR protein XRCC1 binds and is recruited to the site of damage [18][20]. Another function of PARylation is the relaxation of chromatin structure by PARylating of H2AX histone, making the DNA damage more accessible for repair proteins [21][22].

1.1.2.2 Mismatch repair

The mismatch repair (MMR) pathway recognizes and corrects wrongly incorporated bases in the newly synthetised DNA strand. This happens during replication, repair or recombination when the polymerase incorrectly elongates the DNA strand. It is estimated that for a proof-reading polymerase the frequency of wrongly incorporated bases is 10^{-7} per nucleotide [23] while the ratio lays way higher for non-proofreading polymerases, MMR is decreasing this number to almost zero. For this reason mutations in genes coding for MMR cause cancer susceptibility syndromes with a "mutator" phenotype like Lynch syndrome or hereditary non-polyposis colorectal cancer [24].

MMR is detecting and initiating repair through a dimeric heterocomplex of the MutS (Siegel Mutator) and MutL (Salmonella LT7 Mutator) homologs. Both are heterocomplexes as well and can bind different subunits, thus broadens the substrate specificity as the different subunits show preferences for different damages. In eukaryotes, MSH2-MSH6 (MutSα) is the main subcomplex for single base mismatches or two base insertions or deletions (InDels), in contrast MSH2-MSH3 (MutSβ) repairs larger InDels, MutLα is the main repair homolog consisting of MLH1-PMS2 [25][26].

MMR proteins recognize specifically the nascent DNA strand to repair the damage: in prokaryotes, the recognition and discrimination between the two DNA strands is facilitated by the unmethylated status of the newly synthetized DNA strand while in eukaryotes the mechanism is not yet understood [27].

The binding of MutSα to a mismatch activates its ATPase activity and triggers a conformational change that promotes the binding of MutLα so that the dimer forms a clamp that can move along the DNA [28][29][30][31]. Then PCNA activates MutLα to incises the strand both 5' and 3' to the mismatch. The MutSα homolog recruits exonuclease 1 (EXO1) to digest the daughter strand and RPA coates the created ssDNA [32][33]. Synthesis of the new strand is dependent on leading or lagging strand with polymerase ε and polymerase δ respectively filling the gap [34][35].

1.1.2.3 Nucleotide excision repair and photosensitivity syndromes

Nucleotide excision repair (NER) can recognize and repair a variety of different DNA damages but its main target are lesions that distort the DNA double helix such as the one caused by UV radiation (cyclopyrimidine dimers (CPDs), 6-4 photoproducts (6-4PP)), and cyclopurines caused by reactive oxygen species (ROS) [36][37]. NER molecular pathway is divided in two separate sub-pathways (figure 2).

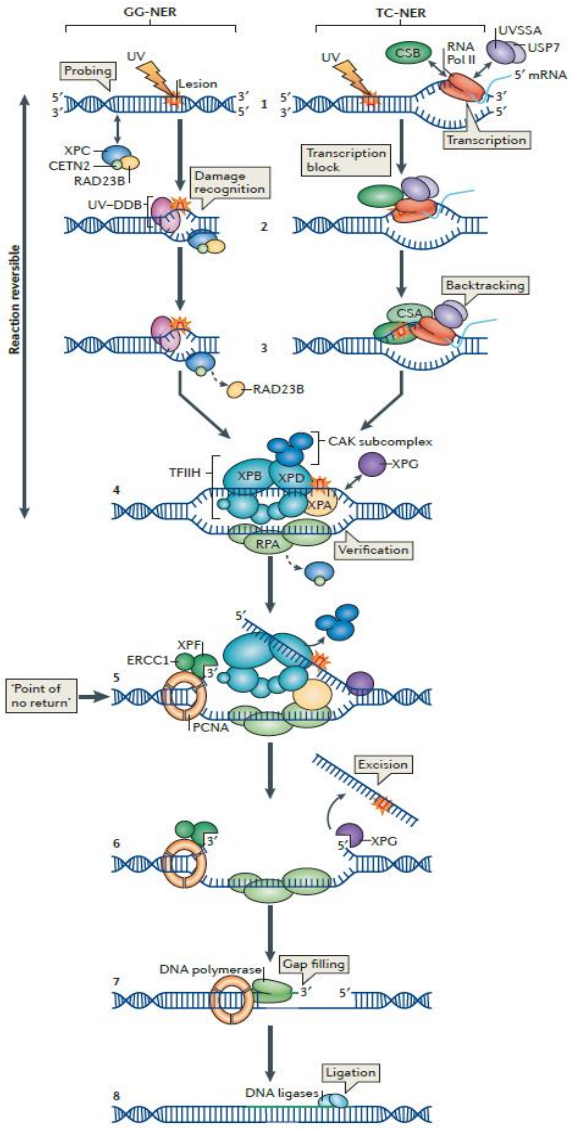

Figure 2: Schematic of the NER pathway with the two DNA damage recognition pathways GGR and TCR, taken from [36]

One is the global genome repair (GGR) and the other one is the transcription coupled repair (TCR). Both share the same steps to incise, elongate and ligate the affected DNA segment.

For the GGR the sensor protein xeroderma pigmentosum group C (XPC) with the help of RAD23B and CETN2 probes the entire genome for helix distorting lesions [36][38][39]. The primary function of RAD23B seems to be the stabilization of XPC: after damage recognition, RAD23B disassociates from the complex with XPC and makes it unstable allowing the subsequent steps of the pathway to take place [40]. The XPC complex is associated with UV-damage-binding proteins 1 (UV-DDB1) and XPE/UV-DDB2 which are necessary for detecting CPDs as these lesions do not destabilize the DNA helix much [41][42].

In the TCR damage recognition pathway, in contrast, NER factors are only recruited when UV-damage stalls the transcription machinery. The arrested RNA-Polymerase II is the signal that recruits Cockayne syndrome WD repeat proteins A (CSA or ERCC8), CSB (or ERCC6), XPA-binding protein 2 (XAB2), UV-stimulated scaffold protein A (UVSSA), ubiquitin-specific-processing protease 7 (USP7), high mobility group nucleosome-binding domain-containing protein 1 (HMGN1), and transcription initiation factor TFIIH (or XPB) [37][43]. It is believed that CSA and CSB are backtracking the RNA polymerase to access the damage and recruit the NER proteins to the site of damage [37].

After the initial step of damage recognition, the GGR and TCR converge in a common pathway to further process the damage [38]. The XPB-XPD complex opens the double strand through its ATPase activity and XPD opens the strand in the opposite direction [36]. The formed single strand DNA (ssDNA) is protected by replication protein A (RPA). XPA binds to RPA and acts as a damage verification [36]. XPA also binds to ERCC1 of the ERCC1-XPF heterodimer and recruits it to the damage. XPF too binds to RPA and is activated by it [44]. XPF (the gene is *ERCC4*) encodes a 5‘ flap endonuclease that incises 5’ to the DNA lesion. After that, the PCNA is loaded on the strand and recruits the polymerase that fills the gap. On the 3’ site of the lesion the nuclease XPG cuts the ssDNA and creates a 22 – 30 nt gap [45] only after XPF made the incision [46].

The 3’ hydroxyl group created by the XPF incision can be used by polymerases to initiate repair synthesis. This filling of the gap is the last step of the repair mechanism. It can be accomplished by DNA polymerase (DNA pol) δ, DNA pol ε or DNA pol κ and the ligase of the nicks by ligase 1 or ligase 3. Studies have revealed that depending on the status of cells, replicating or non-

replicating different DNA polymerases and ligases are used [47][48]. The following chapters will discuss some of the syndromes associated with mutations in NER proteins.

1.1.2.3.1 Xeroderma pigmentosum

One of the diseases that can originate from mutations in genes involved in the NER pathway is Xeroderma pigmentosum (XP), which is an autosomal recessive inherited disorder that is characterised by extreme photosensitivity and a high frequency of skin cancer. This is due to DNA damage inflicted by UV radiation from sun exposure and that in normal individuals is repaired by the NER pathway. Some patients instead of sunburn and photosensitivity manifest abnormal skin pigmentation and lentiginosis, a few cases show also progressive neurological abnormalities. Ocular abnormalities and increased risk of squamous cell carcinomas (SCC) are also common in XP patients [49].

XP is caused by inherited defects in eight XP genes (complementation groups XPA to XPG and XPV): the proteins from XPA to XPG are involved in the removal of UV- damage as shown in figure 2 and XPV is involved in replication bypass of UV-damage [49]. As already mentioned the symptoms can be very varied and differ from patient to patient: mixed forms of XP and Cockayne syndrome (CS), Segmental progeria (XFE), or Fanconi anaemia (FA) have been described [50][51]. While it is not possible to make definite genotype phenotype correlations, it seems that genes involved in GGR are more prone to cause XP while genes further downstream of damage recognition are more prone to cause mixed symptoms.

XP is molecularly diagnosed by efficiency of unscheduled DNA synthesis (UDS) after UV radiation as the newly synthesised ssDNA in the NER process can be measured and distinguished from the DNA replication occurring during the S-phase of the cell cycle.

1.1.2.3.2 Cockayne syndrome

Cockayne syndrome (CS) is a rare genetic disease with an autosomal recessive inheritance pattern, characterised by developmental abnormalities, microcephaly, growth retardation, neurological and cognitive deficits, premature aging and in some cases photosensitivity which, opposed to XP, does not lead to pigmentation abnormalities or skin cancer [52][53][54].

CS is caused by mutations in CSA and CSB but CS caused by mutations in XPB, XPD, XPG or XPF can be accompanied by additional symptoms that are more common in XP [51][54]. The diagnosis of CS is realized by the reduced recovery of RNA and DNA synthesis after UV radiation

[55]. CS is caused by a defect in TCR but there are some sources that implicate CSA and CSB patients with mitochondrial diseases due to their involvement in mitochondrial DNA repair [56][57]. But as the main difference of CS to other disorders with an underlying defect in DNA repair is that patience do not develop cancer because of the inability of their cells to proliferate which is caused by the defect in TCR.

1.1.2.3.3 Segmental progeria syndrome (XFE)

Segmental progeria syndrome is a collective term for rare diseases that cause symptoms associated with premature aging in all tissues. There are some cases described where mutations in *XPF* cause XFE [58][59]. One described mechanism of is the mislocalization of the mutant protein in the cytoplasm and ineffective translocation to the nucleus for NER, these patients suffer severe photosensitivity, neurological and musculoskeletal abnormalities as well as hematopoietic symptoms, which very likely is due to the nuclease participating in the Fanconi anaemia pathway [60] (see chapter 1.1.2.4).

1.1.2.4 Interstrand cross-link repair and Fanconi anaemia

Fanconi anaemia (FA) is rare genetic disease with heterogeneous clinical features but the most common symptoms shared by patients are bone marrow failure in the first two decades of life, a highly increased risk for SCC of the head and neck (HNSCC), hematopoietic malignancies, and birth defects such as radial malformations, skin abnormalities, and organ abnormalities [61][62][63][64][65][66].

There are very few correlations between genotype-phenotype and the penetrance of the symptoms is incomplete and inconsistent. For that reason the diagnosis is done by testing the cellular phenotype for spontaneous and interstrand cross-links (ICLs) induced increase of chromosome breaks in mitotic cells derived from patients [67]. Another characteristic of FA cells is the stalling of the cell cycle from the G2-phase to mitosis which is highly increased after treatment with certain chemotherapeutics like mitomycin C (MMC), diepoxybutane (DEB), cisplatin or psoralen [68][69][70].

As mentioned above, FA patients exhibit a highly increased cancer risk stemming from the inability of patient cells to correctly repair ICLs. This causes a severe problem for the cancer treatment of these patients as they are particularly sensitive to ICL inducing

chemotherapeutics, leaving surgery as the only safe option. Noteworthy is the fact that several genes of the FA pathway are also hereditary breast and ovarian cancer susceptibility genes like BRCA1/FANCS, BRCA2/FANCD1, RAD51C/FANCO, PALB2/FANCN and FANCM [71][72][73]. Patients with biallelic mutations in these genes develop severe forms of FA and are more likely to be affected by multiple cancers. Heterozygote carriers of these genes do not exhibit FA features, but have a live long increased risk for breast and ovarian cancer [74].

FA is inherited mainly in an autosomal recessive manner by mutations in 23 genes FANCA, -C, -D1/BRCA2, -D2, -E, -F, -G, -I, -J/BRIP1, -L, -M, -N/PALB2, -O/RAD51C, -P/SLX4, -Q/XPF, -S/BRCA1, -T/UBE2T, -U/XRCC2, -V/REV7, -W/RFWD3, -Y/FAAP100, with the exception of FANCB which is inherited X-chromosomal [75] and FANCR/RAD51 which has an autosomal dominant inheritance pattern [76].

Mutations in these genes disrupt the FA/BRCA pathway that is the only repair mechanism to counter ICLs during the S-phase of the cell cycle at stalled replication forks. ICLs are especially difficult to repair because they covalently bind the two DNA strands together impairing replication during which the separation of both strands is needed otherwise the replication fork stalls. If stalled forks persist too long they turn into double strand breaks (DSB) [77], a highly toxic DNA damage for cells. The FA/BRCA pathway repairs the DNA damage through a highly regulated activation and inactivation of proteins and uses homologous recombination (HR), an error-free process of DSB repair that requires the presence of a sister chromatid, to contrast ICLs damage in the S-phase of the cell cycle. There are also evidences, that cells can repair ICLs outside of the S-phase cell cycle over a different mechanism, similar to BER [78].

1.1.2.4.1 The FA core complex

The FA/BRCA pathway can be separated into three steps with a set of different proteins involved in each; the first group of proteins are part of the FA core complex a multiprotein E3-ubiquitin ligase that consists of FANCA, FANCB, FANCC, FANCE, FANCF, FANCG, FANCL as well as Fanconi anaemia associated proteins (FAAP) 100 and FAAP20 [79][80]. This complex can be further split in three subcomplexes, one is the A-G-20 subcomplex (FANCA, FANCG, FAAP20) that binds to the DNA strand, C-E-F subcomplex (FANCC, FANCE, FANCF) and the B-L-100 subcomplex (FANCB, FANCL, FAAP100) which is the active ubiquitin transferring unit [80].

The complex works in concert with FANCT which is the E2-conjugating enzyme passing the ubiquitin to FANCL [81].

The core complex activates the pathway by monoubiquitinating a heterodimer complex of FANCD2 and FANCI (ID2). This is a key event in the FA/BRCA pathway: without it the action of downstream proteins, which confer the actual repair, cannot take place. Mutations in any of the proteins of the core-complex or in FANCT abolish ID2 complex monoubiquitination. An exception is FANCM which is not necessary for ID2 ubiquitination [82].

1.1.2.4.2 The ID2 complex

The ID2-complex monoubiquitination on lysine 561 for FANCD2 and lysine 523 in FANCI [83] [84], acts as an activation signal for the actual DNA repair. For a stable monoubiquitination of the ID2-complex, FANCI is first phosphorylated by ATR [85], which assembles the complex, than the monoubiquitination of FANCD2 triggers a conformational change of FANCD2 to form a clamp on dsDNA (Figure 3) while the monoubiquitination of FANCI sterically protects FANCD2 monoubiquitination from USP-UAF1 mediated deubiquitination [86][87][88].

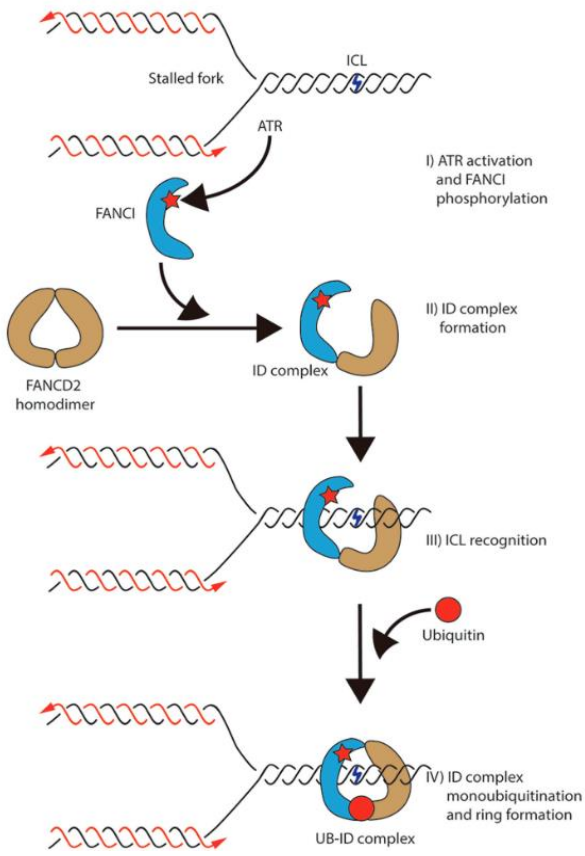

Figure 3: Schematic assembly of the ID2-complex taken from [88]

The ubiquitination is also necessary for the localisation into nuclear foci at phosphorylation marked histones yH2AX and interaction with the downstream proteins which mediate the actual repair like BRCA1 [89][90]. As mentioned in chapter 1.1.2.4 the pathway is highly regulated through activation and inactivation of proteins. For the ID2 complex to work properly it needs to be inactivated by the deubiquitination of FANCD2 through the ubiquitin specific protease 1 USP1-UFA1 complex, for the DNA repair to be accomplished. Mouse embryonic fibroblasts (MEFs) Usp1-/- exhibit a FA molecular phenotype with impaired Fancd2 foci formation and defective HR [91].

USP1 is activated by building a complex with USP1 associated factor 1 (UAF1) that interacts with FANCI to de-ubiquitinate FANCD2 [92]. The USP1 transcription is tightly bound to the cell cycle with the highest expression during exit of S-phase or after passing the G_2M-block when DNA repair is complete [93].

1.1.2.4.3 The downstream proteins and the unhooking of the ICL

The classification of downstream proteins arose historically as they are not needed to monoubiquitinate the ID2-complex and are therefore downstream of it in the pathway in contrast to the core complex proteins which are necessary for ubiquitination which places them upstream of the ID2 complex.

The downstream proteins mediate the actual repair of the ICL by unhooking the two strands and creating a DSB on one of them while producing a second strand with a covalently bound base adduct. The strand with the base adduct is repaired through translesion synthesis (TLS) while the DSB is substrate for HR (Figure 4).

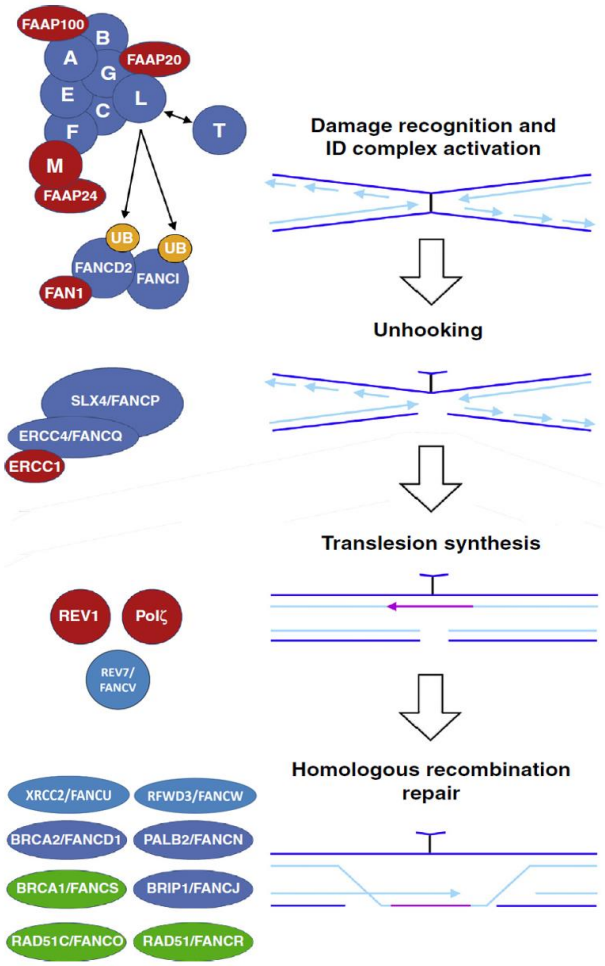

Figure 4: FA/BRCA pathway of ICL repair genes in blue are classic FA causing, in red FA-associated genes and in green FA-like genes adapted from [74]

The unhooking of the ICL is initiated by a dual incision on either side of the ICL when two replication forks collide [94]. The SLX4 protein is a large protein that functions as a docking platform for several endonuclease like XPF/ERCC1, MUS81-EME1 and SLX1, its enzymatic interactor during DNA repair [95]. The SLX4-SLX1 complex participates in Holiday-Junction (HJ) resolution, HJ are four-arm branched dsDNA structures that arise as intermediates of HR repair. SLX4 orchestars the nucleases it docks by regulation of substrate specificity and enhancing activity [96]. The ERCC1-XPF complex, of which XPF is the enzymatic subunit, is involved in the incision of the converged ICL as mutations in *ERCC4,* the gene encoding XPF, cause FA subtype FANCQ [97][98][99] (figure 5).

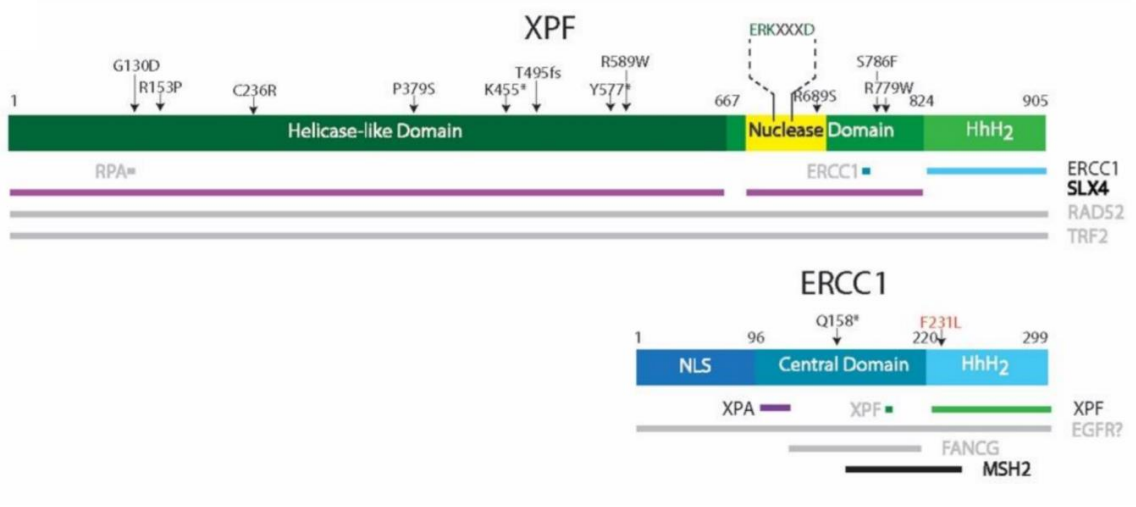

Figure 5: Model of XPF and ERCC1 proteins with functional domains (different colours), interactions sites with different repair proteins (gray; evidence for interaction) and known mutation sites (adapted form [103])

As stated in the previous chapters, XPF was first described as a mutated gene in Xeroderma Pigmentosum complementation group F [100] with defects in the NER pathway but can cause different diseases depending on the mutation [51].

The complete lack of XPF in humans seems to be incompatible with postnatal survival [101]. XPF is a 916 aa protein that forms a stable heterodimer with ERCC1 that allows for its 3' flap endonuclease activity. The XPF protein recognizes ssDNA through its C-terminal Helix-hairpin-Helix HhH domain and ERCC1 binds preferentially to the dsDNA through its HhH domain, this forms a structure specific nuclease complex that determines the cutting position [102][103].

In the highly regulated process of ICL repair the interaction between SLX4 and XPF is necessary for proper function [96]. XPF is a 3' flap nuclease that incises 3' of the ICL for unhooking but, as mentioned above, this leaves a missing nuclease for the 5' incision. There are conflicting evidence that brought up the possibility that XPF is cutting bilateral incisions though interactions with RPA [104] nevertheless this needs further investigation and the involvement of other 5' nucleases have still to be considered.

Another nuclease complex that docks to SLX4 and is a possible candidate for the 5' incision to the ICL is MUS81-EME1. MUS81 is the catalytic subunit of the structure specific nuclease complex and cuts 3'-flaps, replication forts and splayed arms [105]. It docks to SLX4 as the XPF-ERCC1 complex and there is probably competition in binding [106].

The SNM1 nucleases, SNM1A and SNM1B, are processing exonucleases that digest form 5' to 3' past ICLs [107]. It is probable that all nucleases are involved to process different fork structures or repair intermediates and, that they can work in tandem or in a competitive way. New approaches and further studies need to determine the exact involvement of these enzymes in the unhooking of the damage, as of today there are only FA patients for the XPF mutations.

1.1.2.4.4 Translesion synthesis

Now that the ICL is unhooked DNA replication is performed above the strand that carries the residual ICL adduct (Figure 4) by specific translesion synthesis polymerases that can bypass gaps or damaged bases. Polymerases REV1 and/or Polζ are responsible for filling the gap [104][108]. REV7, encoded by *FANCV* a recognized FA gene, is a subunit of polζ together with REV3 POLD2 and POLD3. REV1 is a cytidine-transferase that incorporates a cytidine in an abasic site [109].

The extended nascent strand is ligated and repaired. On the homologous strand the ICL, needs to be eliminated by a still unknown mechanism that could involve the NER or BER proteins while the DSB on the opposite strand is repaired by HR with the newly repaired double strand as substrate for HR (Figure 4).

1.1.2.5 DNA double strand breaks repair

DSB are toxic DNA intermediates for cells, as they can get fused to telomers (the ends of chromosomes) or degraded causing genetic information loss. Cells have two main mechanisms to repair DSB, HR which as mentioned above, is an error-free way of repair and the error-prone non-homologous end joining (NHEJ). There are two more pathway to repair DSB that are prone to cause deletions and are therefore alternatives to NHEJ, the microhomology mediated repair (MHMR) and single strand annealing (SSA) [110] (figure 6).

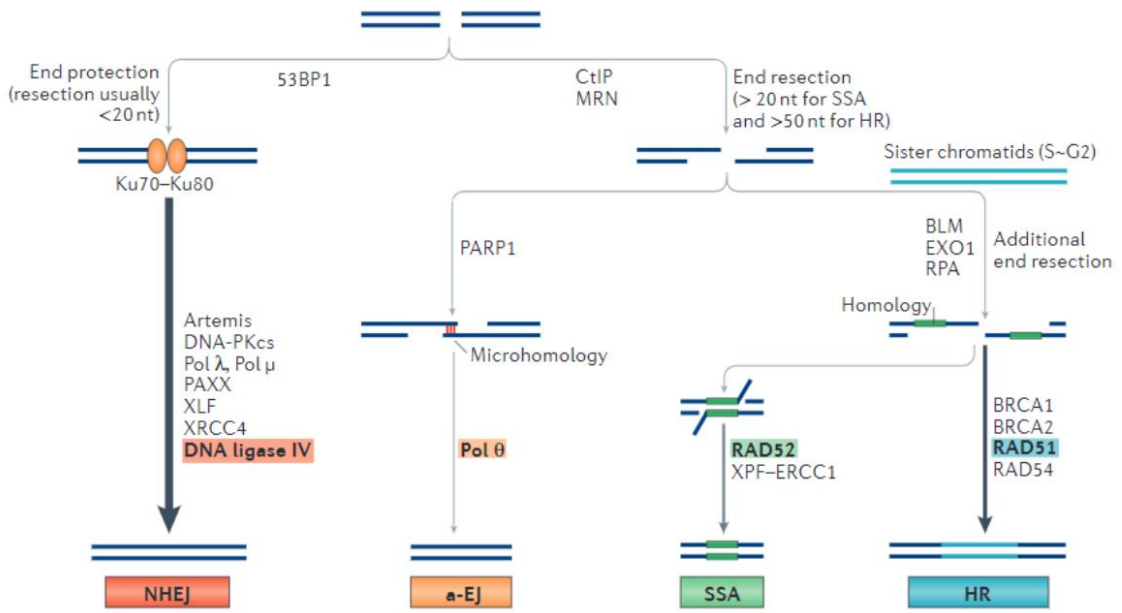

Figure 6: The different pathways to repair DSB; from left to right NHEJ, MMR (here alternative End Joining), SSA and HR the first determination between the NHEJ and homology dependent pathways is end resection or end protection, the main proteins involved in the repair process are listed and the determinates are marked in colour (taken form [110])

1.1.2.5.1 Homologous recombination

HR only functions during the S-phase or early G2-phase of the cell cycle and the reason is that the chromosomal organization allows for an available sister chromatid as homologous template. In the case of ICL repair the homologous template used is the strand that was repaired through TLS.

The process of HR is initiated through 5'- end resection, followed by strand invasion and homology search, the elongation of the strand, and resolution of the created holiday junction. The end resection is the critical step in pathway choice for the repair of the DSB and is mediated through the BRCA1-BRAD1 complex [111][112][113]. Historically BRCA1 was thought to participate in the resection, based on its interaction with the MRN complex (MRE11, RAD50, NBS1) [114], but recently there are convincing evidences that BRCA1 is preventing or abolishing 53BP1 binding at the DSB site and therefore allowing end resection [112]. BRCA1-BRAD1 complex recruits CTIP and the MRN complex which has a endo- and exonuclease function. MRE11 cuts the strand close to the DSB and resects it with its 3'-5' exonuclease activity

[115]. Then the 3' overhang is extended by BLM/DNA2 or the EXO1 exonucleases creating a free ssDNA which is immediately coated with RPA to protect it from nucleolytic degradation.

For the strand invasion, the RAD51 (FANCR) nucleofilament formation is necessary: for this, RAD51 needs to substitute RPA on the ssDNA and therefore the two proteins are competing with each other. For the exchange of RPA for RAD51 the mediator protein complex BRCA2-DSS1-PALB2 is necessary [116][117] and growing evidence suggest that under specific circumstances the loading requires also RAD52 [118][119]. There are other mediators of strand invasion like the five RAD51 paralogs RAD51B, RAD51C/FANCO, RAD51D and XRCC2/FANCU [120].

The recruitment of RPA to ssDNA triggers the ATR-ATRIP (ATR interacting protein) cascade into motion producing the phosphorylation of FANCJ/BRIP1 though cyclin-dependent kinase (CDK) which in turn is a signal for acetylating FANCJ/BRIP1 for its interaction with CTIP. This interaction promotes end resection too, it is independent of BRCA1 but dependent on FANCJs own helicase activity [121]. Another mediator protein is FANCW that ubiquitinates RPA for proteasomal degradation [122]. The nucleofilament invades the dsDNA and forms a D-loop and the strand is extended by at least polymerase eta (polη) or delta4 (polδ4) [123][124]. There are two mechanisms to resolve the D-loop: one is the synthesis dependent strand annealing (SDSA) the other is by holliday junction resolution (Figure 7). In humans there is a preference to SDSA as a holliday junction resolution bears the possibility of a chromosome crossover while SDSA does not [125][126][127]. HR is completed with ligation of the DNA strand.

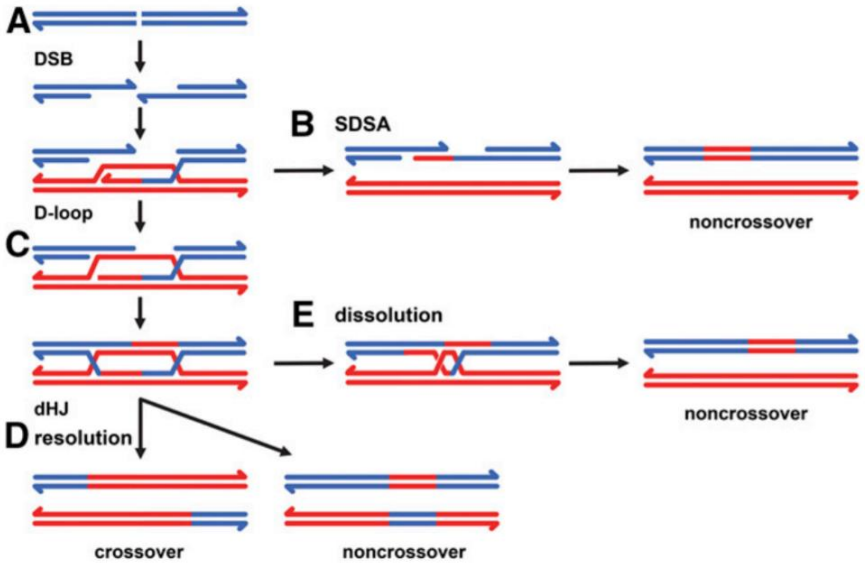

Figure 7: schematic of homologous recombination; A) DSB resection to have 3' overhangs following strand invasion and extension B) SDSA resolve and gap filling C) formation of a holliday junction E) dissolution of the holliday junction D) resolution of the holliday junction can either be non-crossover or the nucleolytic resolution with crossover (taken from [126])

1.1.2.5.2 Non-homologous end joining and alternative DSB repair

The NHEJ pathway does not require a sequence homology and it is initiated by 53BP1 binding that protects the DSB end from resection. It is active during the whole cell cycle and requires DNA-dependent protein kinase (DNA-PK) that comprises of the heterodimer KU70/80 and the catalytic subunit (DNA-PKc). The involved proteins anyway can change depending on the structure of the of the DNA ends that need to be ligated [128]. For blunt DNA end this could be only Ku–XRCC4–DNA ligase IV complex (not the DNA-PKcs) for ligation of the two ends. The ligation can be stimulated by a complex of XRCC4 and XLF [110]. If there are incompatible ends, for example one end has an overhang while the other is blunt, that composition needs the extra involvement of nucleases to trim the overhang. For 5' overhang the pathway utilizes DNA-PKcs and Artemis, while for the trimming of 3' overhangs a polymerase from the X-family (mainly pol μ) is required [128].

The MHMR pathway could be a back-up pathway if NHEJ or HR are not working but it normally occurs also at 10 - 20 % level in normal cells [129]. It depends on end resection up to a microhomology sequence on both strands from 2 nt up to 20 nt (Figure 6). The homology is stabilizing the DNA for ligation. PARP1 seems to promote MHMR [130] and Polθ (Polymerase

theta) is essential for MHMR. Polθ is known to stabilize the annealing of long overhangs with a short homology [131]. Additionally it contains a terminal transferase activity with which it can add nucleotides to create sequence homology independent of a template [132]. If homology is achieved, the gaps or single strands just needs to be extended and ligated by ligase 1 (LIG1) or ligase 4 (LIG4). This pathway can create small deletions or insertion mutations.

The SSA pathway, same as the MHMR, do not relay on the KU homologues and needs a short patch of homology. For the SSA pathway homology needs to be longer and end resection by MRN and CtIP creates 15 – 20 nt 3' overhangs that can be extended by EXO1, BLM or DNA2 nuclease [110][133]. The single strands are coated in RPA protein to protect them, and the annealing is mediated by RAD52. The annealed sequence produced overhangs that need to be trimmed for ligation by XPF-ERCC1 and/or MSH2-MSH3 (Figure 6)[134].

1.2 Synthetic lethality and viability

1.2.1 The concept of synthetic lethality and viability in oncology

Cancer is a disease caused by unregulated cell growth of abnormal cells that can invade the nearby tissue. The unregulated cell growth is the result of accumulated mutations which give the tumor cells a survival advantage but at the same time these mutations leave the tumor cell dependent on other proteins or pathways to compensate for the lack of these mutated genes.

The reliance of cancer on specific pathways can be exploited for treatment in the form of SL [135]. SL is when inactivation of two genes simultaneously leads to cell death while each of the genes separately inactivated do not. What makes this approach so appealing is the high specificity of the treatment, as only cancer cells that are dependent on the compensatory pathway are affected while healthy cells are not. This approach is more readily available with the advance of more faster and powerful methods for profiling expression and mutation landscape of the cancer and it pushes the boundaries in the direction of personalized medicine [136].

As mentioned PARP1 recruits XRCC1 to SSB and in its absence (or XRCC1s absence) HR, RAD51 foci and yH2AX foci are increased suggesting a dependence of cells on HR in the absence of

PARP1. This was the first evidence of SL between *PARP1* and genes involved in HR such as BRCA1 and BRCA2 (Figure 8) [137][138].

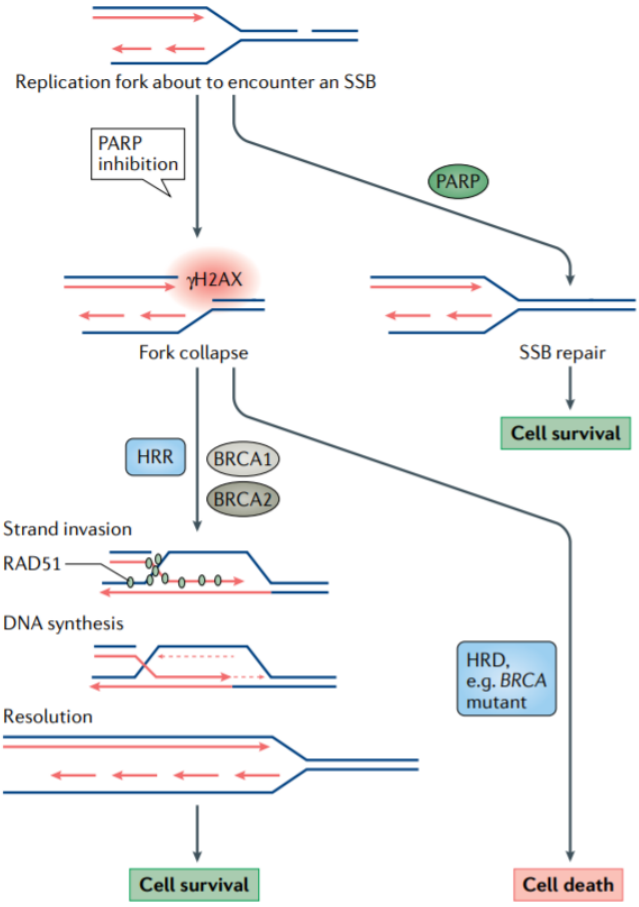

Figure 8: Schema of synthetic lethality with between PARP1 and HR deficiency (taken form [144])

The first PARP inhibitors were already described in 1980 but the development and finally the first registration as cancer treatment took until 2014 with Olaparib as a new class of anticancer drug [139]. Currently there are several other inhibitors in clinical trials phase 1-3, designed on the basis of SL: ATR, DNA-PK, WEE1 and CHK1 [140] and one PARP1 inhibitor Olaparib in phase four. At the moment Olaparib is used for the treatment of HR defective triple negative breast and ovarian cancers [140][141].

The mechanism of PARP1 inhibition, the main target of Olaparib, is the competitive inhibition of the active site with NAD+. This obstructs the PARylation of PARP1 itself and of other proteins and, moreover, it blocks the dissociation of PARP1 from DNA. This trapping of PARP1 impedes

the other repair proteins to access the damaged DNA. This trapping effect was published very early in the discovery PARP showing that a PARP1 free cell extract could repair a nicked plasmid while instead a cell extract containing both PARP1 and the inhibitor could not [142].

The emerging of resistance to any cancer drug is common feature of all cancers, as the nature of cancer cells is the accumulation of mutations that confer a selective advantage. There are several described mechanisms that grant resistance to PARP inhibitors, one being the restauration of the HR pathway. This is possible due to secondary mutations restabilising BRCA1, BRCA2, RAD51C, RAD51D and PALB2 functions [143][144]. Besides that, HR can also be restored by loss of 53BP1 which is essential for NHEJ pathway choice [145][146].

Other mechanism of resistance are the increase of PARP1 expression, increase of PARylation, mutation of the active site of PARP1 or the removal of the inhibitor with efflux transporter [144].

A further mechanism of resistance is called synthetic viability: an additional mutation in another gene confers survival despite the HR deficiency and the inhibition of PARP1. One example of synthetic viability is the stabilization of replication forks through abolishing the excessive end resection. This is achieved by mutations in the MRE11 gene which is part of the MRN complex and responsible for end resection in HR [147].

1.2.2 Synthetic lethal/viable interaction of the FA pathway

As introduced before the FA/BRCA pathway consist of several stages of repair steps and the HR is just the last step to repair the created DSB. As a result of the application of SL between PARP inhibitors and HR deficiency in cancer, and seeing that HR is part of the FA pathway, there is now an increased interest studying in the FA pathway. For one, FA has an very intricate association with cancer and there is multiple evidence that FA proteins are frequently mutated in cancer, making it a potent target for SL as cancer treatment [148][149][150].

Finding synthetic lethal interactions of the FA pathway has a huge potential because FA proteins themselves can be mutated in cancer frequently and treated with an inhibitor for the synthetic interaction partner or the FA pathway could be inhibited broadening the application field. At the moment there is not yet a specific inhibitor for the FA pathway but several paper

are urging the for a development of an inhibitor that would target the FANCD2 monoubiquitination [151].

For the FA pathway various synthetic interactions were reported in the last years, one of the most well-known interactions is the SL of FA core complex proteins including FANCD2 and Ataxia telangiectasia mutated (ATM) [152]. This interaction could be verified in mouse double KO of $FANCG^{-/-}$ and $ATM^{-/-}$ though embryonic lethality and with an ATM inhibitor. The survival of FA cells, at least for core complex and FANCD2 KO cells depends on an increased activation of ATM [149][153].

ATM is a central serin/threonin protein kinase of the DNA damage response [154][155]. It is thought to balance the pathway choice between HR and cNHEJ in response to genotoxic stress like DSB through the activation of the MRN complex (MRE11-RAD50-NBS1) but it is also involved in the response to oxidative stress and mitophagy [156]. Several FA proteins are ATM substrates [157] as well and it seems possible that with an impaired ICL repair the cells need to channel DNA repair into another functional pathway like cNHEJ. ATM is not the only kinase that is synthetically lethal in the absence of the FA/BRCA pathway so are CHK1, SIK2 and WEE1 [158][159][160]. All of these kinases participate in the cell cycle.

Not only kinases are synthetically lethal with the FA/BRCA pathway, for example mutations in the enzymes catabolizing alcohol: alcohol dehydrogenase 5 (ADH5) and aldehyde dehydrogenase 2 (ALDH2) are synthetically lethal with FA as well. The breakdown of alcohol starts with the generation of acetaldehyde by ADH5 and the aldehyde is than oxidized to acetate by ALDH2. Aldehydes are known for causing ICLs and the fast breakdown of this cytotoxic by-product of metabolism is important more so in FA cells as they lack the proper repair pathway. This interaction could be proven by in mice [161] and in a study of Japanese FA patients, that carry heterozygote or in rare cases homozygote mutations in ALDH2 [162][163], a mutation that is more prevalent in east-Asia. This SL interaction gained more attention recently, when it was published that in a subset of acute myeloid leukaemia ALDH2 is frequently silenced and the cancer cells dependent on the function of the FA pathway to repair damage caused by endogenous aldehydes [164]. The research proposed that in ALDH2 silenced cells are dependent on the repair of ICLs that are caused by the abundance of toxic aldehydes that accumulate because the degradation block due to the silencing of ALDH2. If the cancer cells lack ICL repair ICLs enrich in the DNA until triggers the p53 mediated apoptosis. This is the first

example of the application of SL between FA and ALDH2 as a potential cancer target in a subset of hematologic malignancy.

Further SL interactions of FA proteins were found between the DNA polymerases Polι, Polθ [165][166] and in BRCA deficient cells with FEN1 and APEX2 [167].

All of the mentioned interactions are synthetically lethal but there also some described synthetic viable interactions. BRCA1/2 or PALB2 and RAD52 co-inhibitions are synthetically lethal [119], but when the Exonuclease/Endonuclease/Phosphatase Domain-1 protein (EEPD1) is depleted in parallel, the cells are rescued [168].

It is believed that RAD52 is mediating, at stalled replication forks, a backup pathway for HR or facilitating entrance to HR independent of BRCA1 or BRCA2. To initiate HR a free 3' ssDNA overhang is necessary at the stalled fork, to load RAD51 onto for strand invasion. For this single strand DNA, 5'-end resection is necessary, and this would be promoted in healthy cells by BRCA1. In cells lacking BRCA1, the EEPD1 adapts this role by cutting the stalled fork and initiates EXO1 mediated 5'-end resection and generates the substrate for RAD51. The presence of EEPD1 forces the cells into HR repair through end resection, creating a dead end. If EEPD1 is missing in the double KO cells, it is then possible to repair the damage over MHMR. This is further corroborated by the fact that the depletion of Polθ in triple KO cells of BRCA1, RAD52, and EEPD1 is again synthetic lethal [168].

Another application for the concept of synthetic viability is as a potential cure for FA. There has been work stating that the inhibition of the cNHEJ pathway can rescue the FA phenotype, in chicken DT40, in *C. elegance* and in a human cell line [169][170].

In the DT40 chicken cell line the depletion of Ku70 in a FANCC KO background was synthetically viable however DNA-PK_{CS} nor LIG4 could rescue the FA phenotype. In contrast, in the *C. elegance* model, in a FCD-2 (FANCD2 homolog) background the depletion of LIG4 serves as a synthetic viable interaction attenuating the cisplatin sensitivity [170]. In the human glioblastoma cell line MO59J (DNA-PKcs deficient) the siRNA inhibition of FANCD2 did not sensitise the cells to MMC as it did to the DNA-PKcs expressing cell line. Even though all these finding are promising, so far there is no treatment available based on these interactions, but further research into synthetic viability could be fruitful for the development of a treatment.

1.3 The CRISPR/Cas9 system and gene editing

The CRISPR (clustered, regularly, interspaced short palindromic repeats) are patterns present in the genomes of bacteria and archaea that code for an adaptive immune system against phages and invading plasmids [171]. This system, like restriction enzymes, can be utilized for targeted gene editing in cells [172].

There are three different types of CRISPR known differentiating in the sequence and structure of the Cas proteins [173] but only type 2 systems are used in gene editing as it is the simplest system. For an endogenous system of type 2 CRISPR/Cas9 the CRISPR-associated endonuclease Cas9/Csn1 (Cas9), the CRISPR RNA (crRNA) and the transactivating crRNA (tracrRNA) are necessary to function. Immunity is achieved in three steps: the foreign ribonucleic acid sequence is cut into small fragments by Cas enzymes, called protospacer and incorporated into the CRISPR locus. Then the locus is transcribed into long precursor crRNA the tracrRNA hybridizes to the palindromic sequence of the precursor followed by cleavage of endogenous RNase III, creating mature crRNAs, which consist of one spacer and a partial repeat sequence (Figure 9).

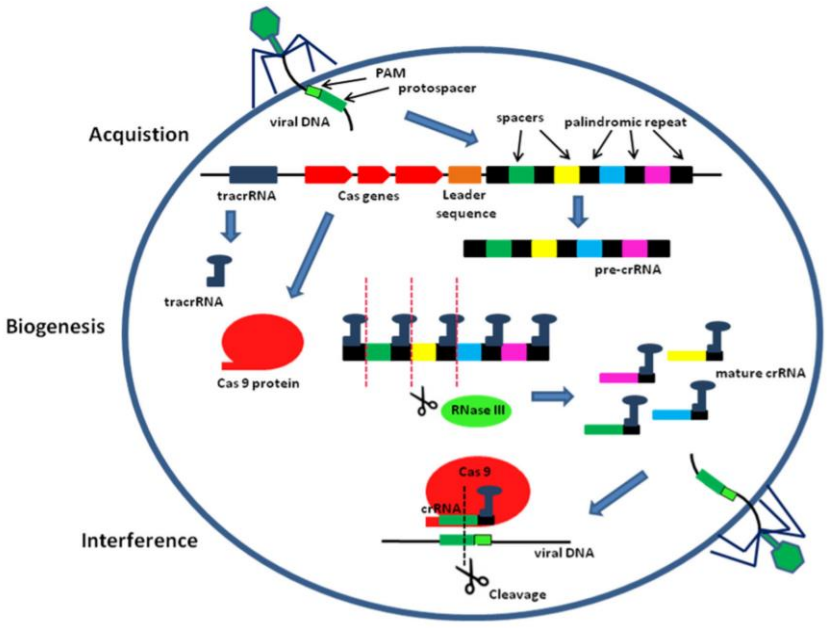

Figure 9: Schema of CRISPR locus in the acquisition step with tracrRNA in grey key-shapes, Cas genes/protein in red, the palindromic sequence in black and the different spacer/foreign DNA in different colours. The PAM sequence is marked on the viral DNA; In the biogenesis step tracrRNA and pre-crRNA are transcribed and processed after hybridisation with tracerRNA, the mature crRNA is integrated into a Cas9 proteins and guides the enzyme to a homologous sequence which is cut after PAM verification. (taken from [174])

If these mature crRNA guide the Cas9 protein to the complementary foreign nucleic acids, the complex degrades the DNA sequences of the invading species [174] by cutting 3 bp upstream of the PAM sequence and creating a DSB [175] . The protospacer adjacent motifs (PAMs) is an important sequence motif for recognition of the viral genome. This PAM motif makes the distinction between the incorporated spacer of the CRISPR locus and the actual viral genome, that should be degraded. For that reason protospacer sequences do not contain PAM sites [176]. The identity of the PAM sequence depends on the species of the Cas9 [177].The crRNA sequence of the Cas9 typically corresponds to foreign viral genomes as an acquired immune system, but it can be substituted by any sequence, harbouring a PAM on the strand to be targeted by the Cas9 protein [178].

This system is now exploited to for easy gene editing in eukaryotic cells. For it to work, it only needs: Cas9, the crRNA, which in the setting of gene editing is more commonly called small guide RNA (sgRNA), and either the tracrRNA or a chimeric form of sgRNA and tracrRNA, all of the components can be introduced on a plasmid into cells. Another more temporary form of delivery of the CRISPR/Cas9 system into cells is as riboprotein, which is common in gene therapy where the integration of foreign DNA into the genome of the cell is unfavourable [179][180].

As mention the Cas9 induces a site-specific DSB. The repair of this break can happen over HR or one of the error-prone DSB repair pathways. HR repair can be exploited for inducing specific mutations by suppling in donor sequence that carries the desired mutation while NHEJ produces mutations randomly. The sgRNA ensures a sequence specific cutting of the target gene with minimal off-targets making it perfect for gene correcting in therapy or the creation of a knock-down cell line for basic research. The success of this method is seen in the great variety of modulations and applications of the CRISPR/Cas9 method.

In this work a dual plasmid approach was used through lentiviral particle delivery and a chimeric tracrRNA-sgRNA. No donor sequence was used to insert a specific mutation but instead clones were screened for incorrect repair and mutations.

2 Objectives

The main objective of this thesis is to identify novel synthetic lethal and viable interactions between DNA repair pathways with a focus on the repair of interstand cross-links by the FA/BRCA pathway. For this aim the following subobjectives were stipulated:

- Creating FANCA and FANCD2 KO clones with fluorescent marker for testing of synthetic lethality/viability

- Establishing a cell-based colour competition system of cytometer measurement for testing synthetic lethality/viability in different backgrounds

- Testing for synthetic lethality/viability between DNA repair pathways through the colour competition assay

- Find novel synthetic lethal and/or viable interaction among FA- BRCA pathway and other DNA repair pathways

3 Material und Methods

3.1 Cell lines and plasmids

In Table 1 are all cell lines listed that were used in the thesis with their origins, culture medium and introduced plasmids and resistances.

Table 1: Cell lines, stable integrated plasmids and culture medium (see end of table for components)

Name	Tissue of origin	Cell line characteristics
ATM GFP	human transformed patient fibroblast	AT patient, transduced with pLKO5.sgNT.EFS.GFP, green fluorescent, medium 2
ATM KO	human transformed patient fibroblast	AT patient; ATM deficient cell line, medium 2
ATM tRFP	human transformed patient fibroblast	AT patient, transduced with pLKO5.sgNT.EFS.tRFP, red fluorescent, medium 2
Fibroblast BRCA2 KO	human transformed patient fibroblast	HR deficient, BRCA2 KO, patient cell line, medium 2
Fibroblast BRCA2 KO GFP	human transformed patient fibroblast	Fibroblast BRCA2 KO transduced with pLKO5.sgNT.EFS.GFP, medium 2
Fibroblast BRCA2 KO tRFP	human transformed patient fibroblast	Fibroblast BRCA2 KO transduced with pLKO5.sgNT.EFS.tRFP, medium 2
HCT116	human colorectal carcinoma fibroblasts	Mismatch repair deficient mlh1, medium 1
HCT116 GPF	human colorectal carcinoma fibroblasts	HCT116 transduced wit pLKO5.sgNT.EFS.GFP, green fluorescent, medium 1
HCT116 tRFP	human colorectal carcinoma fibroblasts	HCT116 transduced wit pLKO5.sgNT.EFS.tRFP, red fluorescent, medium 1
HEK 293	human embryonic kidney fibroblast cells	Immortalized, medium 2
HEK tRFP	human embryonic kidney fibroblast cells	HEK 293 transduced with pLKO5.sgNT.EFS.tRFP, red fluorescent, medium 2
HEK BRCA2 KO	human embryonic kidney fibroblast cells	HR deficient BRCA2 KO, medium 2
HEK BRCA2 KO GFP	human embryonic kidney fibroblast cells	HEK BRCA2 KO transduced with pLKO5.sgNT.EFS.GFP, green fluorescent, medium 2
HEK BRCA2 KO tRFP	human embryonic kidney fibroblast cells	HEK BRCA2 KO transduced with pLKO5.sgNT.EFS.tRFP, red fluorescent, medium 2
HEK XPF KO	human embryonic kidney fibroblast cells	Deficient in NER and ICL repair, medium 1

HEK XPF KO + wt	human embryonic kidney fibroblast cells	HEK XPF KO transduced with pUltra + TAPtag-XPF-HA, medium 2, puromycin resistance
HEK XPF KO + wt	human embryonic kidney fibroblast cells	HEK XPF KO transduced with pLKO5.sgNT.EFS.tRFP, medium 2, puromycin resistance
HEK XPF KO + wt	human embryonic kidney fibroblast cells	HEK XPF KO transduced with pLKO5.sgNT.EFS.GFP, medium 2, puromycin resistance
HEK XPF KO C236R	human embryonic kidney fibroblast cells	HEK XPF KO transduced with plasmid pUltra + TAP-XPF-HA with C236R, medium 2, blasticidin
HEK XPF KO C236R GFP	human embryonic kidney fibroblast cells	HEK XPF KO C236R transduced with pLKO5.sgNT.EFS.tRFP, medium 2, blasticidin resistance
HEK XPF KO C236R tRFP	human embryonic kidney fibroblast cells	HEK XPF KO C236R transduced with pLKO5.sgNT.EFS.GFP, medium 2, blasticidin resistance
HEK XPF KO GFP	human embryonic kidney fibroblast cells	HEK XPF KO transduced with pLKO5.sgNT.EFS.GFP, medium 1, blasticidin resistance
HEK XPF KO I225M	human embryonic kidney fibroblast cells	HEK XPF KO transduced with plasmid pUltra + TAP-XPF-HA with I225M, medium 1, blasticidin resistance
HEK XPF KO I225M GFP	human embryonic kidney fibroblast cells	HEK XPF KO I225M transduced with pLKO5.sgNT.EFS.tRFP, medium 1, blasticidin resistance
HEK XPF KO I225M tRFP	human embryonic kidney fibroblast cells	HEK XPF KO I225M transduced with pLKO5.sgNT.EFS.GFP, medium 1, blasticidin resistance
HEK XPF KO L230P	human embryonic kidney fibroblast cells	HEK XPF KO transduced with plasmid pUltra + TAP-XPF-HA with L230P, medium 1, blasticidin resistance
HEK XPF KO L230P GFP	human embryonic kidney fibroblast cells	HEK XPF KO L230P transduced with pLKO5.sgNT.EFS.tRFP, medium 1, blasticidin resistance
HEK XPF KO L230P tRFP	human embryonic kidney fibroblast cells	HEK XPF KO L230P transduced with pLKO5.sgNT.EFS.GFP, medium 1, blasticidin resistance
HEK XPF KO R153P	human embryonic kidney fibroblast cells	HEK XPF KO transduced with plasmid pUltra + TAP-XPF-HA with C236R, medium 2, blasticidin resistance
HEK XPF KO R153P GFP	human embryonic kidney fibroblast cells	HEK XPF KO C236R transduced with pLKO5.sgNT.EFS.tRFP, medium 2, blasticidin resistance
HEK XPF KO R153P tRFP	human embryonic kidney fibroblast cells	HEK XPF KO C236R transduced with pLKO5.sgNT.EFS.GFP, medium 2, blasticidin resistance

HEK XPF KO tRFP	human embryonic kidney fibroblast cells	HEK XPF KO transduced with pLKO5.sgNT.EFS.tRFP, medium 1, blasticidin resistance
HeLa XPF KO	human adenocacinoma epithelial cell line	transduced with sgXPF lentiCRISP_v2, medium 2, puromycin resistance
HeLa XPF KO GFP	human adenocacinoma epithelial cell line	HeLa XPF KO transduced with pLKO5.sgNT.EFS.GFP, medium 2, puromycin resistance
HeLa XPF KO tRFP	human adenocacinoma epithelial cell line	HeLa XPF KO transduced with pLKO5.sgNT.EFS.tRFP, medium 2, puromycin resistance
LoVo	human adenocarcinoma fibroblasts from colon	Mismatch repair deficient *MSH2,* medium 3
LoVo GFP	human adenocarcinoma fibroblasts from colon	LoVo transduced wit pLKO5.sgNT.EFS.GFP, green fluorescent, medium 3
LoVo tRFP	human adenocarcinoma fibroblasts from colon	LoVo transduced wit pLKO5.sgNT.EFS.tRFP, red fluorescent, medium 3
PN	Transformed human fibroblasts	wildtype control, medium 3
PN GPF	Transformed human fibroblasts	PN transduced with pLKO5.sgNT.EFS.tRFP, medium 3
PN tRFP	Transformed human fibroblasts	PN transduced with pLKO5.sgNT.EFS.GFP, medium 3
RPE1 p53 KO	human immortalized retina pigmented epithelium cells	transduced with lentiBLAST; p53 deficient, medium 1, blasticidin resistance
RPE1 p53 KO FANCA KO GFP	human immortalized retina pigmented epithelium cells	RPE1 p53 KO cells transduced with pLKP5.sgFANCA.EFS.GFP, medium 1, blasticidin resistance
RPE1 p53 KO tRFP	human immortalized retina pigmented epithelium cells	RPE1 p53 KO cells transduced with pLKP5.sgNT.EFS.tRFP, medium 1, blasticidin resistance
U2OS	human osteosarcoma cell line	medium 1
U2OS Cas9	human osteosarcoma cell line	transduced with plasmid lentiCas9-BLAST, medium 1, blasticidin resistance
U2OS FANCA KO	human osteosarcoma cell line	U2OS Cas9 transduced with pLKO5.sgFANCD2.EFS.GFP, green fluorescent, medium 1, blasticidin resistance
U2OS FANCD2 KO	human osteosarcoma cell line	U2OS Cas9 transduced with pLKO5.sgPARP1.EFS.GFP, green fluorescent, medium 1, blasticidin resistance
U2OS GFP	human osteosarcoma cell line	U2OS Cas9 transduced with plasmid pLKO5.sgNT.EFS.GFP, green fluorescent, medium 1, blasticidin resistance

U2OS PARP1 KO GPF	human osteosarcoma cell line	U2OS Cas9 transduced with pLKO5.sgFANCA.EFS.GFP, green fluorescent, medium 1, blasticidin resistance
U2OS tRFP	human osteosarcoma cell line	U2OS Cas9 transduced with plasmid pLKO5.sgNT.EFS.tRFP, Red fluorescent, medium 1, blasticidin resistance
XPA corrected	human transformed patient fibroblast	XPA KO transduced wildtype xpa gene, medium 1
XPA corrected GFP	human transformed patient fibroblast	XPA KO corrected transduced wit pLKO5.sgNT.EFS.GFP, green fluorescent, medium 1
XPA corrected tRFP	human transformed patient fibroblast	XPA KO corrected transduced wit pLKO5.sgNT.EFS.tRFP, red fluorescent, medium 1
XPA KO	human transformed patient fibroblast	NER deficient XPA KO cell line, medium 1
XPA KO GFP	human transformed patient fibroblast	XPA KO transduced wit pLKO5.sgNT.EFS.GFP, green fluorescent, medium 1
XPA KO tRFP	human transformed patient fibroblast	XPA KO transduced wit pLKO5.sgNT.EFS.tRFP, red fluorescent, medium 1

Medium 1: DMEM (biowest L0104-500) with 10 % Serum (biowest FBS S181B) + 1:10000 Plasmocin
Medium 2: DMEM with 15 % Serum + 1:10000 Plasmocin
Medium 3: DMEM with 20 % Serum + 1:10000 Plasmocin

In Table 2 are listed all bought and generated plasmids for the CRISPR/Cas9 gene editing and the shRNA inhibition as well as the plasmid needed for the virus particle production.

Table 2: Plasmids used for clone creation and shRNA inhibition

Name	Description
lentiCas9-BLAST	Lentiviral vector of S. pyrogenes Cas9 addgene #52962, blasticidin selection marker
pLKO5.sgRNA.EFS.GFP	3rd generation lentiviral vector, sgRNA spacer for delivery, without Cas9, GFP marker, EFS Promoter driven addgene #57822
pLKO5.sgRNA.EFS.tRFP	3rd generation lentiviral vector, sgRNA scaffold with spacer, without Cas9, tRFP marker EFS Promoter driven addgene #57823
pLKO5.NT.GFP	pLKO5.sgRNA.EFS.GFP with sgRNA spacer substituted by non-human sgRNA target as control plasmid, GFP
pLKO5.NT.tRFP	pLKO5.sgRNA.EFS.tRFP with sgRNA spacer substituted by non-human sgRNA target as control plasmid, tRFP
pLKO5.FANCA.GFP	pLKO5.sgRNA.EFS.tRFP with sgRNA spacer substituted by sgRNA for *fanca* target as control plasmid, GFP
pLKO5.FANCD2.GFP	pLKO5.sgRNA.EFS.tRFP with sgRNA spacer substituted by sgRNA for *fancd2* target as control plasmid, GFP
pLKO5.PARP1.tRFP	pLKO5.sgRNA.EFS.tRFP with sgRNA spacer substituted by sgRNA for parp1 target as control plasmid, GFP
pLKO5.PARP1.GFP	pLKO5.sgRNA.EFS.tRFP with sgRNA spacer substituted by sgRNA for parp1 target as control plasmid, tRPF
pLKO1.shRNA.FANCA	pLKO.1_shRNA TRCN0000296799 shRNA for FANCA inhibition, sigma mission (Merck), puromycin selection marker
pLKO1.shRNA.FANCD2 40	pLKO.1_shRNA TRCN0000082840 shRNA for FANCD2 inhibition, sigma mission (Merck), puromycin selection marker
pLKO1.shRNA.NT	pLKO.1_shRNA_non-targeting, sigma mission (Merck), puromycin selection marker
pLKO1.shRNA.FEN1	pLKO.1_shRNA TRCN0000049731 shRNA for FEN1 inhibition, sigma mission (Merck), puromycin selection marker
psPAX2	2nd generation lentiviral packaging plasmid, psPAX2 was a gift from Didier Trono (Addgene plasmid # 12260 ; http://n2t.net/addgene:12260 ; RRID:Addgene_12260)
pENV	3rd generation lentiviral packaging plasmid pMD2.G was a gift from Didier Trono (Addgene plasmid # 12259 ; http://n2t.net/addgene:12259 ; RRID:Addgene_12259)

3.2 Establishing of U2OS and RPE1 know-out cell lines with the CRISPR/Cas9 method

3.2.1 sgRNA target sequence selection

In order to generate the sgRNA for the CRISPR/Cas9 knock-out cell line the Breaking Cas web tool was used [181] and chosen was the suggested sequences that were the closest to the N-terminal of the protein and which had no or the least predicted off-targets.

All sequences were created over the web tool except for BRCA1 which was from a publication [182] that stated to have obtained a BRCA1 KO clone by using the CRISPR/Cas9 method. The sgRNA sequences that were cloned by different methods in the pLKO5 plasmid backbone are listed in table 3.

Table 3: sgRNA sequences used for establishing KO clones

Gene	Sequence 5' - 3'	Exon
BRCA1	GTCTCCACAAAGTGTGACCA	2
BRCA1 _2	GACGTCTGTCTACATTGAAT	5
BRCA1 _3	TTCTGAAGATACCGTTAATA	6
FANCA	GGATGGTTGCCTCTAGCGTG	4
FANCD2	AACAGCCATGGATACACTTG	11
PARP1	CGAGTCGAGTACGCCAAGAG	1
Non-target	GGACGCCCTAATGCCCATCG	NA

3.2.2 Vector construction

The guide sequences were constructed after the lentiviral protocol from GeCKO Lentiviral CRISPR toolbox “Target guide sequence cloning protocol” with the exception that the oligonucleotide sequences were ordered 5’-phosphorylated for the sense and the antisense sequence (BRCA1, BRCA1_2, BRCA1_3 non-target and PARP1).

The digestion reaction of the original pLKO5_GFP and tRFP plasmid is described in table 4 below. This reaction cuts the spacer and opens the backbone for ligation of the sgRNA.

Table 4: Digestion mix for cutting pLKO5 plasmid to replace the spacer

Volume in µl	Content
X (1 ug)	Plasmid
1	BsmBI (NEB)
5	10x NEBuffer 3.1
44 - X	H_2O
50	total Volume

The reaction was incubated for 2 h and 30 min at 55 °C and afterwards heat-inactivated at 80 °C for 10 min. The whole reaction was loaded on a 1 % agarose gel for purification and the DNA was isolated with the Macherey-Nagel Kit NucleoSpin Gel and PCR Clean-up with the protocol "DNA extraction from agarose gels" with an elution volume of 10 µl.

The sense and antisense oligonucleotides ware annealed in the thermoblock following the protocol below in a concentration of 100 µM each in a 10 µl volume.

Table 5: Protocol for annealing of the sense and antisense oligonucleotides to create the sgRNA

Temperature in °C	Time in min
37	30
95	5
RT	10

After the annealing the oligos were diluted 1:200 for the ligation. Table 6 lists the components of the ligation reaction of pLKO5 plasmid backbone with the annealed oligonucleotides.

Table 6: Ligation mix for the ligation of the pLKO5 backbone with the annealed sgRNA

Volume in µl	Content
X (50 ng)	digested Plasmid
1	diluted Oligo
5	2x Quick Ligase Buffer (NEB)
0.5	Quick Ligase (NEB)
3.5 - X	H_2O
10	total Volume

The Ligation reaction was incubated 15 min at RT. The plasmids were than transformed into *Stl3* bacteria by pipetting the whole ligation mix onto competent cells and incubating 30 min on ice followed by the heat-shock of 30 sec at 42 °C. Then followed up by 2 min on ice and the addition of 250 µl SOC-Medium the bacteria were grown 1 h at 37 °C and 220 rpm. From this suspension 100 µl were plated on a Agar plate with Ampicillin selection. While one plate was plated with a more concentrated cell suspension both were grown overnight at 37 °C.

For the creation of the red and green control (non-targeting sgRNA; NT) plasmid as well as the FANCA and FANCD2 a site directed mutagenesis Kit from NEB (E0554S) was used. Primer were created by the webtool provided by NEB "NEBaseChanger" and are listed in the table 7 below.

Table 7: Primer for the site directed mutagenesis of pLKO5 plasmid with gRNA; in lower case overlapping sequence of the plasmid in upper case gRNA

Name	5' - 3' Sequence
DSt024_FA-A f	gcctctagcgGTTTTAGAGCTAGAAATAGCAAG
DSt024_FA-A r	aaccatcccgCGGTGTTTCGTCCTTTCC
NT_pLKO5 F	atgcccatcgGTTTTAGAGCTAGAAATAGCAAG
NT_pLKO5 R	tagggcgtccCGGTGTTTCGTCCTTTCCAC
DSt022_FANCD2_f	gtacacttgGTTTTAGAGCTAGAAATAGCAAG
DSt023_FANCD2_r	catggctgttCGGTGTTTCGTCCTTTCC

For the site-directed mutagenesis the PCR reaction was pipetted after the following scheme in table 8, the PCR reaction components were provided in the kit.

Table 8: PCR pipetting scheme for site directed mutagenesis of pLKO5 sgRNA integration

Volume in µl	Content
6.25	2x Q5-Master Mix
1.25	Primer Forward (5 µM)
1.25	Primer Reverse (5 µM)
12 (3 ng)	Plasmid
4.3	H_2O
25.05	Total Volume

The thermocycler conditions for the site-directed mutagenesis PCR of the non-target sequence is depicted in table 9.

Table 9: Thermocycler condition for site directed mutagenesis PCR of pLKO5 with non-targeting sgRNA

Temperature in °C	Time	
95	30 sec	
98	10 sec	
61	20 sec	x25 cycles
72	3 min 30 sec	
72	2 min	

The thermocycler conditions for the site-directed mutagenesis PCR for guide RNA of FANCA and FANCD2 is depicted in table 10.

Table 10: Thermocycler conditions for site directed mutagenesis PCR of pLKO5 with sgRNA for FANCA or FANCD2

Temperature in °C	Time	
95	30 sec	
98	10 sec	
62	20 sec	x25 cycles
72	3 min 30 sec	
72	2 min	

The finished PCR was used directly for the kinase, ligase and DpnI digestion reaction which is a one-step reaction in the Q5-Kit with a 5 min incubation step at room temperature (table 11).

Table 11: KDL reaction to finish the site directed mutagenesis of pLKO5 with inserted sgRNA

Volume in µl	Content
1	PCR product
5	2x KDL reaction buffer
1	10x KLD enzyme mix
3	H_2O
10	total Volume

The plasmids created via both methods, the traditional cloning and the site-directed mutagenesis, were transformed into bacteria via the heat-shock protocol (see above). The only difference was the use of C2987 *E.coli* competent cells for the Q5-site directed mutagenesis.

From the grown bacteria of each reaction 16 colonies were picked for minipreparations (minipreps) of bacteria, which consist of 4 ml LB-medium with 1:1000 dilution of ampicillin, incubated overnight at 37 °C and 220 rpm shaking. From these minipreps the plasmids were isolated by E.Z.N.A. Plasmid DNA Mini Kit I from Omega with the "Plasmid DNA Extraction and Purification from *E.coli* culture"

For the sequencing all plasmids were brought to the same concentration of 100 ng/µl for sanger sequencing and 5 µl of plasmid (500 ng) and 5 µl Primer (hU6_seq 5´-3´ ACTATCATATGCTTACCGTAAC), in a 5 µM concentration, were sent to sequence through the Macrogen EZ-sequencing service. The results were visualised with BioEditor or the Sequencher bioinformatic software.

The verified plasmids were amplified in a maxiprep; 250 ml LB-medium with 1:1000 ampicillin at 37 °C overnight and 220 rpm shaking. The next day the plasmids were isolated with Macherey-Nagel Kit: Plasmid DNA purification NucleoBond and brought to a 1 µg/ml concentration for further use.

3.2.3 Lentiviral particle production

To create infectious lentiviral particles, HEK cells in passage five or six were seeded in a 10 cm diameter dish. The 4x 10^6 cells were grown in 10 ml over night and the next day the medium (see table 1) was changed to only 9 ml of volume and supplied with 3 µl of 100 mM of chloroquine. The cells were incubated for the duration of the preparation of the Chalphos-Kit infection solution.

The transfection solution A for generating lentiviral particles was prepared in the order following table 12 for one dish.

Table 12: Pipetting scheme for the generation of transfection solution A for lentiviral particle production

Volume in µl	Content
10 (10 ng)	Plasmid
6.5 (6.5 ng)	psAX2 packaging plasmid
3.5 (3.5 ng)	ENV lenti VSV G plasmid
87	Calcium Solution (Calphos)
593	sterile H2O
700	total Volume

After preparing solution A, it was carefully vortexed while one volume of 2x HBS (Calphos) Buffer was added dropwise to the transfection solution A. The finished transfection solution was incubated for 15 min at room temperature and vortexed again before added dropwise to the HEK packaging cells. The plates were incubated overnight, the next day the medium was changed to fresh 9 ml medium. The following day the supernatant of the plates was collected and stored at 4 °C while 9 ml of new medium were added to the cells.

The last day the collection of the supernatant was repeated and the all supernatant was centrifuged in Millipore Utra-15 centrifugal filter units for concentration of the infectious particles at 4000 rpm during 30 min at 6 °C. The collected lentiviral particle was stored in cryovials and frozen at -80 °C until further use.

3.2.4 Cell transduction and clone selection

For the lentiviral infection to create knock-down cells lines with the CRISPR/Cas9 system 200000 cells (U2OS or RPE1) were seeded in a 6-well plate and incubated overnight. The next day the wells were supplemented with 1:1000 polybrene and incubated 1 h before the transduction with the lentiviral particle.

U2OS or RPE1 cells were first infected with the lentiCas9-Blast plasmid with 25 µl volume of lentiviral particles in a medium of 2 ml. The cells were incubated with the virus particles for 72 h before the medium was changed to a blasticidin (2 µg/µl concentration) containing selection medium. For the positive selection of cells that integrated the plasmid, the cells were grown for 5 days on the selection medium.

To create stable KO cell lines the pLKO5 plasmids were being transduced into the previously selected, Cas9 expressing cells. For the transduction 200 000 cells were seeded in 2 ml medium of a 6-well plate well and incubated 72 h. The efficiency of transfection was controlled by fluorescence expression under a microscope first and then the cell pools were sorted for fluorescence with the FACSAria 2 (DB Bioscience) cell sorter and regrown.

From the sorted pools, single cell clones were seeded in 96-well plates through dilution. Per well 0,3 cells were calculated and per cell line 3x 96-well were seeded. All plates were incubated

at 37 °C and 5 % CO_2 and grown for circa 3 weeks with regular checks under the microscope for progress.

As a fast screening method, clones were split into two wells of a 96-well plate, one well for a fast western blot analysis, the other one to grow. For this fast screen by western blot, the clones were washed with 1x PBS and 40 µl Lämmli-Buffer was added directly into the well, the cell suspension was scratched from the surface and transferred to a 1.5 ml tube. The suspension was incubated 10 min on ice and centrifuged for 5 min at maximum speed before the samples were denatured for 5 min at 95 °C and 30 µl were loaded on a polyacrylamide gel. All clones which showed protein bands for the desired KO were discarded.

3.2.5 Western blot validation of knock-out clones

All promising clones from the quick screening were grown in 6-well plates to confluency and harvested by trypsinizing them. The pellets were washed and either weighted or cells were counted beforehand. The cell were lysed with 50 µl RIPA/mg of cell pellet of 1x RIPA buffer (Table 14) or 3x 10^6 cell per 50 µl respectively.

Before suspending the pellet in the RIPA (Millipore cat.no 20-188) aliquot, Benzonase (VWR International cat.no 7074-6-3) was added to it 1:1000 to digest DNA in the sample. The composition of RIPA buffer is noted in table 13.

Table 13: Content of RIPA buffer for protein extraction

Volume	Content
1 ml	10x RIPA Lysis Buffer (Millipore)
2 ml	5x cOmplete ULTRA tablets Protease inhibitor (Roche)
1 tablet	10x PhosSTOP Phosphatase inhibitor (Roche)
7 ml	H_2O
10 ml	total Volume

Protein extraction was achieved by the following protocol:

10 min at room temperature, followed by either sonication 2x for 15 sec and 25 % amplitude or by freezing overnight. Then 10 min of centrifugation at 10 °C at maximum speed.

The protein extract was then quantified with the Bradford method (Bio-Rad Protein Assay Dye Reagent Concentrate #5000006) For the Bradford protein measurement the 5x Bradford solution was diluted to 1x and pipetted 99 µl into a 96-well plate before the 1 µl protein extract was added and incubated at room temperature for 2 min. For measurement of the absorbance the Thermo scientific Multiskan Sky was used at wavelength 595 nm.

With the information from the protein extraction and a standard curve, the protein concentration was calculated and 50 mg of protein was loaded on a polyacrylamide gel. The samples were then mixed depending on the concentration with 2x Lämmli buffer (sigma cat.no. S3401-10VL) and denaturized 5 min at 95 °C.

Depending on the molecular weight of the protein gels between 5 % and 10 % polyacrylamide were used. Gels were run for approximately 1 h at 150 V. After the running-front left the gel, the blotting was done with the BIO-RAD Trans-Blot Turbo Transfer system onto a nitrocellulose membrane. To avoid unspecific binding of primary antibody the membrane was blocked in a solution of 5 % milk powder in 1x TBST (for 10x TBS: 4.85 g Tris-HCl, 16 g NaCl in 1 l H_2O pH 7.4; 1x TBST: 1:10 TBS add 1 ml of Tween) for an hour at room temperature.

The incubation with primary antibody was overnight at 4 °C followed the next day by 4 washing steps, each 5 min at room temperature with 5 ml of 1x TBST and the incubation with the correlating secondary antibody 1:3000 dilution of the secondary antibody (Anit-mouse Bethyl A90-116P, Anit-rabbit Bethyl A120-101P) in 5 % milk powder in 1x TBST for 1 h at room temperature. 4x washing with 5 ml 1x TBST before the revealing with the gene genomic aperture and the gene snap software.

Table 14 is a list of all used primary antibodies in this work.

Table 14: Primary antibodies and dilutions in 5 % milk in 1x TBST for Western blot revealing

Protein	Reference	Dilution	Western blot revealing solution
ATM	ab78	1:1000	Pierce
BRCA1	calbiochem ms110	1:800	Cresiendo
BRCA2	ab123491	1:800	Cresiendo
Cas9	ab204448	1:1000	Pierce
Clathrin	ab21679	1:1000	Pierce
FANCA	Bethyl A301-980A-M	1:1000	Cresiendo
FANCD2	ab108928	1:2000	Pierce
FEN1	Bethyl A300-255A-M	1:2000	Pierce
GAPDH	ab9485	1:2500	Pierce
PARP1	ab32138-100	1:800	Cresiendo
Vinculin	ab130007	1:2500	Pierce
XPF	Invitrigen MA5-12054	1:1000	Pierce

3.2.6 Sanger sequencing of the obtained knock-out clones

For identifying the mutation of each clone, the exon which was targeted by the sgRNA was amplified by PCR with the IBIAN®-Taq DNA Polymerase from IBIAN lab according to the manufacturer manual.

Table 15 lists all used primer combinations for amplification of the DNA fragments for mutation characterisation by sanger sequencing.

Table 15: Primer for PCR of mutated genomic DNA for sequencing of mutations caused by CRISPR/Cas9

Primer name	5'-3' sequence	gene
DSt005_F	TAGGGGTGGATATGGGTGAA	BRCA1
DSt006_R	GTTGCAGTGAGCCAAGATCA	BRCA1
DSt011_PARP1_1_F	CGGGTCCTCCAAAGAGCTAC	PARP1
DSt012_PARP1_1_r	CAAAGCGAAAGGCAACACCA	PARP1
DSt015_BRCA1_2_f	TCTTTTGAGCTCCCAGGCAC	BRCA1
DSt016_BRCA1_2_r	TGATTCTAGTCTGGAGAAACACCA	BRCA1
DSt017_BRCA1_3_f	TCAAGTATCAGCTTCAAAATATGCT	BRCA1
DSt018_BRCA1_3_r	AAGGTGGGAACTGCGTCTTT	BRCA1
DSt022_FANCD2_f	GGAAGATGGAGTAAGAGAAGT	FANCD2
DSt023_FANCD2_r	TGCTCATTCATAGTGGGTAG	FANCD2
MP_FANCA_Fw	GTGAGCTGCTTGGATCATCA	FANCA
MP_FANCA_Rv	TACTCTCTGCTCCACAGTCA	FANCA

Table 16 shows the reaction composition for the PCR to amplify the DNA fragments targeted by CRISPR/Cas9 for sanger sequencing.

Table 16: PCR reaction for FANCA and FANCD2 with IBIAN Taq

Volume in µl	Component
5	PCR-Buffer 10x
1 (40mM)	dNTPs
1.00	Primer
1	Primer
0.5	IBIAN-taq
1 (50 ng)	DNA
40.5	H2O
50	total

The PCR reaction for amplification of the DNA fragments of FANCA and FANCD2 that were targeted by CIRSPR/Cas9 is below in table 17, the exons were amplified with the same protocol.

Table 17: Thermocycler conditions for FANCA and FANCD2

Temperature in C	Time	
94	5 min	
94	45 sec	
64	1 min	x20
72	1 min	
72	7 min	

The PARP1 fragment was amplified with a special polymerase Kapa2G Robust PCR Kit (Kapa Biosystems) due to its very high GC-content, the composition of the PCR reaction shown below in table 18.

Table 18: PCR reaction after the manual of Kapa2G Robust

Volume in µl	Component
5	Buffer A
5	Enhancer
0.5	dNTPs
1,25	Primer
1,25	Primer
0,2	Polymerase
1 (50 ng)	DNA
10,80	H2O
25	total

In table 19 is the thermocycler protocol described for amplifying the DNA fragment of PARP1 that was targeted with the sgRNA for creating a KO clone.

Table 19: Thermocycler conditions for PARP1

Temperature in C	Time	
95	5 min	
95	15 sec	
60	15 sec	x35
72	30 sec	
72	1 min	

The amplified fragments were sanger sequenced over the EZ system over Macrogen.

3.2.7 Functional studies and survival assays

3.2.7.1 Colony forming assay

For the colony forming assay (CFA) 350 of shRNA or siRNA infected cells were seeded in 6-well plates and incubated for 16 days. The cells were fixed with trichloro acid (TCA) which was added directly to the medium of the wells, for a final 10 % TCA solution and incubated overnight at 4 °C. The plates were washed 6x under flowing tap water and dried before they were stained with 800 µl of a 0.057 % (wt/vol) sulforhodaminde B solution in 1 % acetic acid for 30 min at room temperature and slow shaking. After the incubation the dye is washed out 3x with 1 % acetic acid and dried. The colonies were counted manually.

3.2.7.2 Sulforhodamine B survival

The sulforhodamine B survival (SRB) is done in a 96-well plate using twelve wells per concentration of treatment. All cell lines origin from U2OS were seeded 1000 cells per well and treated the next day with Diepoxybutane (DEB, Sigma cat.no. 202533-16) with concentrations 0, 25, 50, 100 and 200 ng/ml or Olaparib (AZD-2281, Selleckchem cat.no. S1060) 0, 5, 50, 500, 5000 nM. The cells were grown for around 5 days until the wells of the untreated control reached confluence. TCA was added to the wells to a final concentration of 10 % and incubated overnight at 4 °C.

The plates were washed 6x under tap water and dried. After drying the wells were incubated with 50 µl of a 0.057 % (wt/vol) sulforhadamine B solved in 1 % acetic acid for 30 min and washed 3x with 1 % acetic acid and dried. For the measurement of absorbance at 510 nm the stain was solved in 100 µl of 10 mM tris(hydroxymethyl)aminomethane (TRIS) at pH 10.5 and incubated for 1 h at room temperature, shaking. The absorbance was measured with Thermo scientific Multiskan Sky at 510nm absorbance.

Out of the obtained dataset outlyers were identified with the interquarentil range (IQR). To calculate the IQR first the three quarentils of the twelve samples were calculated.

$$Q1 = \frac{1}{4(n+1)th}$$

$$Q3 = \frac{1}{4(n+1)th}$$

$$Q2 = Q3 - Q1$$

With the IQR the upper and lower limit were calculated, samples under the lower limit or higher than the upper limit were excluded from calculating the mean of each dose for the survival curve.

$$Lower\ fence = Q1 - (Q2 * 1{,}5)$$

$$Upper\ fence = Q3 + (Q2 * 1{,}5)$$

3.2.7.3 Micronuclei-chromosome-fragility and cell cycle

On day one the cells were seeded into 96-well plates 10 000 cells for U2OS and RPE1 in 200 µl and 20-25 000 cells for the HEK cell lines. On day two the cells are treated with DEB (DEB, Sigma cat.no. 202533-16) in concentrations 0, 25, 50 and 100 ng/ml and on day four the plates are processed.

The plate was incubated on ice for 20 min followed by the aspiration of the medium and staining of the cells with 0,025 mg/ml Ethidium monoazide (EMA; Thermo Fisher cat.no. E1374) and incubation on ice for 30 min with exposure to visible light.

Cold 1x PBS + 2 % FBS was added to the EMA and the wells were aspirated. 50 µl of Lysis buffer 1 (before use of the lysis buffer added 4′,6-diamidino-2-phenylindole (2 µg/ml DAPI; Invitrogen cat.mo. D21490) and RNase A (1 mg/ml; Thermo Fisher cat.no. 12091021)) were added:

Table 20 lists all components of MN lysis buffer 1 prior to the addition of DAPI and RNase A for the first step of lysis of the cells that are being prepared for MN measurement.

Table 20: Components of MN lysis buffer 1

Weight in mg	Concentration in mg/ml	Component
58.4	0.584	NaCl
100	1	$Na_3C_3H_5O(COO)_3$
solve in 100 ml		H_2O
add 30 µl	0.3 µl/ml	IGEPAL

Incubation for 1h at 37 °C to the lysis buffer 1 was added 50 µl lysis buffer 2 (before use added DAPI (2 µg/ml)) and incubated for 30 min at RT in the dark. Table 21 shows the components of MN lysis buffer 2 prior to DAPI addition for the completion of the cell lysis for MN measurement.

Table 21: Components of MN lysis buffer 2

Weight in g	Concentration in mg/ml	Component
8.56	85.6	Saccharose
1.5	15	Citric acid ($C_6H_8O_7$)
solve in 100 ml		H_2O

The plates can be stored up to 4 days at 4 °C in the dark before measurement at the cytometer.

The cytometer measurement was done like described in "In Vitro MicroFlow® 96 Well Plate Format" from Litron Laboratiries with the exception of the used DNA dye. Instead DAPI was used of the SYTOX® Green nucleic acid stain. The cytometer set-up conditions are described in the manual and measured were 75 µl volume of each sample with the MACSQant from Miltenyi. The cell cycle histogram of DAPI stained cells was used to identify the G1 cell cycle fraction and a gated were all events starting from $1/100^{th}$ of the G1 peak and encompassing all nuclei in any of the cell cycle phases. The Events $1/100^{th}$ of the G1 peak are considered MN.

The following clean up steps of the measured data as described in the manual was done over the FACSs software FLOWJOW (like exclusion of duplets, and cell fragments). The cell cycle was measured at the same time under the same conditions as the MN and samples that counted less than 5000 nuclei were excluded from further analysis.

3.2.7.4 UV-sensitivity survival

For the determination of UVC sensitivity the cells were seeded 50 % confluence in 2 ml of medium a 35 mm diameter dish. 24 h after seeding the medium was aspirated and the cells were washed with 1x PBS and irradiated without liquid at 0, 2, 5, 10 and 15 J/m^2 (254 nm; 15 W UVC Lamp G15-T18 Philips). The medium was added back to the cells and the surviving cells were counted after 72 h with the Backman-Coulter cell counter.

3.3 SiRNA transfection for protein knock-down

siRNA transfections were done in 6-well plates with 200 000 cells per well independent of the cell line. Following the seeding, the next day, the medium of the cells was changed to 1 ml of OptiMEM (Gibco™ Thermo fisher cat.no. 31985062).

In two 1.5 ml tubes the transfection solutions were prepared separately for the siRNA and for the lipofectamine. For the siRNA 30 pmol (3 µl of a 10 µM stock) of siRNA in 150 µl OptiMEM per well were mixed and in the other 1.5 ml tube 9 µl of lipofectamine in 150 µl OptiMEM (RNAiMAX Invitrogen) per well were mixed.

The solutions were incubated for 1 min at room temperature before they were pipetted together as a mixture and incubated for 5 min at room temperature before 300 µl of the mixture was added to the cells and incubated 16 h at 37 °C before the medium was changed to normal DMEM cell culture medium.

Table 22 lists all used siRNA sequences in the CCA.

Table 22: siRNA sequences for silenced genes

Gene	sequence 5' - 3'	Supplier
ATM	AACAUACUACUCAAAGACAUU	merck
ATM_as	AAUGUCUUUGAGUAGUAUGUU	merck
BRCA1	GUGGGUGUUGGACAGUGUA	sigma
BRCA1_as	UACACUGUCCAACACCCAC	sigma
BRCA2	GGAUUAUACAUAUUUCGCA	sigma
BRCA2_as	UGCGAAAUAUGUAUAAUCC	sigma
FANCA	AAGGGUCAAGAGGGAAAAAUA	sigma
FANCA_as	UAUUUUUCCCUCUUGACCCUU	sigma
FANCD2	esiRNA	sigma
Luciferase	CGUACGCGGAAUACUUCGA	sigma
Luciferase_as	UCGAAGUAUUCCGCGUACG	sigma
MLH1	AACUGUUCUACCAGAUACUCAUU	sigma
MLH1_as	AAUGAGUAUCUGGUAGAACAGUU	sigma

3.4 Cytometer based Colour Competition Assay (CCA)

3.4.1 Set up conditions and controls

At first the population doubling time was established for the U2OS conU2, FANCA and FANCD2 as well as for cell line RPE1 by seeding 20 000 cell in a 6 well-plate and counting cells for time points 24 h, 48 h, 72 h, 96 h and 120 h to calculate the doubling time.

For conU2 and FANCA KO mutant the doubling time was 24 h independent, the doubling time for FANCD2 KO was 25 h with this knowledge the incubation time for measuring the CCA was decided to be at least 5 days, meaning that the cells went through at least 4 cells cycles after treatment.

On day one the cells were seeded 200 000 cells per well (in a 6-well plate) in total and while 100 000 cells were the NT GFP control and the other half was from the same background but carrying the NT tRFP protein. On day two the cells were treated with Diepoxibutane (DEB;

cat.no 202533-16 sigma), Olaparib (cat.no S1060 selleckchem) siRNA or shRNA on day three the medium was changed for lentiviral transduced shRNA to 1 µg/ml puromycin containing DMEM medium and for siRNA as described in the anterior chapter.

On day nine the cells were measured. For longer cultures only 100 000 cells were seeded as a standard, if the cells grew confluent before measurement they were passed to a 25 cm^2 flask.

To find the most complete inhibition for each shRNA the a kinetic experiment was carried out for the following time points and seeding volume 24 h; 800 000 cells, 48 h; 600 000 cells, 72 h; 500 000 cells, four days 400 000 cell, six days 400 000 cells, eight days 200 000 cells, ten days 200 000 cells, 12 days 100 000 cells and 14 days 100 000 cells. The inhibition was visualized by immunoblot detection (see table 15 for antibodies).

As proof of concept for the CCA already published SL interactions between BRCA1/2 and Olaparib, shFEN1 or PARP1 KO and siBRCA1 and between the Fanconi pathway proteins and siATM were used.

3.4.2 Set up of cell lines with parental control cell line

For KO cell lines that were created form a parental cell line, like U2OS clone FANCA, FANCD2 and PARP1 this parental cell line U2OS Cas9 was transduced with plasmid (pLKO5.sgNT.EFS.tRFP) coding for a red fluorescent protein (tRFP) this created cell line was used as control (conU2). conU2 or RPE1 Cas9 tRFP cells (control cell line for RPE1 Cas9 FANCA KO GFP) were mixed 1:1 with the KO cells before seeding. 50 000 cells/colour in the 6-well plate which makes in total 100 000 cells in one 6-well plate well.

On day two the cells were treated according to the protocol of siRNA or shRNA virus particle above, control cells were treated with shNT. On day three the medium was changed for the cells transduced with the lentivirus particle to a selection medium containing 1 µg/ml Puromycin, for the siRNA to cell culture medium (see table 1 for culture medium of different cell lines).

For the cytometer measurement the cells were trypsinized and collected in 1x PBS with 2.5 % of fetal bovine serum (FBS, serum) the total volume of the sample was 1 ml and the samples were kept in the dark until measurement with one of the following flow cytometer: FACSCanto

(BD Biosciences), MACSQuant® Analyzer 10 Flow Cytometer or MACSQuant® VYB Flow Cytometer.

3.4.3 Set up of cell lines without a parental control cell line

For cell lines that had no parental or complemented control, first the cell lines were transduced with the pLKO5.sgNT.EFS.GFP or pLKO5.sgNT.EFS.tRFP plasmid to express GFP or the tRFP fluorescent marker.

Instead of mixing the two cell lines beforehand, they were seeded separately and treated on day two, the tRFP expressing cell line with NT shRNA and the GFP expressing cell line with a target shRNA, on day three they were detached and mixed 1:1 before they were seeded in one well with selection medium. The measurement was according to chapter 3.2.3.2

If the cells were treated additionally with a drug this was done on day three with the change of the medium, treatment with DEB was incubated with the cells until measurement at the cytometer.

3.4.4 Colour competition assay with inhibitors

For studies with inhibitors 200 000 cells in total in a 6-well plate were grown overnight and treated the with the inhibitor for 24 h bevor the medium was changed to normal cell culture medium. The cells were measured after five days of growth with the inhibitor (FEN1 inhibitor: LNT1 Tocris Cat.No. 6510 and XPF inhibitor: NSC16168, MCE Cat.No. HY-100690)

3.4.5 Set up of cell liens without selection marker

For the siRNA transfection were selection marker are not possible non-independent replicates in 96-well plates were chosen to be useed to homogenise the results.

The cells were treated as described in the chapter above cells without parental cell line but instead of growing the cells after the siRNA treatment in the 6-well plates they were seeded as

12 non-independent replicates in a 96-well plate 1000 cells/colour. The MACSQuant® Analyzer 10 Flow Cytometer and MACSQuant® VYB Flow Cytometer are adaptable for measurements in 96-well plates.

The resulting data was screened for outlyer as described in the SRB survival after calculating the percentage of tRFP and GFP expressing cells.

3.4.6 Cytometer measurement and data analysis of the CCA

The measured cells were plotted as function of SSC-A vs the FSC-A and the living cell population was selected, this population was then plotted on FSC-H vs FSC-A to see population's distribution of size to eliminate duplets. The single cells were than plotted as a function of PE-A (recognizes the tRFP) and FITC-A (recognises the GFP) to see distinct populations in with tRFP, GPF or without colour. For each sample 10 000 events of single cells were gated.

The combined amount of tRFP positive cells and GFP positive cells were set to 100 % and the percentage of red and green expressing populations were calculated. Form this the fold increase to the shNT or untreated control was used to plot the results.

For the plotting the GraphPad software was used and the mean as well as the standard deviation (SD) or standard error of the mean (SEM) of the repeats was calculated by the software. We tested for statistical significance between control cell line and the KO mutant by first testing for a parametric distribution of the data as suggested by the software with D'Agostino-Pearson omnibus normality test as well as with the Kolmogorov-Smirnov test with Dallal-Wilkinson-Lillifor P-value provided by the programme. If a normality distribution was confirmed the unpaired t-test with a significance level of <0.05 was applied. If there results were non parametric the unpaired Mann-Whitney test was executed as suggested by the GraphPad software.

4 Results and Discussion

4.1 Establishing of the U2OS knock-out cell lines with the CRISPR/Cas9 method

4.1.1 Expression of Cas9 and fluorescence proteins

The purpose of this thesis was to find new synthetic lethal or viable interactions of FA proteins with other DNA repair pathways. FANCA is a protein of the FA core-complex that monoubiquitinates the ID2-complex, it is also the most commonly mutated FA protein. The monoubiquitination of the ID2-complex is an essential step for recruiting the downstream proteins to repair damage, both proteins, FANCA and FANCD2, have a central function in the pathway, for that reason generating knock-down cells of these two genes was accomplished through the CRISPR/Cas9 system.

The first step for establishing a KO cell line with the CRISPR/Cas9 system is the introduction of the Cas9 enzyme into the chosen cell line. The addgene plasmid lentiCas9-Blast is carrying the Cas9 nuclease and the selection marker blasticidin. The cells were transduced with lentiviral particles and selected with blasticidin for one week. The expression of Cas9 was confirmed by western blot (WB). Figure 10 shows a WB of U2OS cells that are either not transduced with the lentiCas9-Blast plasmid (Figure 10 pocket one) or transduced (figure 10 pocket two and three) with Cas9 an additional fibroblast control cell line PN (figure 10 pocket three)was also transduced.

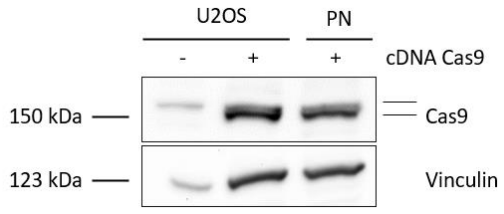

Figure 10: ***Western blot of Cas9 expression****; 10 % PAA gel with antibodies against Cas9 and loading control Vinculin; first pocket: U2OS cells not transduced with the lentiCas9-blast plasmid carrying the Cas9, second pocket: U2OS cells transduced with lentiCas9-blast, third pocket: fibroblast cell line PN transduced with lentiCas9-blast*

In the transduced cell lines there are two bands at the molecular weight of Cas9 (150 kDa) while there is only one band in the control cell line. The untranduced U2OS cells are clearly missing

the second band which is positioned slightly lower on the membrane leading to the conclusion that the second band on the blot, which is only present in the two transduced cell lines, is the Cas9 protein. Therefore, the cell pool was transduced with the second plasmid (pLKO5) that carries the sgRNA and GPF or in the case of the control, the non-targeting sgRNA (sgNT) and the tRFP.

The fluorescence of the cell lines was first confirmed by microscopy (figure 11) before they were sorted by FACS and regrown for single cell clones.

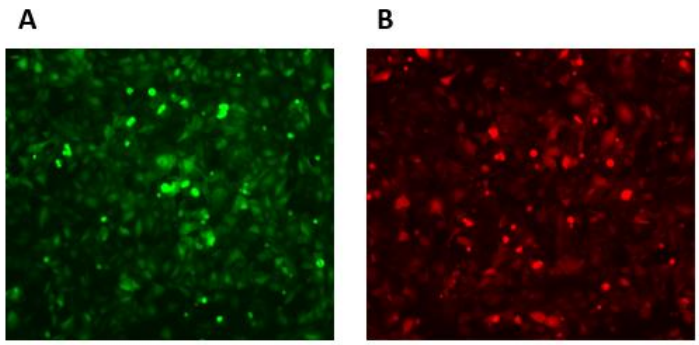

Figure 11: ***Control of pLKO5 transduction in U2OS Cas9 cells by fluorescent microscopy;*** *10x Magnitude, 72 h after transduction A: U2OS Cas9 + pLKO5.sgFANCA.GFP, B: U2OS Cas9 + pLKO5.sgNT.tRFP*

The detection of the red fluorescent protein was possible over the PE detector of the cytometer. The cell line U2OS Cas9 + pLKO5.sgNT.tRFP will be call conU2 from here on and serves as a control to U2OS FANCA KO, U2OS FANCD2 KO and U2OS PARP1 KO cells.

4.1.2 Characterisation of the FANCA KO clone

After the transduction of the sgRNA and the single cell cloning, the expression of a chosen FANCA clone was visualized on a WB (figure 12 A). As mentioned before, the main function of the FA core complex, which FANCA is part of, is the monoubiquitination of the ID2-complex. FANCA KO patient cells are incapable of monoubiquitinating of FANCD2. This deficiency can be visualized by WB through which it is possible to detect monoubiquitinated FANCD2 as well as the unmodified protein in healthy controls. This is what can be seen in conU2 cells in figure 12

B, it shows two bands at 164 kDa and approximately 172 kDa for FANCD2, the monoubiquitinated form is exactly 8.6 kDa heavier than the unmodified one.

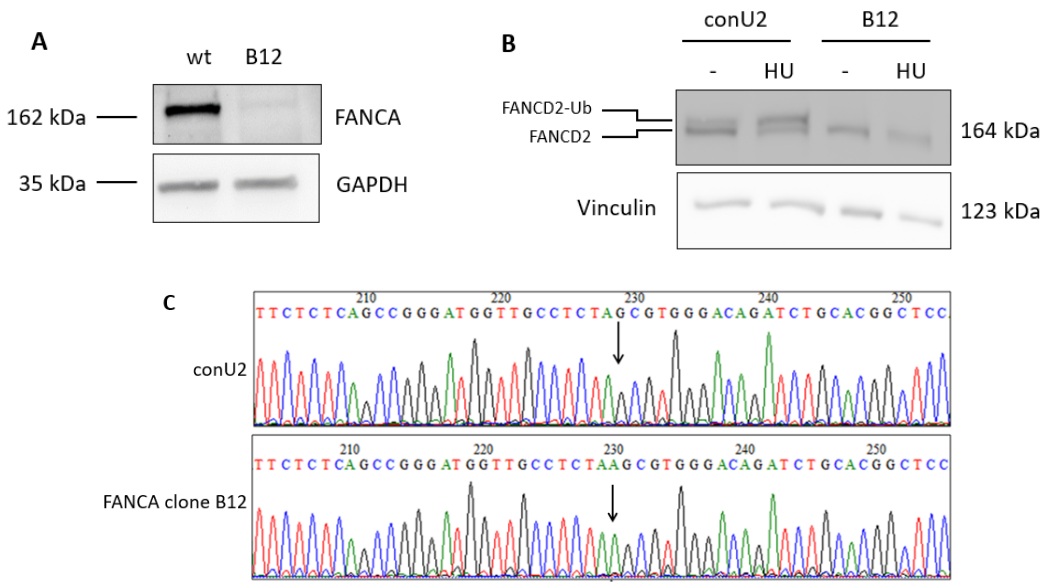

Figure 12: Characterisation of FANCA KO clone B12, A: ***WB of FANCA expression****; 7.5 % PAA gel, FANCA antibody and GAPDH loading control, pocket left conU2, right pocket U2OS Cas9 + pLKP5.sgFANCA.GFP clone B12; B:* ***WB of FANCD2 monoubiquitination****: 10 % PAA gel FANCD2 primary antibody and loading control Vinculin, pockets one and two conU2 without HU treatment and with 2 mM HU, pockets three and four U2OS Cas9 FANCA clone B12 without and with 2 mM HU treatment; C:* ***Sequence of FANCA KO clone B12****; reference sequence top and clone sequence bottom, arrows indicate the mutation position*

The treatment of hydroxyurea (HU) mimics replication fork stalling at ICLs and induces an increase in FANCD2 monoubiquitination. The conU2 cells exhibit the behaviour of healthy cells, when unchallenged there is only a faint band for monoubuquitinated FANCD2 but with the HU treatment the FANCD2 ubiquitination increases. In the FANCA KO clone on the other hand, there is no second band, independent of HU treatment. This is seen in patient cells with mutations in the core complex proteins and what would be expected of a FANCA KO clone.

The sequencing of U2OS FANCA KO clone B12 for mutation characterization showed a homozygote insertion of an adenine c.358_359insA resulting in frame shift and subsequent stop codon (p.S120Kfs*61) (Figure 12 C). Further prove of the creation of a FANCA KO clone provided the molecular phenotype of sensitivity to DEB and Olaparib (figure 13), as well as the induced chromosome fragility and the stalling of FA cells at G_2/M cell cycle checkpoint (figure 13 A and B).

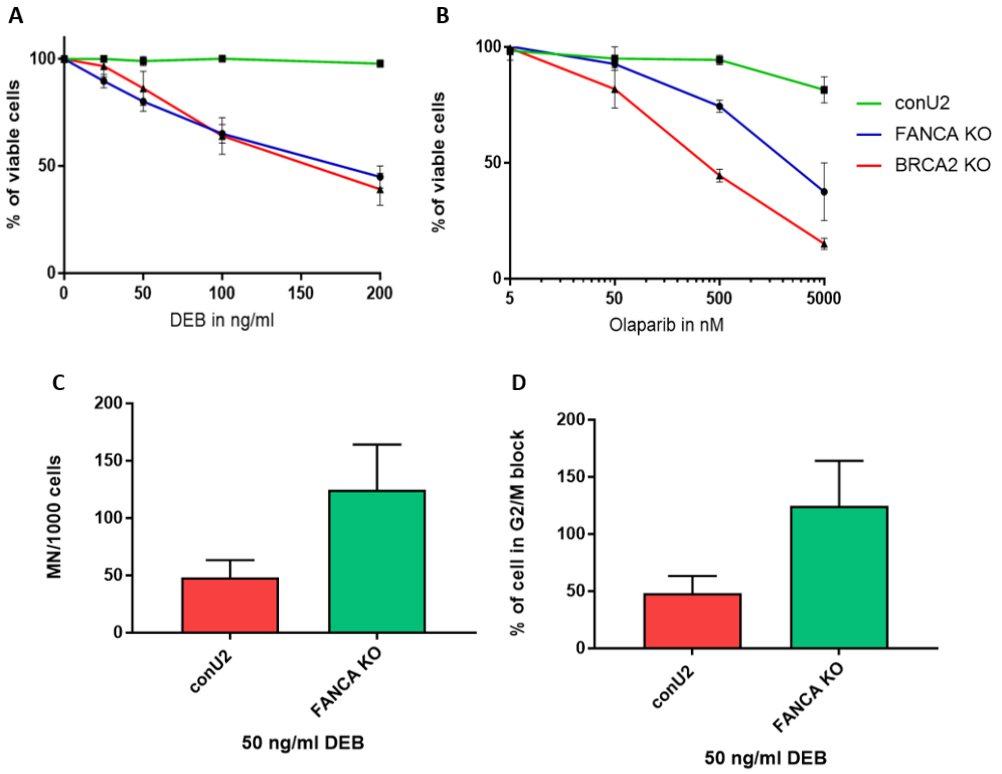

Figure 13: Functional assays for characterisation of the U2OS Cas9 FANCA KO clone B12 phenotype, A and B: ***SRB survival assays of FANCA KO clone B12 with SD****; in green U2OS Cas9 pLKO5.sgNT.tRFP, in red HEK BRCA2 KO as sensitivity control, in blue U2OS Cas9 FANCA KO clone B12, left survival with increasing doses of DEB, right survival with increasing doses of Olaparib, D and D:* ***Chromosome fragility measure by MN and G_2M block with SD****; left MN/1000 cells of conU2 compared to U2OS Cas9 FANCA clone B12 treated with 50 ng/ml DEB, right G_2M-block conU2 and U2OS Cas9 FANCA clone B12 with 50 ng/ml DEB treatment*

FA cells are highly sensitive to ICL including agents, in contrast, cells proficient for the FA pathway like conU2 are very little effected by DEB. The created U2OS FANCA KO cell line was challenged with DEB in a SRB survival assay (figure 13 A): the conU2 cell line (green) does not show sensitivity to DEB, in red is the HEK BRCA2 KO cell line used as a positive control since BRCA2 KO cells are highly sensitive to DEB. The U2OS FANCA KO cell line (in blue) demonstrates a high sensitivity to DEB, showing the expected behaviour of a FA cell line while the conU2 cells are unaffected.

FA upstream cells are moderately sensitive to Olaparib treatment and this is demonstrated in figure 13 B were the U2OS FANCA KO survival lies between the unaffected conU2 and the highly sensitive HEK BRCA2 KO.

Spontaneous and induced chromosome fragility is a hallmark of FA molecular phenotype and is demonstrated for the generated FANCA KO clone in figure 13 C though the MN analysis of the FANCA KO compared to the conU2 with 50 ng/ml DEB treatment. The same is valid for the G_2/M cell cycle arrest in FA cells, shown in figure 13 D in the graph. Overall, the experiments demonstrated the creation of a stable FANCA KO cell line that is expressing GFP and behaves like expected of a FA cell line.

4.1.3 Characterisation of the FANCD2 KO clone

One of the U2OS FANCD2 KO clones was not showing protein on the WB at the size of 164 kDa (figure 14) and this clone, U2OS FANCD2 KO clone C9, was selected for sanger sequencing. The PCR showed a homozygote insertion of approximately 200 bp (figure 14 B)

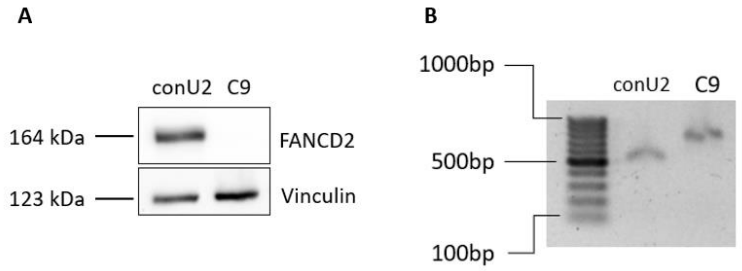

Figure 14: Identification of a U2OS Cas9 FANCD2 KO clone C9, A: ***WB of FANCD2 expression****; 7.5 % PAA gel FANCD2 antibody and Vinculin loading control, left pocket: conU2, right pocket: U2OS Cas9 FAND2 clone C9, B:* ***SDS-PAGE of PCR FANCD2 Exon 11****; 0.8 % Agarose gel of FANCD2 Exon 11 PCR with primer from table 16, left pocket: conU2 with expected fragment size of 570 nt, right pocket: U2OS Cas9 FANCD2 clone C9 with one band at approximately 200 nt bigger*

The sanger sequencing than revealed a deletion of 5 nucleotides and at the same position as the insertion of 238 nt resulting in a frame shift and a pre-mature stop codon (p.L295Mfs*3) (c.883_888delinsATGACTTGAGAAAATCATTTATTAGAGTATGAAAATAAAGGACATACTTAGTTG CCATTAAGTTACCGTTTATAGTATGTTTCTTTAAAAATTGTTTTGACTGCAAAAAATAATACATGC TCATTATAAAAATTCAAATAATAAAAGTAGAAACAAGAAGCCTTCCATCACAATCCCCACTACCCA GAGAACACCACTATTTAGTTTGGTATGTATCCTTCCCCGCAAAAAGGAAAAA).

The sensitivity to DEB and Olaparib was tested next. In figure 15 A and B are the graphs shown for the SRB survival with DEB or Olaparib treatment. The FANCD2 KO clone C9 (blue) exhibit a

high sensitivity comparable with the HEK BRCA2 KO cell line (red), this HEK BRCA2 KO cell line serves as a positive control for DEB and Olaparib sensitivity. In contrast, the conU2 cell line does not show any sensitivity.

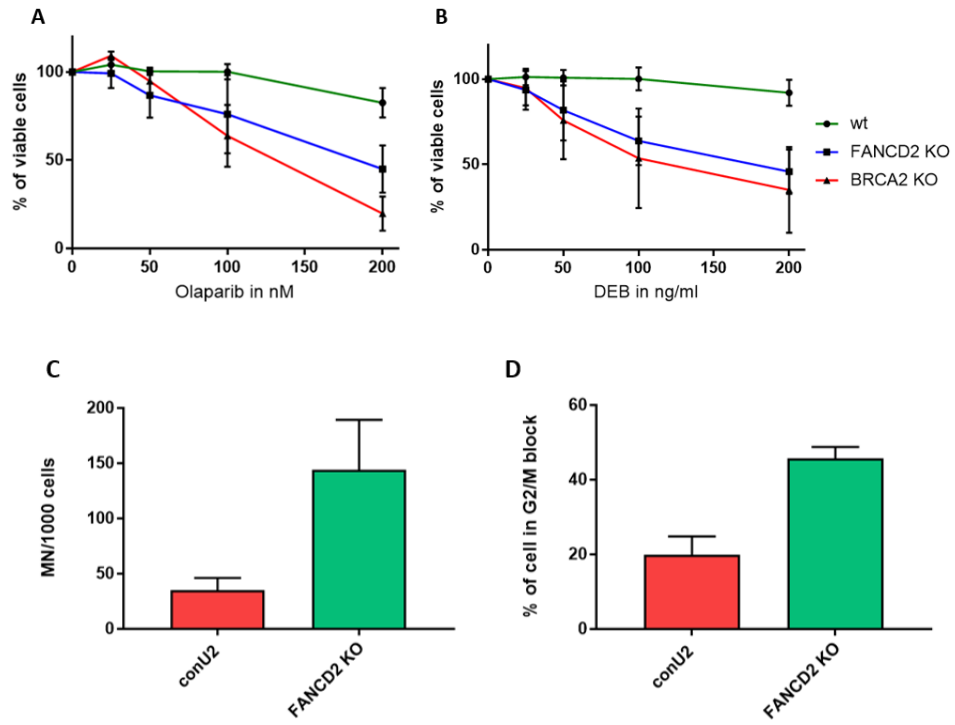

Figure 15: Characterisation of U2OS FANCA KO clone C9, A and B: ***SRB survival assays of FANCD2 KO clone C9 with SD****; in green conU2, in red HEK BRCA2 KO as sensitivity control, in blue U2OS Cas9 FANCD2 KO clone C9, left survival with increasing doses of DEB, right survival with increasing doses of Olaparib, C and D:* ***Chromosome fragility measure by MN and G_2M block with SD****; left MN/1000 cells of conU2 compared to U2OS Cas9 FANCD2 clone C9 treated with 50 ng/ml DEB, right G_2M-block conU2 and U2OS Cas9 FANCD2 clone C9 with 50 ng/ml DEB treatment*

In figure 15 B the graph, which depicts the sensitivity to Olaparib is shown, conU2 does not experience sensitivity compared to HEK BRCA2 KO and U2OS FANCD2 KO as already seen in the FANCA KO clone. This proves the chemosensitivity of U2OS FANCD2 KO clone C9 to Olaparib and is in accordance with the FA molecular phenotype.

Regarding the chromosome fragility of the U2OS FANCD2 KO clone C9 it is, as expected, more than the double of the conU2 at 50 ng/ml DEB dose (Figure 15 C) and the G_2/M-block of the FANCD2 KO cells is very high compared to the control. Summing up we conclude, that the produced cell line demonstrates typical FA molecular phenotypes.

4.1.4 Characterisation of the PARP1 KO clone

Among the clones generated using the sgRNA for *PARP1*, clone A3 in figure 16 was investigated further. The WB of PARP1 did not show expression of the protein (figure 16 A). The sanger sequencing (figure 16 B) revealed a homozygote insertion of adenine at position cDNA.188_189insA resulting in a frame shift and a premature stop codon (S16Efs*30).

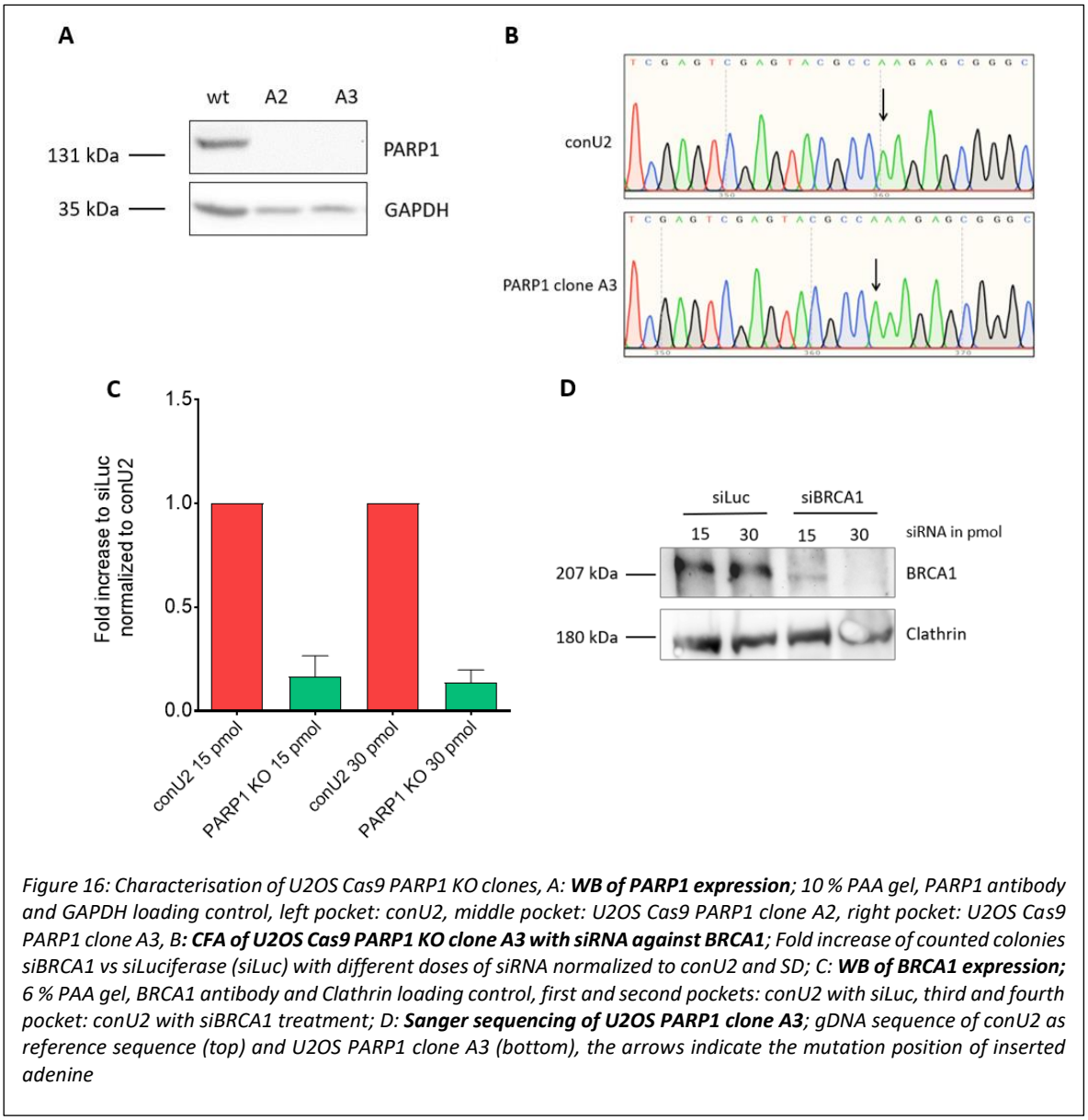

Figure 16: Characterisation of U2OS Cas9 PARP1 KO clones, A: ***WB of PARP1 expression****; 10 % PAA gel, PARP1 antibody and GAPDH loading control, left pocket: conU2, middle pocket: U2OS Cas9 PARP1 clone A2, right pocket: U2OS Cas9 PARP1 clone A3, B****: CFA of U2OS Cas9 PARP1 KO clone A3 with siRNA against BRCA1****; Fold increase of counted colonies siBRCA1 vs siLuciferase (siLuc) with different doses of siRNA normalized to conU2 and SD; C:* ***WB of BRCA1 expression;*** *6 % PAA gel, BRCA1 antibody and Clathrin loading control, first and second pockets: conU2 with siLuc, third and fourth pocket: conU2 with siBRCA1 treatment; D:* ***Sanger sequencing of U2OS PARP1 clone A3****; gDNA sequence of conU2 as reference sequence (top) and U2OS PARP1 clone A3 (bottom), the arrows indicate the mutation position of inserted adenine*

The described synthetic lethality of PARP1 with BRCA1 was used to functionally test the U2OS Cas9 PARP1 clone A3 with a Colony Forming Assay (CFA). The CFA could confirm the synthetic lethality of U2OS Cas9 PARP1 KO clone A3 with siBRCA treatment in a dose dependent manner (figure 16 C) and together with the data from the sanger sequencing, the PARP1 WB and the synthetic lethality, this leads to the conclusion that the created clone is indeed a PARP1 KO clone.

For this work, U2OS BRCA1 KO clones were tried to be established with the CRISPR/Cas9 system and a sgRNA published [182], stating that it successfully generated a BRCA1 KO clone with the mentioned sequence. In the frame of this thesis it was not possible to obtain BRCA1 KO clones even using two other sgRNAs or combinations of more than one sgRNA, generated by the BreakingCas web tool.

4.2 Theory of Colour competition assay

On of the objectives of this thesis was to establish a method to test for synthetic lethal or viable interactions with FA proteins. The theory based on which the CCA functions is the growth advantage that either cells with synthetic viability over healthy cells have over synthetic lethal combinations.

In this system, different types of control cells were used depending on the cell line. Either the parental cell line, from which the clones were created was used by transducing it with pLKO5.sgNT.EFS.tRFP or pLKO5.sgNT.EFS.GFP carrying a non-targeting shRNA depending if the KO counterpart was marked with GFP or tRFP. Thus, the cells were mixed and treated with shRNA or siRNA or inhibitor at the same time. The second control was for cell lines without a Wt control like the LoVo and HCT116 cell line. In that case, a tRFP and a GFP expressing cell line was generated and tRFP expressing cells were treated with shNT or siLuc (non-targeting controls) while the GFP expressing cells were treated with shRNA or siRNA for the target gene.

A synthetic lethal interaction would result in the reduction of the GFP expressing cell line compared to the red control and for a synthetic viable interaction an increase the GFP expressing cell line would be seen compared to the red control.

4.3 Searching for synthetic lethality or viability with the cytometer based colour competition assay between FA and different DNA repair pathways

4.3.1 Colour competition assay proof of principle and synthetic lethality controls

Preliminary experiments were run to avoid facing unforeseen interactions or growth differences and to see how accurate cell counting is and what impact it has on the cytometer measurement between conU2 and U2OS Cas9 sgNT.GFP. The cell counting was very accurate with a near 1:1 distribution of conU2 to U2OS Cas9 sgNT.GFP when measured directly after seeding. This distribution was kept over the measured time span of five days. However, longer cultures showed a small growth deficit in cells expressing the tRFP protein compared to the ones carrying the GFP. In order to keep this difference small, tRFP expressing cells were used exclusively for controls while mutants or cells treated with shRNA silencing a gene, expressed the GFP.

After the basic assessment the previously confirmed synthetic lethality between the established U2OS PARP1 KO and the siRNA against BRCA1 was chosen as proof of principle for the colour competition assay (CCA). In the previous chapter a CFA confirmed the PARP1 synthetic lethal interaction with BRCA1 to prove the creation of a PARP1 KO clone. Now this synthetic lethal interaction should be reflected in the CCA (figure 17).

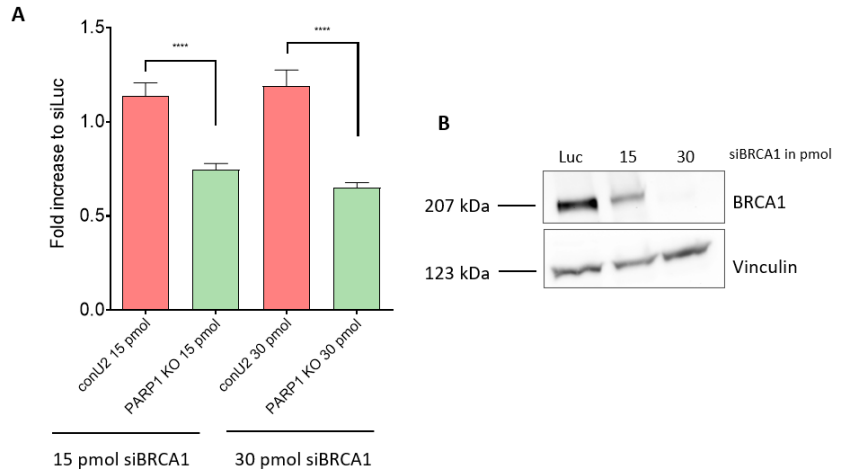

Figure 17: Proof of principle experiment with the CCA A: ***CCA of conU2 vs U2OS PARP1 KO clone A3 with siBRCA1 treatment****; fold increase of siBRCA1 to siLuc with increasing doses of siBRCA1, plotted are five independent experiments, error bars show SD and significant was calculated for an unpaired student t test, B:* ***WB control of conU2 vs U2OS Cas9 PARP1 KO clone A3 siBRCA1 inhibition****; 6 % PAA gel with antibody against BRCA1 and loading control vinculin, left pocket: conU2 vs U2OS Cas9 PARP1 KO clone A3 treated with siLuc as control, middle pocket: conU2 vs U2OS Cas9 PARP1 KO clone A3 treated with 15 pmol of siBRCA1, right pocket: conU2 vs U2OS Cas9 PARP1 KO clone A3 treated with 30 pmol of siBRCA1*

In figure 17 the synthetic lethality of U2OS PARP1 KO cells with siRNA for BRCA1 is confirmed with a reduction of the fold increase of the PARP1 KO to conU2 in a dose dependent manner. This experiment is proofing that the CCA method can detect synthetic lethality. There is a difference in sensitivity between the CFA and the CCA (figure 17) but nevertheless the CCA shows a significant reduction of measured U2OS Cas9 PARP1 KO cells after siBRCA1 treatment.

After proofing that the CCA can reproduce the synthetic lethality of an interaction that was seen before in the CFA, two more published, synthetic lethal interactions were tested. One is the known synthetic lethal interactions of ATM in a FA background [152] and the other is the SL of BRCA2 KO with FEN1 [167].

In figure 18 the CCA of conU2 versus FANCD2 KO is plotted as fold increase to siLuc and the ratio of tRFP to GFP positive cells was measured at different times of growth. This was done to establish the time when the CCA is most sensitive in measuring the SL.

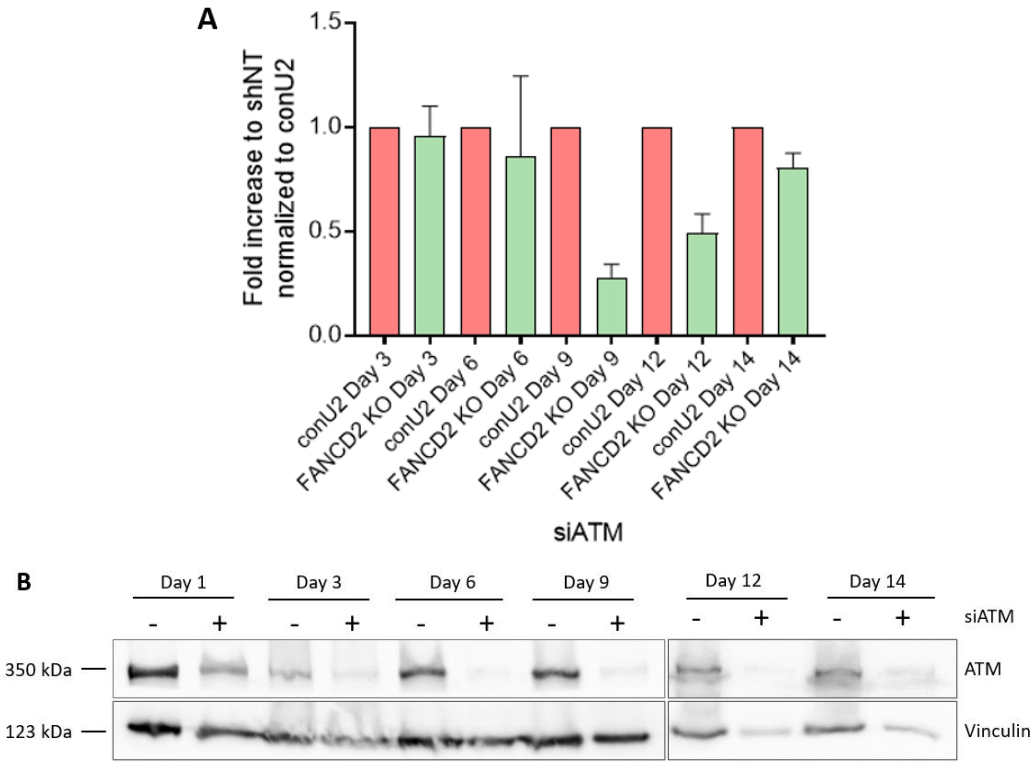

Figure 18: CCA of the published interaction FANCD2 with ATM to determine the time for measurement, A: ***CCA of synthetic lethality control U2OS Cas9 FANCD2 KO clone C9 and siATM;*** *CCA of conU2 vs U2OS Cas9 FANCD2 KO clone C9 with treatment of siATM measurement at different time points after siRNA silencing of ATM with 30 pmol shown as fold increase to siLuc, the error bars are showing SD of two independent repeats; B:* ***WB expression of ATM after siATM treatment****: 6 % PAA gel with antibody against ATM and loading control Vinculin of U2OS Cas9 FANCD2 KO clone C9 and siATM treatment; the placeholder sign indicate that the sample was treated with siLuc and the plus indicate the treatment with 30 pmol siATM*

As shown in figure 18 A the CCA is the most sensitive at day nine and its sensitivity is slowly decreasing from that point on. The loss of sensitivity is probably due to the silencing of the shRNA which occurs naturally by mutating the shRNA sequence. This silencing is also visible in the western blot in figure 18 B, where starting from day six up to day nine the inhibition of ATM expression, in comparison to the loading control, is the greatest. All further CCA experiments were measured at day nine.

In conclusion, the CCA was able recapitulate the SL described between FANCD2 and ATM. In a reverse experiment in fibroblast ATM KO patient derived cells treated with siRNA for FANCA

and FANCD2 cells exhibited a decrease in growth reminiscent of the SL seen in figure 18 (Annex 1).

Another described SL is the interaction between BRCA2 and FEN1 [167]. In figure 19 A, the CCA was tested for its ability to detect this interaction in HEK BRCA2 KO cells with shRNA inhibition of FEN1. The greatest difference in ratio between the control HEK tRFP and HEK BRCA2 KO GFP cell line is again at day nine. The shortest growing time, that had still the greatest difference between control and KO was chosen, which in this case was also at day nine.

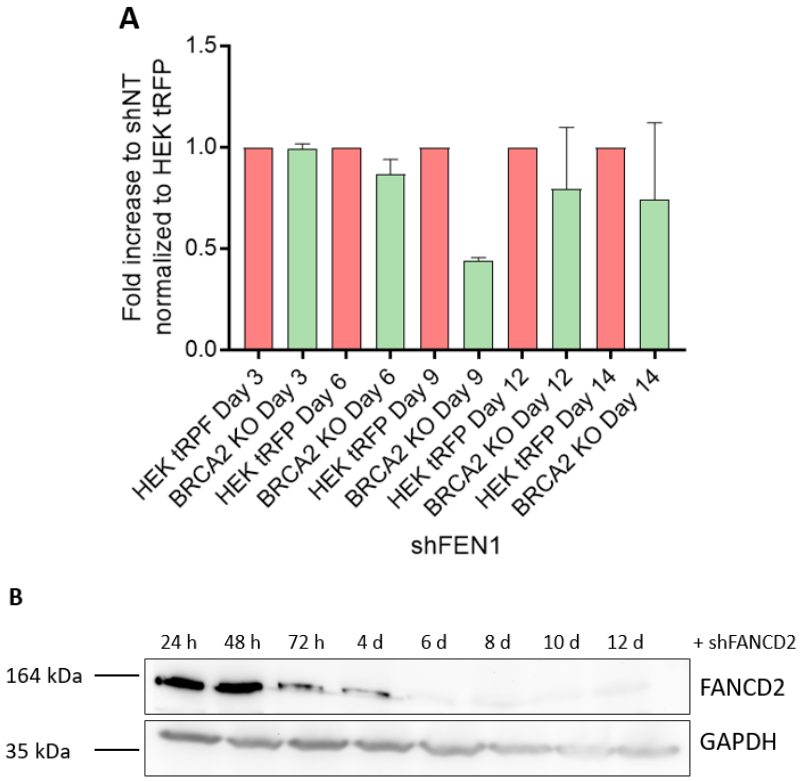

Figure 19: CCA of the published interaction BRCA2KO with FEN1 to determine the time for measurement, A: ***CCA of HEK tRFP vs HEK BRCA2 KO GFP and shFEN1 treatment;*** *CCA of HEK tRFP vs HEK BRCA2 KO GFP with treatment of shFEN1 measurement at different time points three independent repeats plotted as fold increase to shNT, error bars are showing SD, B:* ***WB expression of FEN1 after shFEN1 treatment****: 10 % PAA gel with antibody against FEN1 and loading control Vinculin of HEK tRFP vs HEK BRCA2 KO GFP with shFEN1 treatment*

After being able to establish the sensitivity of the system with shRNA and siRNA the next step was to proof that the CCA was able to detect the SL observed in BRCA1/2 KO cells when treated with the PARP1 inhibitor Olaparib. For this experiment a fibroblast control cell line PN and a fibroblast patient cell line for BRCA2 KO (figure 20 A) was used.

The CCA was able to detect a dose dependent sensitivity to Olaparib in the BRCA2 deficient fibroblast cell line (Figure 20, B) and synthetic lethal behaviour with shFEN1 of the same fibroblast BRCA2 KO cell line as control (Figure 20, C). The HEK BRCA2 KO cell line also showed sensitivity to Olaparib but to a much lesser extend (Annex 2).

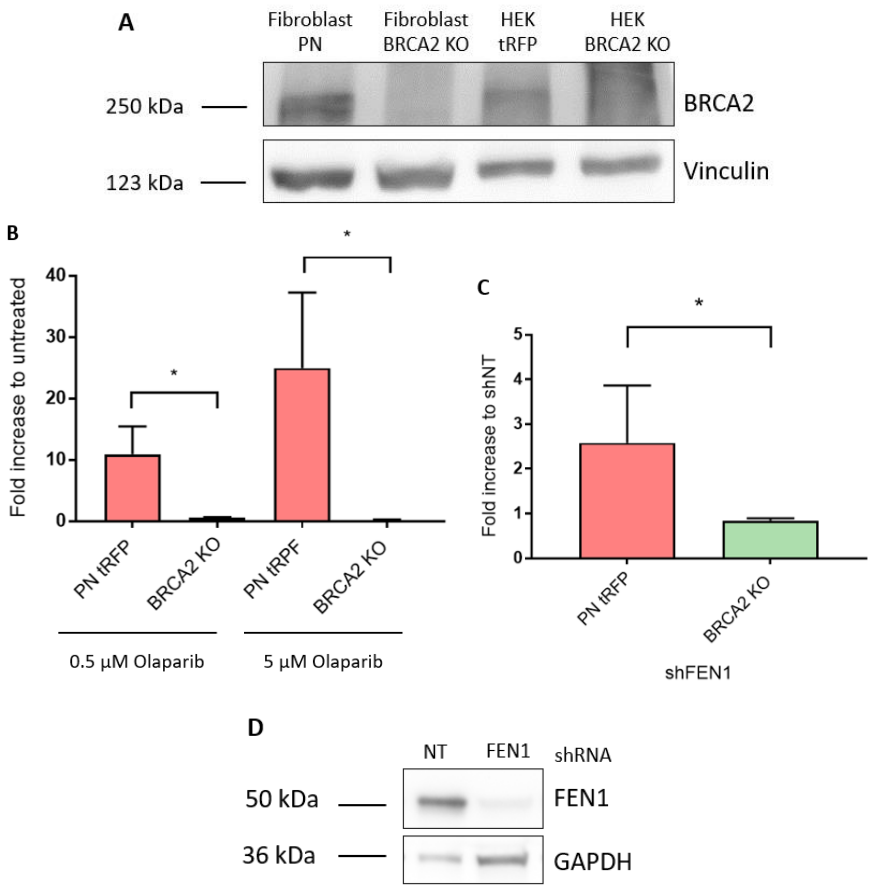

Figure 20: CCA proof of principle with PARP inhibitor Olaprarib and fibroblast BRCA2 KO, A: ***WB of BRCA2 expression;*** *6 % PAA gel with antibody against BRCA2 and loading control Vinculin, Pocket one: BRCA2 proficient Fibroblast cell line PN, Pocket two: Fibroblast BRCA2 KO GFP cell line, Pocket three: HEK tRFP cell line BRCA2 proficient, Pocket four: HEK BRCA2 KO GFP cell line, B:* ***CCA of PN tRFP vs Fibroblast BRCA2 KO GFP with Olaparib treatment;*** *CCA measured at day five, different concentrations of Olaparib and ratio of PN tRFP vs Fibroblast BRCA2 KO GFP of four independent experiments plotted as fold increase to untreated control, error bars show SEM, Significance of unpaired Mann-Whitney test, C:* ***CCA of PN tRFP vs Fibroblast BRCA2 KO GFP with shFEN1 treatment;*** *CCA measured at day nine, treatment with shFEN1 and ratio of PN tRFP vs Fibroblast BRCA2 KO GFP of four independent experiments, plotted as fold increase to shNT, error bars show SEM, Significance calculated with unpaired Mann-Whitney test, D:* ***WB of FEN1 expression in for CCA;*** *10 % PAA gel with antibody against FEN1 and loading control Vinculin, PN tRFP vs Fibroblast BRCA2 KO GFP treated with shRNA; Left Pocket: PN tRFP vs Fibroblast BRCA2 KO GFP treated with shNT;, Right Pocket: PN tRFP vs Fibroblast BRCA2 KO GFP treated with shFEN1*

In summary these results are proof of concept that the CCA was able to detect SL induced by shRNA, siRNA and with an inhibitor. It could recreate the synthetic lethality seen in the CFA as well as the described synthetic lethal interactions with ATM and FEN1.

4.3.2 Testing for synthetic lethality or viability between base excision repair and FA proteins

PARP1 is part of the BER pathway and its inhibition was shown to be synthetically lethal with BRCA1/2, which both are proteins in the downstream part or the FA pathway. This could hint to a synthetic lethality with other FA proteins. To assess if there is any synthetic lethality with upstream FA proteins or with the ID2-complex shRNA was used to test this hypothesis. FANCA is a component of the core-complex and the most frequently mutated FA complementation group as well as shRNA against FANCD2 which is part of the ID2-complex.

Figure 21 A shows the CCA for conU2 versus U2OS Cas9 PARP1 KO with shRNA treatment for FANCA, FANCD2 and PARP1 as an internal control. None of the shRNA treatments showed a difference between the ratio of conU2 and the PARP1 KO. In figure 21 B and C are the WBs of the targeted proteins are seen. The shRNA is down regulating the expression of both proteins, concluding that there is no synthetic lethal or viable interaction between FANCA and PARP1 and neither between FANCD2 and PARP1.

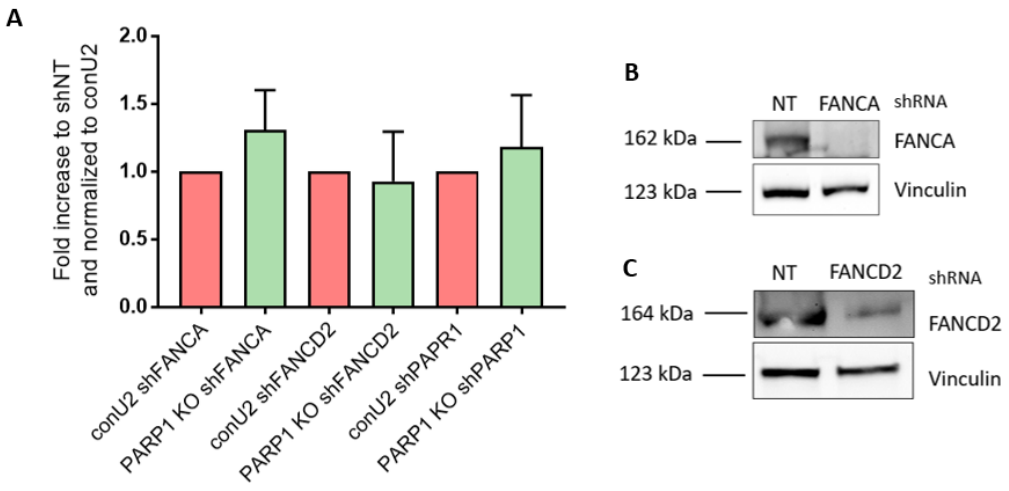

Figure 21:Testing for SL or synthetic viability with BER protein PARP1, A: ***CCA of conU2 vs U2OS Cas9 PARP1 KO clone A3 with shRNA treatment;*** *CCA of conU2 vs U2OS Cas9 PARP1 KO clone A3 treated with shRNA against either FANCA or FANCD2 the shPARP1 is used as an internal control plotted is the fold increase to shNT and normalized to conU2 of three independent repeats and error bars show SD; B and C:* ***WB control of FANCA and FANCD2 expression after shRNA treatment;*** *7.5 % PAA gel with antibody against either FANCA or FANCD2 and loading control vinculin NT indicates the shNT as control*

4.3.3 Testing for synthetic lethality or viability between mismatch repair and FA proteins

The commercially available cell lines LoVo and HCT116 are both from tumour origin of the colon and both have defects in the mismatch repair. LoVo cells are mutated for *MSH2* and HCT116 are deficient for the gene *MLH1*. Both cell lines have a high mutation frequency due to the deficiency in MMR which is, as discussed before, a proof reading mechanism to detect and replace mismatched bases in the DNA.

As there are no parental cell lines available, LoVo MSH2 KO tRFP expressing cells were used to transduce exclusively with shNT and then mixing it with a LoVo MSH2 KO GFP transduced with either shFANCA or shFANCD2. The results were normalized to a sample of LoVo MSH2 KO tRFP shNT vs LoVo MSH2 KO GFP shNT, the same was done for the HCT116 cell line. None of the experiments showed a synthetic lethal or viable interaction, while the WB control shows the silencing of the proteins (Figure 22).

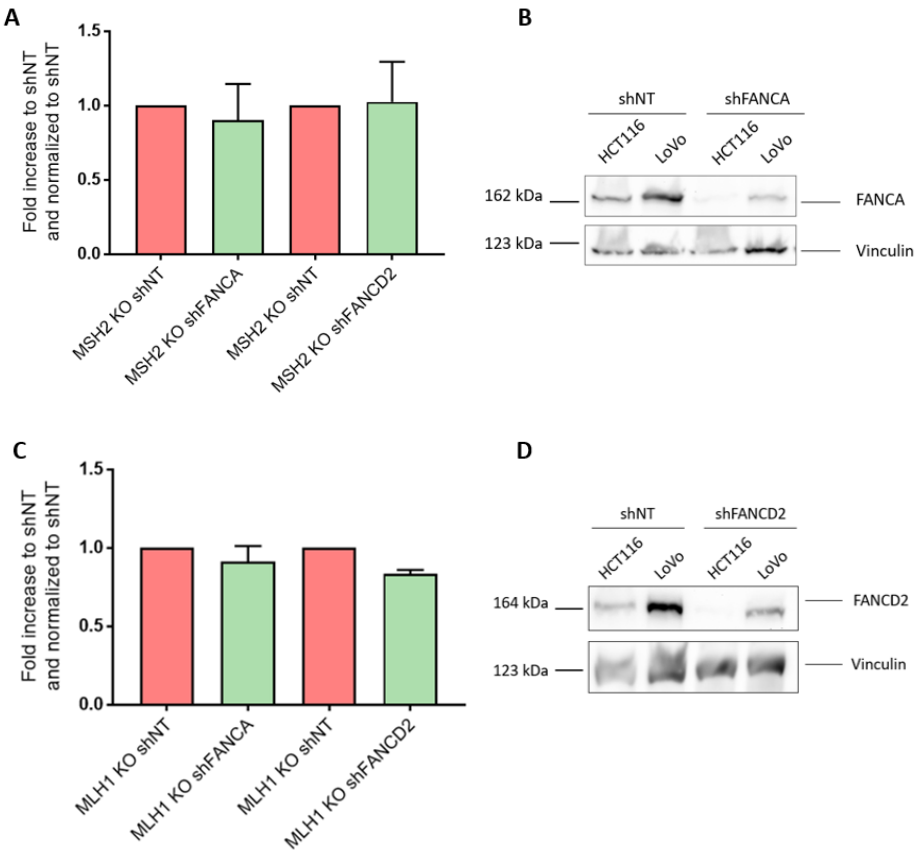

Figure 22: Testing for synthetic lethality or viability with the CCA in MMR deficient cell lines, A: ***CCA of LoVo MSH2 KO shNT vs LoVo MSH2 KO shRNA****; CCA with LoVo cell deficient for MSH2, MSH2 KO tRFP shNT vs MSH2 KO GFP shNT was used as control all sample ratios for tRFP and GFP positive cells are plotted as fold increases to this control, LoVo MSH2 KO tRFP shNT vs LoVo MSH2 KO GFP shRNA was either treated with shFANCA or shFANCD2, samples are normalized to the corresponding LoVo MSH2 KO tRFP shNT, error bars show SD of three independent repeat, B:* ***WB of FANCA expression in LoVo MSH2 KO cells and HCT116 MLH1 KO cells****; 7.5 % PAA gel with antibody against FANCA and loading control Vinculin, First Pocket: HCT116 MLH1 KO shNT, Second Pocket: LoVo MSH2 KO shNT, Third Pocket: HCT116 MLH1 KO shFANCA, Fourth Pocket: LoVo MSH2 KO shFANCA, C:* ***CCA of HCT116 MLH1 KO shNT vs HCT116 MLH1 KO shRNA****; CCA with HCT116 cells that are deficient for MLH1, the HCT116 MLH1 KO tRFP shNT vs HCT116 MLH1 KO GFP shNT was used as control all sample ratios for tRFP and GFP positive cells are plotted as fold increases to this control and are normalized to HCT116 MLH1 KO tRFP shNT samples were either treated with shFANCA or shFANCD2, error bars show SD of three independent repeats, D:* ***WB of FANCD2 expression in LoVo MSH2 KO cells and HCT116 MLH1 KO cells****; 7.5 % PAA gel with antibody against FANCD2 and loading control Vinculin, First Pocket: HCT116 MLH1 KO shNT, Second Pocket: LoVo MSH2 KO shNT, Third Pocket: HCT116 MLH1 KO shFANCD2, Fourth Pocket: LoVo MSH2 KO shFANCD2*

It is of note that the shRNA inhibition of FANCD2 in the HCT116 MLH1 KO background showed a slight reduction compared to the shNT treated cells, though not statistically significant (Figure 22 bottom). Interestingly embryonic lethality in mice between MLH1 and FANCD2 has been reported before [183]. Given that the reduction of tRFP to GFP ratio is very small and second, that the cell line is experiencing a huge mutation burden due to the mutator phenotype of the cell line and additionally that there is already a described embryonic lethality in mice between

MLH1 and FANCD2, it was decided to not investigate further as this work was focusing on finding new interactions.

4.3.4 Testing for synthetic lethality or viability between the nucleotide excision repair and FA proteins

As a representative of the NER pathway patient derived fibroblast XPA KO were employed and as control XPAcorr, which is the corrected patient cell line. These cell lines were already in our group and to prove that the XPA KO cell line is indeed experiencing XP characteristics as well as to proof that the control cell line was corrected, the cells were challenged with an UVC survival. The result can be seen in figure 23 A.

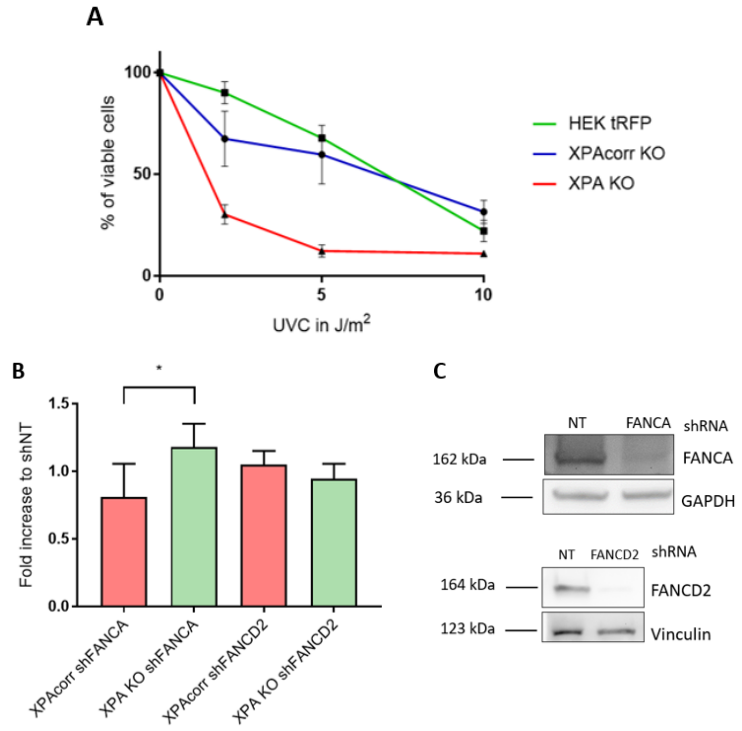

Figure 23: XPA KO and XPAcorr characterisation of UV-sensitivity and CCA testing for synthetic lethal or viable interactions with FA proteins, A: ***CCA of XPAcorr tRFP vs XPA KO GFP treated with shRNA;*** *CCA of XPAcorr tRFP vs XPA KO GFP treated either with shRNA for FANCA or FANCD2 platted is the fold increase to shNT at least three independent repeats are shown and error bars show SD and significance is calculated with an unpaired t test, B:* ***WB control of FANCA and FANCD2 expression after shRNA silencing;*** *10 % PAA gel with antibody against either FANCA or FANCD2 and loaing control for FANCA blot GAPDH and for the FANCD2 blot Vinculin, First pocket: XPAcorr tRFP vs XPA KO GFP shNT, Second pocket: XPAcorr tRFP vs XPA KO GFP treated for either shFANCA or shFANCD2, C:* ***UV-survival;*** *UVC doses 0, 2, 5, and 10 J/m², in green control HEK tRFP, in blue XPAcorr tRFP and in red XPA KO GFP in percentage of viable cells*

In green is a HEK tRFP cell line as control, the XPA KO in red and XPAcorr in blue. While the XPA KO cell line is highly photosensitive with a survival reduction of more than 50 % after 2 J/m^2, the complemented XPAcorr cell line behaves similar to the control and the survival of cells only drops under 50 % after the highest irradiation dose of 10 J/m^2.

The CCA did not reveal any synthetic lethal or viable interaction between XPA and FANCD2, in contrast to XPA with shFANCA. The CCA is showing a synthetic viable interaction between the XPA KO and shRNA inhibition of FANCA (figure 23 B).

The NER pathway is divided into two sub-pathways that recognize DNA damage, the GGR and TCR. After the damage is recognized by either of the sub-pathways, the core NER proteins are responsible for incision, elongation and ligation of the affected DNA segment. XPA is a core protein, that together with XPD (TFIIH) helps positioning the nuclease complex ERCC1-XPF and XPG on the damage to make the incision. XPA is also necessary for recruitment of the ERCC1-XPF complex to the site of damage for its function in NER [184]. This publication [184] gives also proof that XPA and XPF physically interact. This close interaction and the relevance of XPF in NER, makes it reasonable to assume that XPF KO cells could exhibit the same synthetic viability to shRNA inhibition of FANCA as XPA KO cells. To address this question an XPF KO cell line was tested for synthetic viability with shFANCA.

4.3.5 Testing XPF KO and XPF mutants for synthetic lethality or viability with FA proteins

In order to test for the suspected synthetic viable interaction between FANCA and XPF the HEK XPF KO cell line was used with shRNA against FANCA and FANCD2 (figure 24 A). The CCA could confirm the synthetic viability between XPF and FANCA. Contrary to that, XPF KO and FANCD2 inhibition (figure 24 A) was not synthetic lethal nor viable, at least under unchallenged conditions with the CCA. The synthetic viability could be replicated in a HeLa XPF KO cell line (Annex 3). This result does not conclude that the synthetic viability with XPA and FANCA is a result of the inability of XPF to fulfil its function in the NER pathway but it is in supports of this theory.

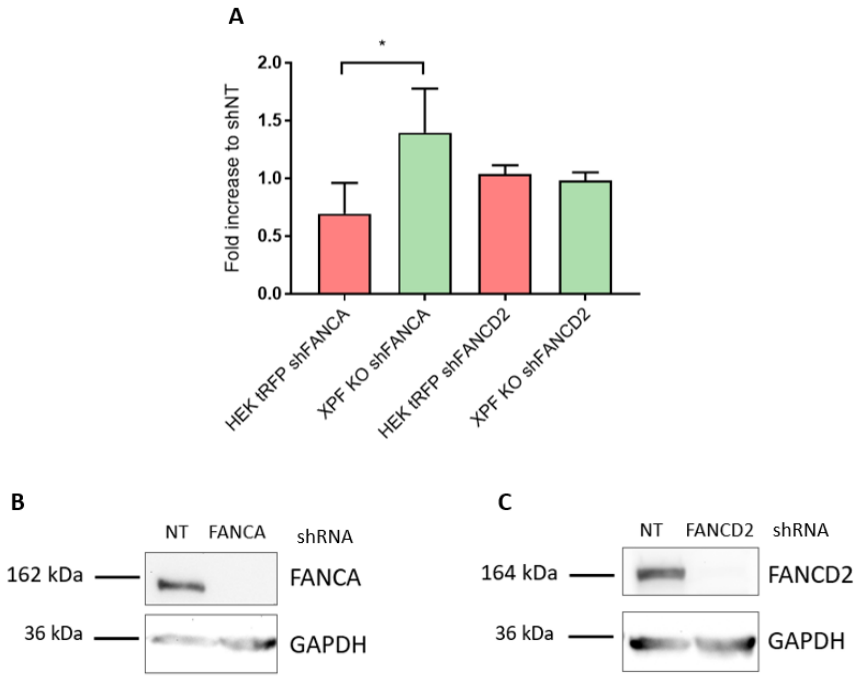

Figure 24: Testing HEK XPF KO for synthetic lethal or viable interaction with the CCA, A: ***CCA of HEK tRFP vs HEK XPF KO treated with shRNA;*** *CCA of HEK tRFP vs HEK XPF KO GFP treated with either shRNA for FANCA or plotted is the fold increase to shNT of four independent repeats error bars show SD and significance was calculated with unpaired Mann-Whitney test, B:* ***WB control of FANCA;*** *10 % PAA gel, HEK tRFP vs HEK XPF KO GFP with loading control GAPDH left pocket: HEK tRFP vs HEK XPF KO GFP shNT, right pocket: HEK tRFP vs HEK XPF KO GFP shFANCA, C:* ***WB control of FANCD2;*** *10 % PAA gel, HEK tRFP vs HEK XPF KO GFP with loading control GAPDH left pocket: HEK tRFP vs HEK XPF KO GFP shNT, right pocket: HEK tRFP vs HEK XPF KO GFP shFANCD2*

XPF is a nuclease that is not only involved in the NER pathway but also in the FA/BRCA pathway, it acts downstream in the FA/BRCA pathway during unhooking of the ICL. While FANCA and FANCD2 are part of the same pathway they act upstream of XPF, FANCA in monoubiquitinating FANCD2 and the ID2-complex in recruiting the downstream proteins. The synthetic viability seen in this experiment is between FANCA and XPF. It would be interesting to test other core-complex proteins for synthetic lethality with XPF, to see if this viability is dependent on the core-complex or maybe only the sub complex of FANCA, FANCG and FAAP20. This work can exclude a synthetic viable interaction with FANCD2, so even if all proteins FANCA, FANCD2, and XPF are part of the same DNA repair pathway, and all pathologic mutations in these genes cause FA, it seems that FANCA or at least the subcomplex of FANCA, FANCG and FAAP20 has an additional role with XPF. This additional role has likely to do with XPFs function in the NER pathway because of the synthetic viability that is seen in XPA KO and FANCA inhibition.

Mutations in the *ERCC4* gene can cause three different syndromes depending on the mutation: FA, XP and CS and mixed forms of the three syndromes like XFE that is accompanied by progeria. In order to test this hypothesis that the observed synthetic viability between XPF and FANCA is because of a deficiency in NER, a CCA was perform with XPF KO cells complemented for XPF carrying mutations that cause these different syndromes. The HEK XPF KO and mutant cell lines were previously created in our laboratory in the frame of a thesis [51]. These different syndromes were used to check if the synthetic viable interaction between FANCA and XPF is because of its participation in NER.

The following XPF mutations were used: the I225M mutation comes from an XP patient, C236R mutation is a CS causing mutation, R153P is a mixed form causing XFE and L230P is causing FA. These clones were tested for synthetic viability with shFANCA in the CCA, to see if this synthetic viability is only occurring when the whole protein is missing or if it is specific to a mutation causing one of the syndromes.

In figure 25 A the CCA is shown as a fold increase to shNT. The expected result if the suppression of NER function of XPF is causing the synthetic lethality would show that cell lines XPF KO and XPF KO + I225M are synthetic viable, the mixed form that causes XFE could probably show a slight increase in the mutant ratio compared to the shNT treated control. There should be no synthetic viability seen with the XPF KO + L230P mutation that causes FA nor with the Wt sequence of the protein. This is what can be seen in the graph (figure 25 A), the XPF KO cell line, the mutant XPF KO + I225M and the XFE mixed form (XPF KO + R153P) are exhibiting synthetic viable tendency while the mutant for CS has only a slight increase in ratio of tRFP verses GFP and shRNA silencing of FANCA in the FA mutant or the Wt shows no synthetic viability.

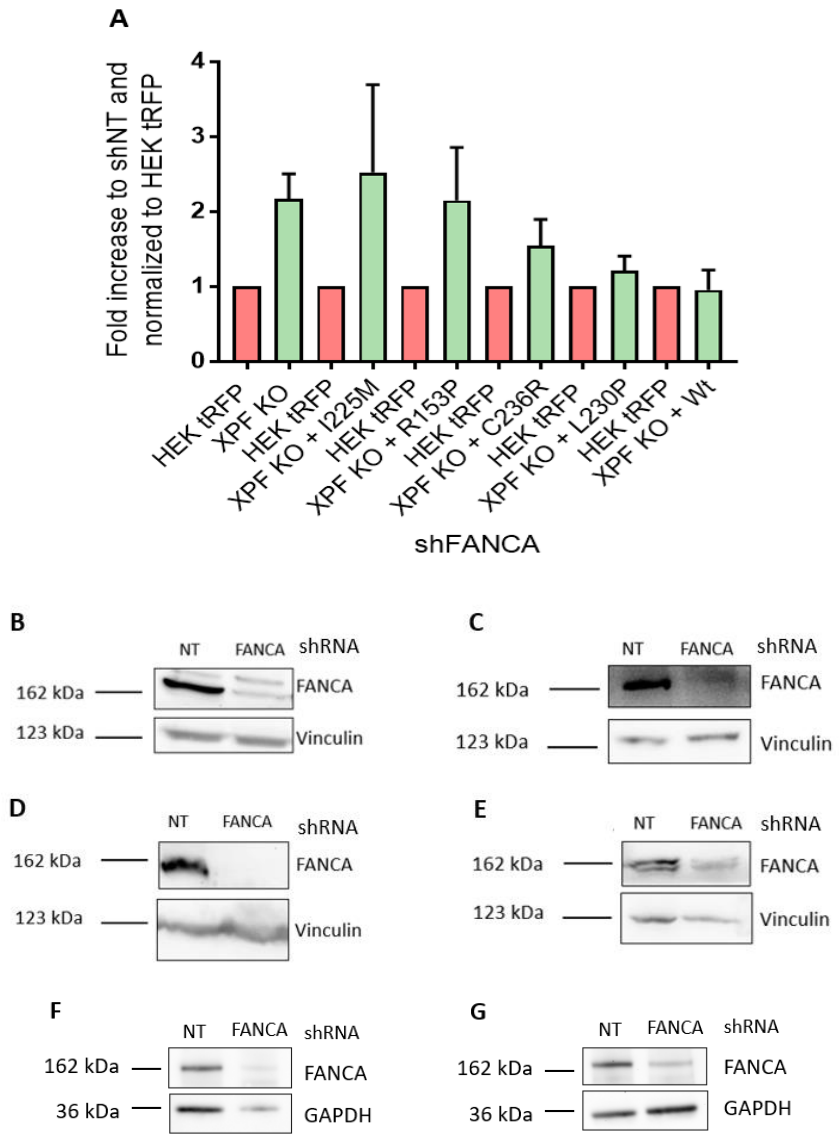

Figure 25: CCA to test for synthetic viable interaction in XPF mutants of different NER deficiency syndromes with FANCA, A: ***CCA of HEK XPF KO mutants and shRNA inhibition of FANCA;*** *CCA of HEK tRFP vs HEK XPF KO mutant treated with shFANCA, plotted are three independent experiments that are normalized to HEK tRFP, error bars show SEM, B:* ***WB control of FANCA expression HEK XPF KO + C236R****; 7.5 % PAA gel with FANCA antibody and loading control Vinculin, HEK tRFP vs HEK XPF KO + C236R, C:* ***WB control of FANCA expression HEK XPF KO****; 7.5 % PAA gel with FANCA antibody and loading control Vinculin, HEK tRFP vs HEK XPF KO, D:* ***WB control of FANCA expression HEK XPF KO + I225M****; 7.5 % PAA gel with FANCA antibody and loading control Vinculin, HEK tRFP vs HEK XPF KO + I225M, E:* ***WB control of FANCA expression HEK XPF KO + L230P****; 7.5 % PAA gel with FANCA antibody and loading control Vinculin, HEK tRFP vs HEK XPF KO + L230P, F:* ***WB control of FANCA expression HEK XPF KO + R153P****; 7.5 % PAA gel with FANCA antibody and loading control Vinculin, HEK tRFP vs HEK XPF KO + R153P, G:* ***WB control of FANCA expression HEK XPF KO + wt****; 7.5 % PAA gel with FANCA antibody and loading control Vinculin, HEK tRFP vs HEK XPF KO + wt*

It is not possible to make concrete conclusions with the high variation in the individual experiments but there seems to be a tendency that the mutations causing XP or the mixed form XFE are more likely to have an impact on this synthetic viability.

Testing more XPF mutants causing these syndromes could provide more insight into this. Another possible step to characterise this synthetic viability could be the testing of XPC deficient cells for synthetic viability with FANCA. XPC is a protein that participates only in the GGR recognition of the DNA damage. If there would be a synthetic viability between XPC and FANCA it would mean, that the mechanism of synthetic viability is not dependent on supressing XPF function in NER but that it is a more general concept involving the GGR. Nevertheless it would be interesting to confirm with further experiments if the XPA synthetic viability with shFANCA is over its interaction with XPF by double inhibition of XPA and XPF or with a XPA mutant that is not able to localise to the site of damage.

XPF shRNA and inhibitor were ordered for testing this synthetic viability in FANCA KO cells but none of the ordered shRNAs against XPF were reducing XPF expression and the results of the XPF inhibitor experiments are inconclusive probably due to handling issues of the inhibitor.

Taken together, the findings of synthetic viability in XPA KO and XPF KO after silencing FANCA and the synthetic viability in the XPF KO, XPF KO + I225M mutant but not in the FA XPF KO + L320P mutant supports the hypothesis that the synthetic viability is due to the suppression of XPF function in NER. As mention, this could mean that the XPA synthetic viability is due to its interaction with XPF as the protein (XPA) is necessary to recruit ERCC1-XPF to the site of damage during NER [184].

Another possibility for the synthetic viable interaction of FANCA and XPF could be the involvement of FANCA in the SSA subpathway of DNA repair in which XPF is participating too [110][185]. As FANCA is promoting SSA it could very well be, that in cells lacking XPF, the repair pathway is stuck without XPF and cannot complete repair. The depletion of FANCA would in that case channel repair directly into a different repair pathway, giving the cells an advantage.

4.3.6 Testing for synthetic lethal or viable interaction in FANCA KO background

In search of synthetic lethal or viable interaction the established FA clone U2OS Cas9 FANCA KO clone B12 GFP, which will be called FANCA KO was tested with the CCA. First the established SL with ATM inhibition was tested by siRNA silencing (Figure 26) as was done with the U2OS FANCD2 KO clone (figure 18) and the U2OS PARP1 KO clone (figure 17).

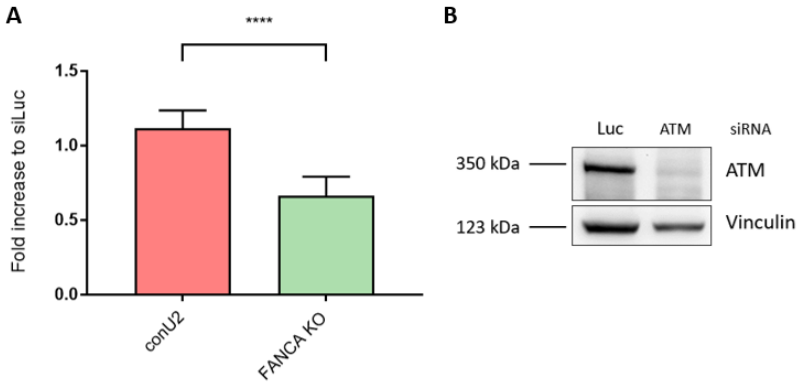

Figure 26: Establishing the synthetic lethality of the FANCA KO clone with siATM, A: ***CCA of conU2 vs U2OS FANCA KO with siATM treatment;*** *CCA of conU2 and FANCA KO with siATM treatment, measurement at day nine, plotted is the fold increase to siLuc and error bars show SD of six independent experiments, significance is calculated with unpaired t test B:* ***WB of ATM expression;*** *5 % PAA gel with antibody against ATM and loading control Vinculin, conU2 vs FANCA KO with siATM treatment*

Next, FANCA KO cells were checked for synthetic lethal or viable interactions. In figure 27 A the CCA is shown with shRNA against FANCA as control, FANCD2, PARP1 and FEN1. It demonstrates that the internal control has no growth advantage nor disadvantage, there is a slight reduction in growth with shRNA for FANCD2 as well es for PARP1 but this work focused on the prominent synthetic viability between FANCA KO and FEN1.

After the discovered synthetic viability a CFA should confirm the synthetic viability but even with different methods of infection or seeding the results remained inconclusive with very high variations between the samples and repeats. Instead, for confirmation of this interaction the CCA was repeated in a different cell line that is not of tumor origin.

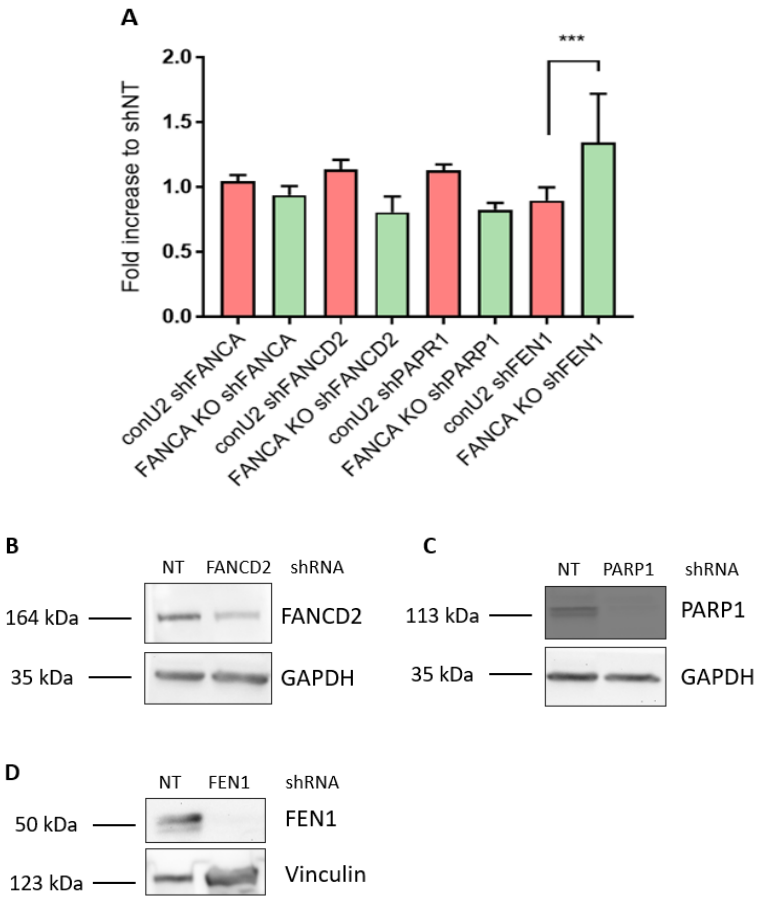

*Figure 27: Testing for synthetic lethal or viable interaction with the CCA in FANCA KO cells, A:**CCA of conU2 vs FANCA KO shRNA treatment:** CCA of conU2 vs FANCA KO and shRNA treatment of shFANCA (control), FANCD2, PARP1 and FEN1 plotted is the fold increase to shNT and error bars show SD of at least three independent experiments, significance test unpaired Mann-Whitney, B**: WB of FANCD2 expression:** 7.5 % PAA gel with antibody against FANCD2 and loading control vinculin, conU2 vs FANCA KO treatment with either shNT control or shFANCD2 C: **WB of FANCD2 expression:** 10 % PAA gel with antibody against PARP1 and loading control vinculin, conU2 vs FANCA KO treatment with either shNT control or shPARP1 D: **WB of FEN1 expression:** 10 % PAA gel with antibody against FEN1 and loading control vinculin, conU2 vs FANCA KO treatment with either shNT control or shFEN1*

For this reason another FANCA KO in the RPE1 background, was generated from a RPE1 p53 KO cell line that was a gift from Daniel Durocher's laboratory. FANCA WB control detected no protein in clone RPE1 Cas9 FANCA KO A1 (figure 28 A), there was also no detectable FANCD2 monoubiquitination (figure 28 B) and the SRB survival with DEB as well as the MN assay confirmed the FA phenotype (figure 28 C and 28 D).

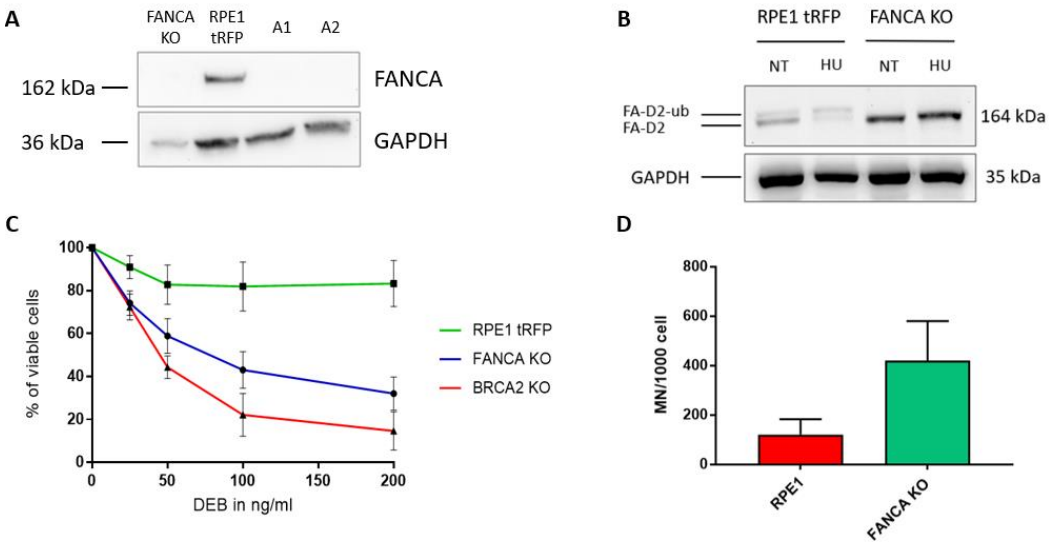

Figure 28: Characterisation of RPE1 Cas9 FANCA KO clone A1, A: ***WB control of FANCA expression in RPE1 Cas9 FANCA KO clones;*** *7.5 % PAA gel with antibody against FANCA and loading control GAPDH, loaded are from left to right; U2OS Cas9 FANCA KO clone B12, RPE1 Cas9 tRFP, RPE1 Cas9 FANCA KO clone A1 GFP, RPE1 Cas9 FANCA KO clone A2 GFP, B:* ***WB control of FANCD2 monoubiquitination;*** *10 % PAA gel with antibody against FANCD2 and loading control GAPDH, first pocket: RPE1 Cas9 tRFP non-treated, second pocket: RPE1 Cas9 tRFP treated with 2mM hydroxyurea, third pocket: RPE1 Cas9 FANCA KO clone A1 GFP non-treated, fourth pocket: RPE1 Cas9 FANCA KO clone A1 GFP treated with 2 mM hydroxyurea, C:* ***SRB survival of RPE1 Cas9 FANCA KO clone A1 after DEB treatment and SD;*** *In green parental control cell line RPE1 Cas9 tRFP, in blue the RPE1 Cas9 FANCA KO clone A1 GFP, in red the positive control for sensitivity HEK BRCA2 KO, D:* ***MN of RPE1 Cas9 tRFP and RPE1 Cas9 FANCA KO clone A1 GFP;*** *RPE1 Cas9 tRFP and RPE1 Cas9 FANCA KO clone A1 GFP were treated with 50 ng/ml of DEB, plotted is SD of three independent experiments.*

The Sanger sequencing revealed two heterozygote mutations in FANCA exon 4 c.358dupA (p.S120Kfs*61) and c.354_360delCTCTAGC (p.S119Wpfs*17).

After confirming the RPE1 Cas9 FANCA KO clone, the CCA was repeated with the established KO for FANCA and shRNA inhibition of FEN1, in figure 29. For simplification the parental control cell line RPE1 Cas9 tRFP is called RPE1 tRFP and RPE1 Cas9 FANCA KO clone A1 GFP is called RPE1 FANCA KO. The CCA could confirm the synthetic viability in a non-tumorgenic background (figure 29), the difference in ratio was not as pronounced as in the U2OS sample but it was significant nevertheless. This finding confirms that the observed synthetic viability is not an tumorgenic artefact.

In order to find out more about the mechanism of the synthetic viable interaction some molecular characteristics of FANCA KO cells were studied to see if the shFEN1 inhibition had an effect on them.

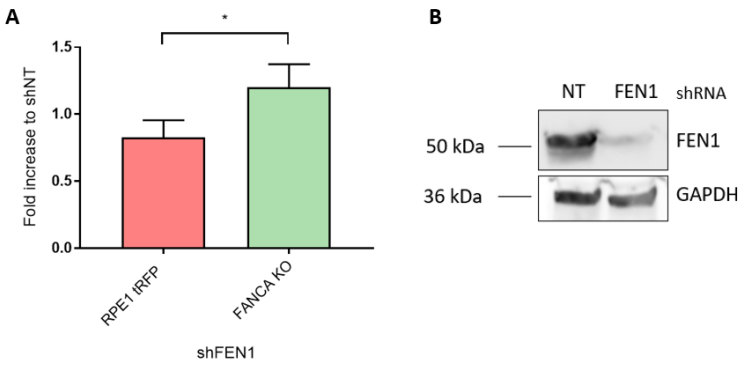

*Figure 29: Confirmation of synthetic viable interaction of FANCA with FEN1 in the REP1 FANCA KO clone, A**: CCA of RPE1 tRFP vs RPE1 FANCA KO with shFEN1 treatment;** CCA of RPE1 tRFP vs RPE1 FANCA KO clone A1 GFP with shFEN1 treatment plotted is the fold increase to shNT of four independent experiments shown is SD and significance was determined by unpaired Mann-Whitney test, B**: WB control of FEN1 expression;** 10 % PAA gel with antibody against FEN1, loading control GAPDH, loaded is RPE1 tRFP vs RPE1 Cas9 FANCA KO clone A1 with shNT treatment left and shFEN1 treatment right*

The most important function of FANCA is the participation in the multiprotein ubiquitin ligase complex that is responsible for the monoubiquitination of FANCD2. A WB of FANCD2 could show if shFEN1 inhibition was able to restore FANCD2 monoubiquitination in FANCA KO cells (Figure 30 A) and if reconstitution of the FA pathway was responsible for the growth advantage. In figure 30 A the WB for the FANCD2 monoubiquitination is shown. FANCA KO cells do not exhibit a second band for monoubiquitinated FANCD2, in neither of the samples treated with HU or untreated, which leads to the conclusion that FEN1 inhibition is not reconstituting the monoubiquitination. In contrast to that, the conU2 control shows in all samples a second band for monoubiquitinated FANCD2 at approximately 172 kDa.

As there was no effect on monoubiquitination the influence of FEN1 on chromosome fragility was explored. FEN1 is a 5'-flap endonuclease that has also exonuclease and gab-nuclease function, it is involved in the BER pathway by cutting the created long-patch flaps and prime the DNA for ligation. It is also involved in the Okazaki-fragment maturation in the removal of RNA primer, in telomere stability and in the DNA fragmentation of apoptotic cells. Because of its function as endonuclease in DNA repair and the high chromosome instability in FA cells it was not unreasonable to theorise that FEN1 could play a role in the chromosome fragility.

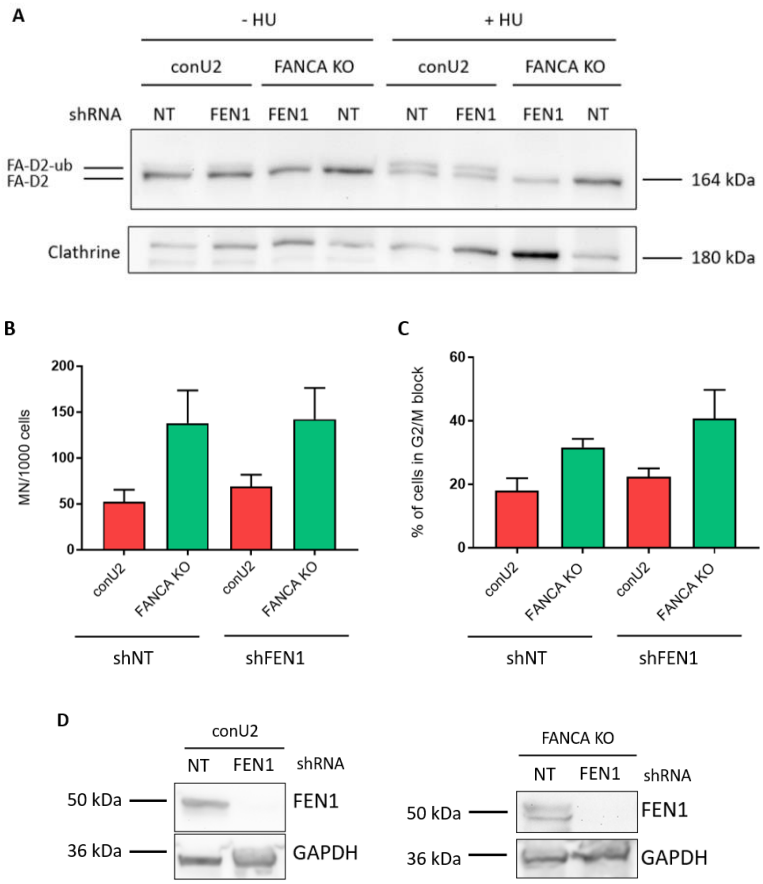

Figure 30: Study of the FANCA FEN1 synthetic viable interaction of restoring the FA pathway, A: ***WB of FANCD2 monoubiquitination with or without shFEN1 treatment;*** *7.5 % PAA gel with antibody against FANCD2, loading control Clathrin, first pocket: conU2 shNT treated, second pocket: conU2 shFEN1 treated, third pocket: U2OS FANCA KO shFEN1 treated, fourth pocket: U2OS FANCA KO shNT treated, fifth pocket: conU2 shNT treated and 2mM hydroxyurea, sixth pocket: conU2 shFEN1 treated and 2mM hydroxyurea, seventh pocket: U2OS FANCA KO shFEN1 treated and 2 mM hydroxyurea, eighth pocket: U2OS FANCA KO shNT treated and 2 mM hydroxyurea, B:* ***MN of conU2 and U2OS FANCA KO GFP treated with either shNT or shFEN1;*** *cells are treated with 5 ng/ml DEB****,*** *plotted are three independent experiments and SD, C:* ***Cell cycle G_2/M block of conU2 and U2OS FANCA KO treated with either shNT or shFEN1;*** *cells are treated with 50 ng/ml DEB plotted are three independent experiments and SD, D:* ***WB control of FEN1 expression in, left conU2 and right U2OS FANCA KO;*** *10 % PAA gel with antibody against FEN1 and loading control GAPDH conU2 or U2OS FANCA KO are treated with shNT or shFEN1*

A MN assay was employed to measure chromosome fragility and the cell cycle to determine if FEN1 inhibition is attenuating the chromosome fragility associated with FA cells or if it has an influence of the stalling of FA cells in the G_2/M cell cycle arrest. The results are shown in figure 30 B the MN and figure 30 C the G_2/M cell cycle arrest. There was no effect on neither chromosome fragility nor on G_2/M block. In the graph for the cells cycle (figure 30 C) the FEN1 treated samples look a little bit higher but with a higher standard deviation. Concluding that

neither FANCD2 monoubiquitination nor the alleviation of chromosome fragility is responsible for synthetic viability of shFEN1 treated FANCA KO cells.

A different approach was to see if the synthetic viability had an influence on the sensitivity of the FANCA KO cells to DEB (figure 31 A). That was not the case which is in accordance the MN assay that showed that FEN1 inhibition had no effect on chromosome fragility.

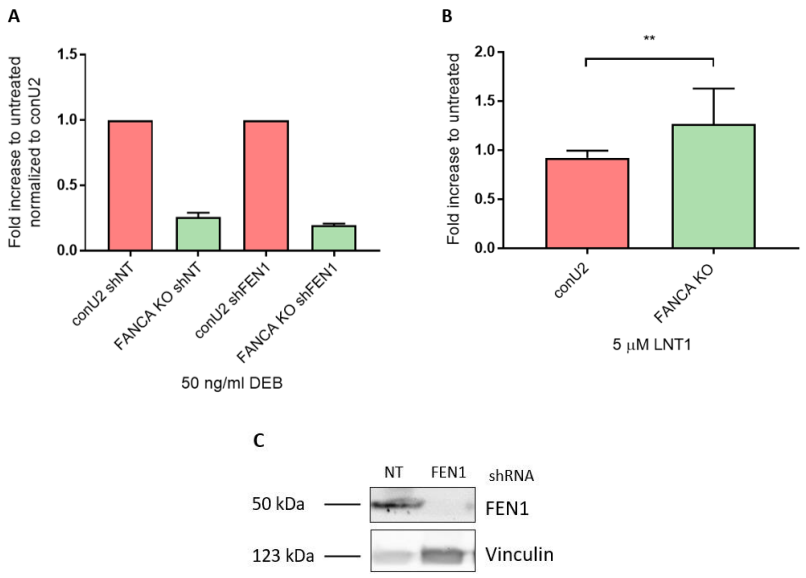

Figure 31: Testing for a reduction in chemosensitivity and validation of the synthetic viable interaction between FANCA and FEN1 with FEN1 inhibitor, A: ***CCA of conU2 vs U2OS FANCA KO with either shNT or shFEN1 treatment;*** *all samples are treated with 50 ng/ml DEB and plotted is the fold increase and SD of three independent experiments normalized to conU2, B:* ***CCA of conU2 vs U2OS FANCA KO with treatment of LNT1 FEN1 inhibitor;*** *conU2 vs U2OS FANCA KO treated with 5 μM of FEN1 inhibitor LNT1 plotted is the fold increase of LNT1 treated cells to DMSO treated cells SD of six independent results and significance was tested with unpaired Mann-Whitney test, C:* ***WB of FEN1 control for CCA with DEB;*** *conU2 vs U2OS FANCA KO treated with either shNT or FEN1*

Lastly the use of a FEN1 inhibitor LNT1 with the CCA could confirm the synthetic viable interaction of FANCA and FEN1 (figure 31 B). The inhibitor LNT1 could recreate the synthetic viability seen with shRNA inhibition. The publication describing the inhibitor states that its function is not degrading the protein but acts as a competitive and uncompetitive inhibitor [186]. It is likely to assume, with this information, that the inhibition of the enzymatic function of FEN1 or the substrate binding is probably responsible for the synthetic viability.

Taken together, synthetic viability could be replicated in two different cell lines one with tumor origin and one retinal epithelium cell line. The synthetic viability could be recreate with an inhibitor for FEN1 and the viability is only present if cells are not challenged with cytotoxic

agents like DEB. This work excludes that FEN1 inhibition is reconstituting the FANCD2 ubiquitination and it does not attenuate the chromosomal fragility measurable with the MN assay neither has it any influence on the cell cycle G_2/M block.

Nevertheless this is the first time that this interaction could be described and even if it has no effect on the sensitivity to cytotoxic agents it seems to improve the cell growth of FANCA cells without increasing the chromosome fragility. It also seems unlikely that FEN1 inhibition changes the cell cycle progression as the shFEN1 treated FANCA KO cells exhibit the same pattern of G_2/M block as the shNT treated. It is more probable that the synthetic viability of shFEN1 inhibition is due to the enzymatic function of FEN1, as the inhibitor experiments suggest. This leads to the question if FANCA is somehow inhibiting or regulating FEN1 activity. There is a publication proofing that FANCA is not only physically interacting with FEN1 but also it is stimulating FEN1 5'-flap nuclease activity [187]. The publication suggesting a role of FANCA stimulation of FEN1 during replication when Okazaki fragment maturation, as FANCA is stimulating FEN1s 5'-flaps endonuclease activity. Maybe the loss of FANCA is inhibiting this FEN1 activity and that leads to a slower replication fork progression or stalling of the replication fork by FEN1. In healthy cells this could be avoided by FANCA stimulation and in cells were both proteins are missing.

4.3.7 Testing for synthetic lethal or viable interactions in FANCD2 KO background

After the discovery of the synthetic viable interaction between FANCA KO cells and FEN1 it was questioned, if the results could be replicated in the FANCD2 KO background. SL for the created U2OS FANCD2 KO and siATM was already established the in figure 19.

The CCA revealed that there is no synthetic viability between FEN1 and FANCD2 KO as expected there is no impact of growth with shFANCA and the internal control for shFANCD2 (figure 32). This result is not surprising as seen before with the shRNA inhibition of FANCD2 in the different DNA repair pathways did not reveal any synthetic lethal or viable interaction. It is not possible to make a statement for the interaction with shPARP1 as the error bar is too big for any conclusion.

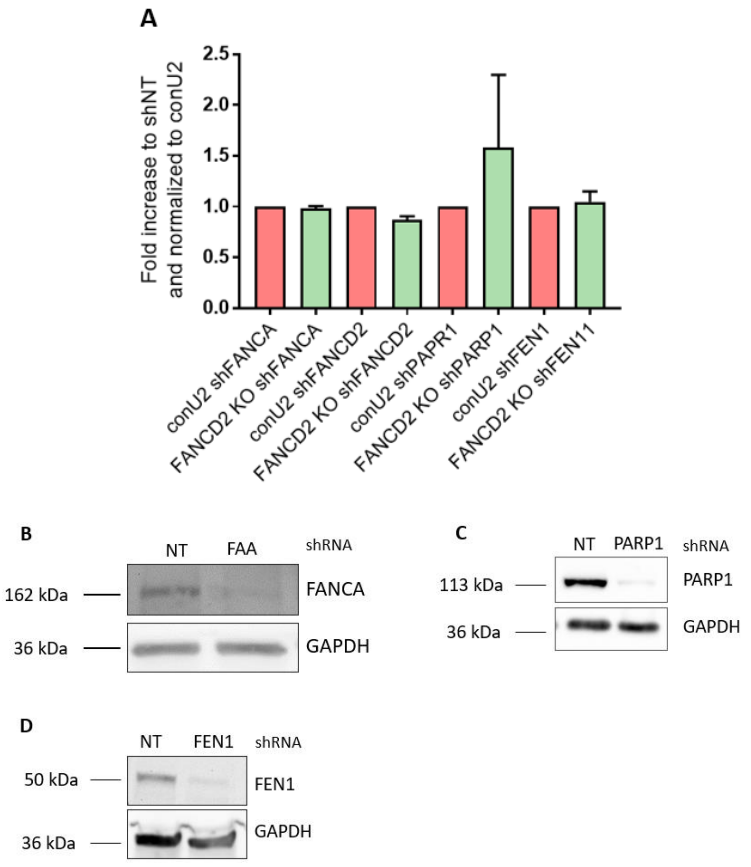

Figure 32: Testing with the CCA for synthetic lethal or viable interactions in FANCD2 KO, A: ***CCA of conU2 vs U2OS FANCD2 KO clone C9 with shRNA treatment****: conU2 vs U2OS FANCD2 KO treated with shRNA against FANCA, FANCD2 internal control, PARP1, FEN1 plotted is the fold increase of shNT and normalized to conU2, error bars show SED of three independent experiments, B:* ***WB control of FANCA expression:*** *7.5 % PAA gel, conU2 vs U2OS FANCD2 KO with shNT or shFANCA treatment, C:* ***WB control of PARP1 expression:*** *7.5 % PAA gel, conU2 vs U2OS FANCD2 KO with shNT or shPARP1 treatment, D:* ***WB control of FEN1 expression:*** *10 % PAA gel, conU2 vs U2OS FANCD2 KO with shNT or shFEN1 treatment*

4.4 Summary of the findings and future perspectives

The established method, the colour competition assay, was able to detect described synthetic lethal interactions with shRNA, siRNA and inhibitor. Nevertheless the CCA was unable to detect synthetic lethal or viable interactions with shFANCA or FANCD2 and BER protein PARP1 or the MMR proteins MSH2 and MLH1.

Instead the CCA revealed a synthetic viable interaction with XPA and shFANCA that could be due to its interaction with XPF. Another CCA with XPF KO cells revealed a viable interaction between XPF KO and shFANCA which supports the idea that the synthetic viable interaction with XPA is due to its recruiting function of XPF in NER. The synthetic viability of XPF with shFANCA could be confirmed in two different cell lines, in of non-tumorogenic origin and of tumor origin, HEK and HeLa cells. The results of the XPF mutant experiments with the CCA showed the tendency that the viability could be related to XPF function in NER. In contrast to these findings the CCA was unable to detect synthetic lethality or viability with shFANCD2 in XPA KO or XPF KO cells.

Furthermore the CCA revealed another synthetic viable interaction between FANCA and FEN1. The findings were replicated in a second cell line that was non-tumorgenic and additionally an inhibitor for FEN1 could recapitulate the synthetic viability. This interaction had no impact on monoubiquitination of FANCD2, chromosome fragility or the cell cycle arrest of the treated FANCA KO cells. Neither did it had any rescuing effect on DEB sensitivity which concludes that a reconstitution or rescue of the FA pathway is not the cause for this synthetic viable interaction. Instead the inhibitor experiments suggest that the viable interaction is due to the enzymatic function or substrate binding of FEN1.

It is interesting that two synthetic viable interactions with FANCA are with proteins that have 5'- flap endonuclease activity and that viability is only with FANCA not with FANCD2. It would be interesting to examine if other proteins of the core-complex are also synthetic viable with these nucleases or if other repair nucleases are synthetic viable with FANCA KO. These results suggest that FA proteins, even if they are in the same pathway have more distinct functions, it would be of interest to test more proteins of the core-complex to see if they also show synthetic viabilities or if FANCA takes a special role.

Overall these findings bear the possibility for potential applications in FA treatment. The synthetic viable interactions are improving FANCA KO cell growth and for the interaction with FEN1, this work could additionally prove, that it is not inducing further DNA damage in treated cells. As FA patients most common symptom is bone marrow failure due to its exhaustion, improving cell growth seems to be a good starting point to investigate its potential for future treatments. Another possibility are short term applications such as improving FA cell growth for the mobilisation of hematopoietic stem cells in FA patients that undergo gene therapy [188][189]. This treatment is only available for FA patients that have mutations in the *FANCA* gene and one of the main concerns with this therapy is the quantity of harvested hematopoietic stem cells. This could be a first step to tackle this issue with a synthetic viability approach as FEN1 as well as XPF are druggable proteins. In any case this work revealed three novel synthetic viable interactions with FANCA that could be exploited in the future for potential treatments.

5 Conclusions

The aim of this thesis was to find novel synthetic lethal or viable interaction between FANCA or FANCD2 with other DNA repair pathways with the newly developed cytometer-based colour competition assay.

- The CCA was not discovering a novel synthetic lethality between FANCA or FANCD2 and other DNA repair pathways.

- The CCA was not detecting any synthetic viability or lethality with between PARP1 KO and FANCA or FANCD2. Neither were there any findings for MMR proteins MSH2 and MLH1

- A novel synthetic viability interaction was revealed between FANCA and XPA, it is likely that this is due to the interaction of XPA with XPF.

- The novel synthetic viability interaction between FANCA and XPF/FANCQ, was identified in HEK and HeLa cells. Further studies with pathway specific mutants of XPF suggest that the synthetic viability is probably due to inhibition of XPF's activity in NER.

- Novel synthetic viability between FANCA and FEN1 was detected in U2OS and RPE1 cells. Inhibition of FEN1 does not rescue chemosensitivity, chromosome fragility or G2/M cell cycle arrest of FANCA cells, suggesting that the observed synthetic viability is not explained by resurrection of the FA/BRCA pathway. The synthetic viability could be mimicked with an inhibitor for FEN1 which makes it probable that the viability is caused by the enzymatic function of FEN1.

6 References

[1] T. Lindahl and B. Nyberg, 'Rate of depurination of native deoxyribonucleic acid', *Biochemistry*, vol. 11, no. 19, pp. 3610–3618, Sep. 1972, doi: 10.1021/bi00769a018.

[2] T. Lindahl, 'Instability and decay of the primary structure of DNA', *Nature*, vol. 362, no. 6422, pp. 709–715, Apr. 1993, doi: 10.1038/362709a0.

[3] C. López-Otín, M. A. Blasco, L. Partridge, M. Serrano, and G. Kroemer, 'The Hallmarks of Aging', *Cell*, vol. 153, no. 6, pp. 1194–1217, Jun. 2013, doi: 10.1016/j.cell.2013.05.039.

[4] W. P. Vermeij, J. H. Hoeijmakers, and J. Pothof, 'Aging: not all DNA damage is equal', *Curr. Opin. Genet. Dev.*, vol. 26, pp. 124–130, Jun. 2014, doi: 10.1016/j.gde.2014.06.006.

[5] C. Schmeer, A. Kretz, D. Wengerodt, M. Stojiljkovic, and O. W. Witte, 'Dissecting Aging and Senescence—Current Concepts and Open Lessons', *Cells*, vol. 8, no. 11, p. 1446, Nov. 2019, doi: 10.3390/cells8111446.

[6] A. Tubbs and A. Nussenzweig, 'Endogenous DNA Damage as a Source of Genomic Instability in Cancer', *Cell*, vol. 168, no. 4, pp. 644–656, Feb. 2017, doi: 10.1016/j.cell.2017.01.002.

[7] H. E. Krokan and M. Bjørås, 'Base Excision Repair', *Cold Spring Harb. Perspect. Biol.*, vol. 5, no. 4, p. a012583, Apr. 2013, doi: 10.1101/cshperspect.a012583.

[8] H. E. Krokan, R. Standal, and G. Slupphaug, 'DNA glycosylases in the base excision repair of DNA', *Biochem. J.*, vol. 325 (Pt 1), pp. 1–16, Jul. 1997, doi: 10.1042/bj3250001.

[9] D. O. Zharkov, 'Base excision DNA repair', *Cell. Mol. Life Sci.*, vol. 65, no. 10, pp. 1544–1565, May 2008, doi: 10.1007/s00018-008-7543-2.

[10] H.-K. Wong and D. M. Wilson III, 'XRCC1 and DNA polymerase β interaction contributes to cellular alkylating-agent resistance and single-strand break repair', *J. Cell. Biochem.*, vol. 95, no. 4, pp. 794–804, 2005, doi: 10.1002/jcb.20448.

[11] E. Cappelli, R. Taylor, M. Cevasco, A. Abbondandolo, K. Caldecott, and G. Frosina, 'Involvement of XRCC1 and DNA Ligase III Gene Products in DNA Base Excision Repair *', *J. Biol. Chem.*, vol. 272, no. 38, pp. 23970–23975, Sep. 1997, doi: 10.1074/jbc.272.38.23970.

[12] C. Cistulli, O. I. Lavrik, R. Prasad, E. Hou, and S. H. Wilson, 'AP endonuclease and poly(ADP-ribose) polymerase-1 interact with the same base excision repair intermediate', *DNA Repair*, vol. 3, no. 6, pp. 581–591, Jun. 2004, doi: 10.1016/j.dnarep.2003.09.012.

[13] Q. Chen *et al.*, 'ADP-ribosylation of histone variant H2AX promotes base excision repair', *EMBO J.*, vol. 40, no. 2, p. e104542, Jan. 2021, doi: 10.15252/embj.2020104542.

[14] J. M. de Murcia *et al.*, 'Requirement of poly(ADP-ribose) polymerase in recovery from DNA damage in mice and in cells', *Proc. Natl. Acad. Sci. U. S. A.*, vol. 94, no. 14, pp. 7303–7307, Jul. 1997, doi: 10.1073/pnas.94.14.7303.

[15] B. F. Pachkowski *et al.*, 'Cells deficient in PARP-1 show an accelerated accumulation of DNA single strand breaks, but not AP sites, over the PARP-1-proficient cells exposed to MMS', *Mutat. Res. - Fundam. Mol. Mech. Mutagen.*, vol. 671, no. 1–2, pp. 93–99, 2009, doi: 10.1016/j.mrfmmm.2009.09.006.

[16] M. D. Vodenicharov, F. R. Sallmann, M. S. Satoh, and G. G. Poirier, 'Base excision repair is efficient in cells lacking poly(ADP-ribose) polymerase 1', *Nucleic Acids Res.*, vol. 28, no. 20, pp. 3887–3896, Oct. 2000, doi: 10.1093/nar/28.20.3887.

[17] Z. Q. Wang *et al.*, 'PARP is important for genomic stability but dispensable in apoptosis', *Genes Dev.*, vol. 11, no. 18, pp. 2347–2358, Sep. 1997, doi: 10.1101/gad.11.18.2347.

[18] K. W. Caldecott, 'Protein ADP-ribosylation and the cellular response to DNA strand breaks', *DNA Repair*, vol. 19, pp. 108–113, Jul. 2014, doi: 10.1016/j.dnarep.2014.03.021.

[19] S. Eustermann *et al.*, 'Structural Basis of Detection and Signaling of DNA Single-Strand Breaks by Human PARP-1', *Mol. Cell*, vol. 60, no. 5, pp. 742–754, Dec. 2015, doi: 10.1016/j.molcel.2015.10.032.

[20] J. Krietsch *et al.*, 'Reprogramming cellular events by poly(ADP-ribose)-binding proteins', *Mol. Aspects Med.*, vol. 34, no. 6, pp. 1066–1087, Dec. 2013, doi: 10.1016/j.mam.2012.12.005.

[21] M. S. Luijsterburg *et al.*, 'DDB2 promotes chromatin decondensation at UV-induced DNA damage', *J. Cell Biol.*, vol. 197, no. 2, pp. 267–281, Apr. 2012, doi: 10.1083/jcb.201106074.

[22] A. Pines *et al.*, 'PARP1 promotes nucleotide excision repair through DDB2 stabilization and recruitment of ALC1', vol. 199, no. 2, 2012, doi: 10.1083/jcb.201112132.

[23] T. A. Kunkel, 'DNA Replication Fidelity *', *J. Biol. Chem.*, vol. 279, no. 17, pp. 16895–16898, Apr. 2004, doi: 10.1074/jbc.R400006200.

[24] R. Fishel *et al.*, 'The human mutator gene homolog MSH2 and its association with hereditary nonpolyposis colon cancer', *Cell*, vol. 75, no. 5, pp. 1027–1038, Dec. 1993, doi: 10.1016/0092-8674(93)90546-3.

[25] S. Gradia, S. Acharya, and R. Fishel, 'The Human Mismatch Recognition Complex hMSH2-hMSH6 Functions as a Novel Molecular Switch', *Cell*, vol. 91, no. 7, pp. 995–1005, Dec. 1997, doi: 10.1016/S0092-8674(00)80490-0.

[26] M. J. Schofield and P. Hsieh, 'DNA mismatch repair: molecular mechanisms and biological function', *Annu. Rev. Microbiol.*, vol. 57, pp. 579–608, 2003, doi: 10.1146/annurev.micro.57.030502.090847.

[27] M. G. Marinus, 'Adenine methylation of Okazaki fragments in Escherichia coli', *J. Bacteriol.*, vol. 128, no. 3, pp. 853–854, Dec. 1976, doi: 10.1128/jb.128.3.853-854.1976.

[28] F. Palombo *et al.*, 'GTBP, a 160-kilodalton protein essential for mismatch-binding activity in human cells', *Science*, vol. 268, no. 5219, pp. 1912–1914, Jun. 1995, doi: 10.1126/science.7604265.

[29] I. Iaccarino, G. Marra, F. Palombo, and J. Jiricny, 'hMSH2 and hMSH6 play distinct roles in mismatch binding and contribute differently to the ATPase activity of hMutSalpha.', *EMBO J.*, vol. 17, no. 9, pp. 2677–2686, May 1998, doi: 10.1093/emboj/17.9.2677.

[30] J. I. Risinger, A. Umar, J. Boyd, A. Berchuck, T. A. Kunkel, and J. C. Barrett, 'Mutation of MSH3 in endometrial cancer and evidence for its functional role in heteroduplex repair', *Nat. Genet.*, vol. 14, no. 1, pp. 102–105, Sep. 1996, doi: 10.1038/ng0996-102.

[31] A. B. Clark, M. E. Cook, H. T. Tran, D. A. Gordenin, M. A. Resnick, and T. A. Kunkel, 'Functional analysis of human MutSalpha and MutSbeta complexes in yeast', *Nucleic Acids Res.*, vol. 27, no. 3, pp. 736–742, Feb. 1999, doi: 10.1093/nar/27.3.736.

[32] J. Genschel, L. R. Bazemore, and P. Modrich, 'Human exonuclease I is required for 5' and 3' mismatch repair', *J. Biol. Chem.*, vol. 277, no. 15, pp. 13302–13311, Apr. 2002, doi: 10.1074/jbc.M111854200.

[33] F. A. Kadyrov, J. Genschel, Y. Fang, E. Penland, W. Edelmann, and P. Modrich, 'A possible mechanism for exonuclease 1-independent eukaryotic mismatch repair', *Proc. Natl. Acad. Sci. U. S. A.*, vol. 106, no. 21, pp. 8495–8500, May 2009, doi: 10.1073/pnas.0903654106.

[34] M. J. Longley, A. J. Pierce, and P. Modrich, 'DNA polymerase delta is required for human mismatch repair in vitro', *J. Biol. Chem.*, vol. 272, no. 16, pp. 10917–10921, Apr. 1997, doi: 10.1074/jbc.272.16.10917.

[35] Y. Zhang *et al.*, 'Reconstitution of 5'-directed human mismatch repair in a purified system', *Cell*, vol. 122, no. 5, pp. 693–705, Sep. 2005, doi: 10.1016/j.cell.2005.06.027.

[36] O. D. Schärer, 'Nucleotide Excision Repair in Eukaryotes', *Cold Spring Harb. Perspect. Biol.*, vol. 5, no. 10, p. a012609, Oct. 2013, doi: 10.1101/cshperspect.a012609.

[37] J. A. Marteijn, H. Lans, W. Vermeulen, and J. H. J. Hoeijmakers, 'Understanding nucleotide excision repair and its roles in cancer and ageing', *Nat. Rev. Mol. Cell Biol.*, vol. 15, no. 7, pp. 465–481, Jul. 2014, doi: 10.1038/nrm3822.

[38] E. Evans, J. G. Moggs, J. R. Hwang, J. M. Egly, and R. D. Wood, 'Mechanism of open complex and dual incision formation by human nucleotide excision repair factors.', *EMBO J.*, vol. 16, no. 21, pp. 6559–6573, Nov. 1997, doi: 10.1093/emboj/16.21.6559.

[39] K. Sugasawa *et al.*, 'Xeroderma Pigmentosum Group C Protein Complex Is the Initiator of Global Genome Nucleotide Excision Repair', *Mol. Cell*, vol. 2, no. 2, pp. 223–232, Aug. 1998, doi: 10.1016/S1097-2765(00)80132-X.

[40] S. Bergink *et al.*, 'Recognition of DNA damage by XPC coincides with disruption of the XPC–RAD23 complex', *J. Cell Biol.*, vol. 196, no. 6, pp. 681–688, Mar. 2012, doi: 10.1083/jcb.201107050.

[41] G. Chu and E. Chang, 'Xeroderma Pigmentosum Group E Cells Lack a Nuclear Factor That Binds to Damaged DNA', *Science*, vol. 242, no. 4878, pp. 564–567, Oct. 1988, doi: 10.1126/science.3175673.

[42] J. Tang and G. Chu, 'Xeroderma pigmentosum complementation group E and UV-damaged DNA-binding protein', *DNA Repair*, vol. 1, no. 8, pp. 601–616, Aug. 2002.

[43] G. Spivak, 'Transcription-Coupled Repair: an update', *Arch. Toxicol.*, vol. 90, no. 11, pp. 2583–2594, Nov. 2016, doi: 10.1007/s00204-016-1820-x.

[44] O. V. Tsodikov *et al.*, 'Structural basis for the recruitment of ERCC1-XPF to nucleotide excision repair complexes by XPA', *EMBO J.*, vol. 26, no. 22, pp. 4768–4776, Nov. 2007, doi: 10.1038/sj.emboj.7601894.

[45] A. F. Fagbemi, B. Orelli, and O. D. Schärer, 'Regulation of endonuclease activity in human nucleotide excision repair', *DNA Repair*, vol. 10, no. 7, pp. 722–729, Jul. 2011, doi: 10.1016/j.dnarep.2011.04.022.

[46] M. Hohl, F. Thorel, S. G. Clarkson, and O. D. Schärer, 'Structural Determinants for Substrate Binding and Catalysis by the Structure-specific Endonuclease XPG *', *J. Biol. Chem.*, vol. 278, no. 21, pp. 19500–19508, May 2003, doi: 10.1074/jbc.M213155200.

[47] T. Ogi *et al.*, 'Three DNA Polymerases, Recruited by Different Mechanisms, Carry Out NER Repair Synthesis in Human Cells', *Mol. Cell*, vol. 37, no. 5, pp. 714–727, Mar. 2010, doi: 10.1016/j.molcel.2010.02.009.

[48] A. R. Lehmann, 'DNA polymerases and repair synthesis in NER in human cells', *DNA Repair*, vol. 10, no. 7, pp. 730–733, Jul. 2011, doi: 10.1016/j.dnarep.2011.04.023.

[49] A. R. Lehmann, D. McGibbon, and M. Stefanini, 'Xeroderma pigmentosum', *Orphanet J. Rare Dis.*, vol. 6, p. 70, Nov. 2011, doi: 10.1186/1750-1172-6-70.

[50] Z. Apostolou, G. Chatzinikolaou, K. Stratigi, and G. A. Garinis, 'Nucleotide Excision Repair and Transcription-Associated Genome Instability', *BioEssays*, vol. 41, no. 4, p. 1800201, 2019, doi: 10.1002/bies.201800201.

[51] M. Marín *et al.*, 'Functional Comparison of XPF Missense Mutations Associated to Multiple DNA Repair Disorders', *Genes*, vol. 10, no. 1, p. E60, Jan. 2019, doi: 10.3390/genes10010060.

[52] E. A. Cockayne, 'Dwarfism with retinal atrophy and deafness', *Arch. Dis. Child.*, vol. 11, no. 61, pp. 1–8, Feb. 1936.

[53] W. J. Kleijer *et al.*, 'Incidence of DNA repair deficiency disorders in western Europe: Xeroderma pigmentosum, Cockayne syndrome and trichothiodystrophy', *DNA Repair*, vol. 7, no. 5, pp. 744–750, May 2008, doi: 10.1016/j.dnarep.2008.01.014.

[54] A. C. Karikkineth, M. Scheibye-Knudsen, E. Fivenson, D. L. Croteau, and V. A. Bohr, 'Cockayne syndrome: Clinical features, model systems and pathways', *Ageing Res. Rev.*, vol. 33, pp. 3–17, Jan. 2017, doi: 10.1016/j.arr.2016.08.002.

[55] L. V. Mayne and A. R. Lehmann, 'Failure of RNA synthesis to recover after UV irradiation: an early defect in cells from individuals with Cockayne's syndrome and xeroderma pigmentosum', *Cancer Res.*, vol. 42, no. 4, pp. 1473–1478, Apr. 1982.

[56] B. Pascucci *et al.*, 'An altered redox balance mediates the hypersensitivity of Cockayne syndrome primary fibroblasts to oxidative stress', *Aging Cell*, vol. 11, no. 3, pp. 520–529, 2012, doi: 10.1111/j.1474-9726.2012.00815.x.

[57] M. Scheibye-Knudsen *et al.*, 'Cockayne syndrome group B protein prevents the accumulation of damaged mitochondria by promoting mitochondrial autophagy', *J. Exp. Med.*, vol. 209, no. 4, pp. 855–869, Apr. 2012, doi: 10.1084/jem.20111721.

[58] T. Mori *et al.*, 'ERCC4 Variants Identified in a Cohort of Patients with Segmental Progeroid Syndromes', doi: 10.1002/humu.23367.

[59] L. J. Niedernhofer *et al.*, 'A new progeroid syndrome reveals that genotoxic stress suppresses the somatotroph axis', *Nature*, vol. 444, no. 7122, pp. 1038–1043, Dec. 2006, doi: 10.1038/nature05456.

[60] A. Ahmad *et al.*, 'Mislocalization of XPF-ERCC1 nuclease contributes to reduced DNA repair in XP-F patients', *PLoS Genet.*, vol. 6, no. 3, p. e1000871, Mar. 2010, doi: 10.1371/journal.pgen.1000871.

[61] S. D. Chirnomas and G. M. Kupfer, 'The Inherited Bone Marrow Failure Syndromes', *Pediatr. Clin. North Am.*, vol. 60, no. 6, p. 10.1016/j.pcl.2013.09.007, Dec. 2013, doi: 10.1016/j.pcl.2013.09.007.

[62] A. D. D'Andrea, N. Dahl, E. C. Guinan, and A. Shimamura, 'Marrow failure', *Hematol. Am. Soc. Hematol. Educ. Program*, pp. 58–72, 2002, doi: 10.1182/asheducation-2002.1.58.

[63] B. P. Alter and P. S. Rosenberg, 'VACTERL-H association and fanconi anemia', *Mol. Syndromol.*, 2013, doi: 10.1159/000346035.

[64] K. Neveling, D. Endt, H. Hoehn, and D. Schindler, 'Genotype–phenotype correlations in Fanconi anemia', *Mutat. Res. Mol. Mech. Mutagen.*, vol. 668, no. 1–2, pp. 73–91, Jul. 2009, doi: 10.1016/j.mrfmmm.2009.05.006.

[65] B. P. Alter *et al.*, 'Malignancies and survival patterns in the National Cancer Institute inherited bone marrow failure syndromes cohort study', *Br. J. Haematol.*, vol. 150, no. 2, pp. 179–188, Jul. 2010, doi: 10.1111/j.1365-2141.2010.08212.x.

[66] C. M. Dutzmann *et al.*, 'Cancer in Children With Fanconi Anemia and Ataxia-Telangiectasia—A Nationwide Register-Based Cohort Study in Germany', *J. Clin. Oncol.*, p. JCO.21.01495, Oct. 2021, doi: 10.1200/JCO.21.01495.

[67] T. M. Schroeder and R. Kurth, 'Spontaneous Chromosomal Breakage and High Incidence of Leukemia in Inherited Disease', *Blood*, vol. 37, no. 1, pp. 96–112, Jan. 1971, doi: 10.1182/blood.V37.1.96.96.

[68] H. Seyschab *et al.*, 'Comparative Evaluation of Diepoxybutane Sensitivity and Cell Cycle Blockage in the Diagnosis of Fanconi Anemia', *Blood*, vol. 85, no. 8, pp. 2233–2237, Apr. 1995, doi: 10.1182/blood.V85.8.2233.bloodjournal8582233.

[69] T. M. Schroeder-Kurth, T. H. Zhu, Y. Hong, and I. Westphal, 'Variation in Cellular Sensitivities Among Fanconi Anemia Patients, Non-Fanconi Anemia Patients, Their Parents and Siblings, and Control Probands', in *Fanconi Anemia: Clinical, Cytogenetic and Experimental Aspects*, T. M. Schroeder-Kurth, A. D. Auerbach, and G. Obe, Eds. Berlin, Heidelberg: Springer, 1989, pp. 105–136. doi: 10.1007/978-3-642-74179-1_10.

[70] P. A. Muniandy, J. Liu, A. Majumdar, S. T. Liu, and M. M. Seidman, 'DNA interstrand crosslink repair in mammalian cells: Step by step', *Critical Reviews in Biochemistry and Molecular Biology*. 2010. doi: 10.3109/10409230903501819.

[71] C. Wendt and S. Margolin, 'Identifying breast cancer susceptibility genes – a review of the genetic background in familial breast cancer', *Acta Oncol.*, vol. 58, no. 2, pp. 135–146, Feb. 2019, doi: 10.1080/0284186X.2018.1529428.

[72] N. Tung *et al.*, 'Frequency of Germline Mutations in 25 Cancer Susceptibility Genes in a Sequential Series of Patients With Breast Cancer', *J. Clin. Oncol.*, vol. 34, no. 13, pp. 1460–1468, May 2016, doi: 10.1200/JCO.2015.65.0747.

[73] M. Bogliolo *et al.*, 'Biallelic truncating FANCM mutations cause early-onset cancer but not Fanconi anemia', *Genet. Med.*, vol. 20, no. 4, pp. 458–463, Apr. 2018, doi: 10.1038/gim.2017.124.

[74] M. Bogliolo and J. Surrallés, 'Fanconi anemia: a model disease for studies on human genetics and advanced therapeutics', *Curr. Opin. Genet. Dev.*, vol. 33, pp. 32–40, Aug. 2015, doi: 10.1016/j.gde.2015.07.002.

[75] A. R. Meetei *et al.*, 'X-linked inheritance of Fanconi anemia complementation group B', *Nat. Genet.*, vol. 36, no. 11, pp. 1219–1224, Nov. 2004, doi: 10.1038/ng1458.

[76] A. T. Wang *et al.*, 'A dominant mutation in human RAD51 reveals its function in DNA interstrand crosslink repair independent of homologous recombination', *Mol. Cell*, vol. 59, no. 3, pp. 478–490, Aug. 2015, doi: 10.1016/j.molcel.2015.07.009.

[77] J. Zhang, J. M. Dewar, M. Budzowska, A. Motnenko, M. A. Cohn, and J. C. Walter, 'DNA interstrand cross-link repair requires replication fork convergence', *Nat. Struct. Mol. Biol.*, vol. 22, no. 3, pp. 242–247, Mar. 2015, doi: 10.1038/nsmb.2956.

[78] N. Li, J. Wang, S. S. Wallace, J. Chen, J. Zhou, and A. D. D'Andrea, 'Cooperation of the NEIL3 and Fanconi anemia/BRCA pathways in interstrand crosslink repair', *Nucleic Acids Res.*, vol. 48, no. 6, pp. 3014–3028, Apr. 2020, doi: 10.1093/nar/gkaa038.

[79] E. Rajendra *et al.*, 'The Genetic and Biochemical Basis of FANCD2 Monoubiquitination', *Mol. Cell*, vol. 54, no. 5, pp. 858–869, Jun. 2014, doi: 10.1016/j.molcel.2014.05.001.

[80] S. Shakeel *et al.*, 'Structure of the Fanconi anaemia monoubiquitin ligase complex', *Nature*, vol. 575, 2019, doi: 10.1038/s41586-019-1703-4.

[81] A. Hira *et al.*, 'Mutations in the Gene Encoding the E2 Conjugating Enzyme UBE2T Cause Fanconi Anemia', *Am. J. Hum. Genet.*, vol. 96, no. 6, pp. 1001–1007, Jun. 2015, doi: 10.1016/j.ajhg.2015.04.022.

[82] T. R. Singh *et al.*, 'Impaired FANCD2 monoubiquitination and hypersensitivity to camptothecin uniquely characterize Fanconi anemia complementation group M', *Blood*, vol. 114, no. 1, pp. 174–180, Jul. 2009, doi: 10.1182/blood-2009-02-207811.

[83] T. Taniguchi, I. Garcia-Higuera, P. R. Andreassen, R. C. Gregory, M. Grompe, and A. D. D'Andrea, 'S-phase–specific interaction of the Fanconi anemia protein, FANCD2, with BRCA1 and RAD51', *Blood*, vol. 100, no. 7, pp. 2414–2420, Oct. 2002, doi: 10.1182/blood-2002-01-0278.

[84] S. Longerich, J. San Filippo, D. Liu, and P. Sung, 'FANCI Binds Branched DNA and Is Monoubiquitinated by UBE2T-FANCL', *J. Biol. Chem.*, vol. 284, no. 35, pp. 23182–23186, Aug. 2009, doi: 10.1074/jbc.C109.038075.

[85] W. Tan, S. van Twest, V. J. Murphy, and A. J. Deans, 'ATR-Mediated FANCI Phosphorylation Regulates Both Ubiquitination and Deubiquitination of FANCD2', *Front. Cell Dev. Biol.*, vol. 8, p. 2, Feb. 2020, doi: 10.3389/fcell.2020.00002.

[86] M. L. Rennie *et al.*, 'Differential functions of FANCI and FANCD2 ubiquitination stabilize ID2 complex on DNA', *EMBO Rep.*, vol. 21, no. 7, p. e50133, Jul. 2020, doi: 10.15252/embr.202050133.

[87] L. Li, W. Tan, and A. J. Deans, 'Structural insight into FANCI–FANCD2 monoubiquitination', *Essays Biochem.*, vol. 64, no. 5, pp. 807–817, Oct. 2020, doi: 10.1042/EBC20200001.

[88] Y. J. Achar and M. Foiani, 'Ubiquitilated Fanconi ID complex embraces DNA', *Cell Res.*, vol. 30, no. 7, pp. 554–555, Jul. 2020, doi: 10.1038/s41422-020-0345-2.

[89] M. Bogliolo *et al.*, 'Histone H2AX and Fanconi anemia FANCD2 function in the same pathway to maintain chromosome stability', *EMBO J.*, vol. 26, no. 5, pp. 1340–1351, Mar. 2007, doi: 10.1038/sj.emboj.7601574.

[90] R. A. Boisvert and N. G. Howlett, 'The Fanconi anemia ID2 complex: Dueling saxes at the crossroads', *Cell Cycle*, vol. 13, no. 19, pp. 2999–3015, Oct. 2014, doi: 10.4161/15384101.2014.956475.

[91] J. M. Kim *et al.*, 'Inactivation of Murine Usp1 Results in Genomic Instability and a Fanconi Anemia Phenotype', *Dev. Cell*, vol. 16, no. 2, pp. 314–320, Feb. 2009, doi: 10.1016/j.devcel.2009.01.001.

[92] K. Yang, G.-L. Moldovan, P. Vinciguerra, J. Murai, S. Takeda, and A. D. D'Andrea, 'Regulation of the Fanconi anemia pathway by a SUMO-like delivery network', *Genes Dev.*, vol. 25, no. 17, pp. 1847–1858, Sep. 2011, doi: 10.1101/gad.17020911.

[93] M. A. Cohn *et al.*, 'A UAF1-containing multisubunit protein complex regulates the Fanconi anemia pathway', *Mol. Cell*, vol. 28, no. 5, pp. 786–797, Dec. 2007, doi: 10.1016/j.molcel.2007.09.031.

[94] M. Räschle *et al.*, 'Mechanism of replication-coupled DNA interstrand cross-link repair', *Cell*, vol. 134, no. 6, pp. 969–980, Sep. 2008, doi: 10.1016/j.cell.2008.08.030.

[95] J. Sarkar *et al.*, 'SLX4 contributes to telomere preservation and regulated processing of telomeric joint molecule intermediates', *Nucleic Acids Res.*, vol. 43, no. 12, pp. 5912–5923, Jul. 2015, doi: 10.1093/nar/gkv522.

[96] M. R. G. Hodskinson *et al.*, 'Mouse SLX4 Is a Tumor Suppressor that Stimulates the Activity of the Nuclease XPF-ERCC1 in DNA Crosslink Repair', *Mol. Cell*, vol. 54, no. 3, pp. 472–484, May 2014, doi: 10.1016/j.molcel.2014.03.014.

[97] K. D. D *et al.*, 'XPF-ERCC1 acts in Unhooking DNA interstrand crosslinks in cooperation with FANCD2 and FANCP/SLX4', *Mol. Cell*, vol. 54, no. 3, Aug. 2014, doi: 10.1016/j.molcel.2014.03.015.

[98] A. R. Meetei *et al.*, 'A novel ubiquitin ligase is deficient in Fanconi anemia', *Nat. Genet.*, vol. 35, no. 2, pp. 165–170, Oct. 2003, doi: 10.1038/ng1241.

[99] M. Bogliolo *et al.*, 'Mutations in ERCC4, Encoding the DNA-Repair Endonuclease XPF, Cause Fanconi Anemia', *Am. J. Hum. Genet.*, vol. 92, no. 5, pp. 800–806, May 2013, doi: 10.1016/j.ajhg.2013.04.002.

[100] A. M. Sijbers *et al.*, 'Xeroderma pigmentosum group F caused by a defect in a structure-specific DNA repair endonuclease', *Cell*, vol. 86, no. 5, pp. 811–822, Sep. 1996, doi: 10.1016/s0092-8674(00)80155-5.

[101] A. Osorio *et al.*, 'Evaluation of rare variants in the new fanconi anemia gene ERCC4 (FANCQ) as familial breast/ovarian cancer susceptibility alleles', *Hum. Mutat.*, vol. 34, no. 12, pp. 1615–1618, Dec. 2013, doi: 10.1002/humu.22438.

[102] D. Das, M. Faridounnia, L. Kovacic, R. Kaptein, R. Boelens, and G. E. Folkers, 'Single-stranded DNA Binding by the Helix-Hairpin-Helix Domain of XPF Protein Contributes to the Substrate Specificity of the ERCC1-XPF Protein Complex', *J. Biol. Chem.*, vol. 292, no. 7, pp. 2842–2853, Feb. 2017, doi: 10.1074/jbc.M116.747857.

[103] M. Faridounnia, G. E. Folkers, and R. Boelens, 'Function and Interactions of ERCC1-XPF in DNA Damage Response', *Molecules*, vol. 23, no. 12, p. 3205, Dec. 2018, doi: 10.3390/molecules23123205.

[104] U. B. Abdullah *et al.*, 'RPA activates the XPF-ERCC1 endonuclease to initiate processing of DNA interstrand crosslinks', *EMBO J.*, vol. 36, no. 14, pp. 2047–2060, Jul. 2017, doi: 10.15252/embj.201796664.

[105] A. Ciccia, N. McDonald, and S. C. West, 'Structural and functional relationships of the XPF/MUS81 family of proteins', *Annu. Rev. Biochem.*, vol. 77, pp. 259–287, 2008, doi: 10.1146/annurev.biochem.77.070306.102408.

[106] I. M. Muñoz *et al.*, 'Coordination of structure-specific nucleases by human SLX4/BTBD12 is required for DNA repair', *Mol. Cell*, vol. 35, no. 1, pp. 116–127, Jul. 2009, doi: 10.1016/j.molcel.2009.06.020.

[107] J. Zhang and J. C. Walter, 'Mechanism and regulation of incisions during DNA interstrand cross-link repair', 2014, doi: 10.1016/j.dnarep.2014.03.018.

[108] D. Bluteau *et al.*, 'Biallelic inactivation of REV7 is associated with Fanconi anemia', *J. Clin. Invest.*, vol. 126, no. 9, pp. 3580–3584, Sep. 2016, doi: 10.1172/JCI88010.

[109] G. P. Crossan and K. J. Patel, 'The Fanconi anaemia pathway orchestrates incisions at sites of crosslinked DNA', *J. Pathol.*, vol. 226, no. 2, pp. 326–337, Jan. 2012, doi: 10.1002/path.3002.

[110] H. H. Y. Chang, N. R. Pannunzio, N. Adachi, and M. R. Lieber, 'Non-homologous DNA end joining and alternative pathways to double-strand break repair', *Nat. Rev. Mol. Cell Biol.*, vol. 18, no. 8, pp. 495–506, Aug. 2017, doi: 10.1038/nrm.2017.48.

[111] W. D. Wright, S. S. Shah, and W.-D. Heyer, 'Homologous recombination and the repair of DNA double-strand breaks', *J. Biol. Chem.*, vol. 293, no. 27, pp. 10524–10535, Jul. 2018, doi: 10.1074/jbc.TM118.000372.

[112] J. Her and S. F. Bunting, 'How cells ensure correct repair of DNA double-strand breaks', *J. Biol. Chem.*, vol. 293, no. 27, pp. 10502–10511, Jul. 2018, doi: 10.1074/jbc.TM118.000371.

[113] M. Tarsounas and P. Sung, 'The antitumorigenic roles of BRCA1–BARD1 in DNA repair and replication', *Nat. Rev. Mol. Cell Biol.*, vol. 21, no. 5, pp. 284–299, May 2020, doi: 10.1038/s41580-020-0218-z.

[114] Q. Zhong *et al.*, 'Association of BRCA1 with the hRad50-hMre11-p95 complex and the DNA damage response', *Science*, vol. 285, no. 5428, pp. 747–750, Jul. 1999, doi: 10.1126/science.285.5428.747.

[115] A. Shibata *et al.*, 'DNA double-strand break repair pathway choice is directed by distinct MRE11 nuclease activities', *Mol. Cell*, vol. 53, no. 1, pp. 7–18, Jan. 2014, doi: 10.1016/j.molcel.2013.11.003.

[116] M. Tarsounas, D. Davies, and S. C. West, 'BRCA2-dependent and independent formation of RAD51 nuclear foci', *Oncogene*, vol. 22, no. 8, pp. 1115–1123, Feb. 2003, doi: 10.1038/sj.onc.1206263.

[117] W. Zhao *et al.*, 'Promotion of BRCA2-Dependent Homologous Recombination by DSS1 via RPA Targeting and DNA Mimicry', *Mol. Cell*, vol. 59, no. 2, pp. 176–187, Jul. 2015, doi: 10.1016/j.molcel.2015.05.032.

[118] H. Wang, S. Li, J. Oaks, J. Ren, L. Li, and X. Wu, 'The concerted roles of FANCM and Rad52 in the protection of common fragile sites', doi: 10.1038/s41467-018-05066-y.

[119] Z. Feng *et al.*, 'Rad52 inactivation is synthetically lethal with BRCA2 deficiency', *Proc. Natl. Acad. Sci.*, vol. 108, no. 2, pp. 686–691, 2011, doi: 10.1073/pnas.1010959107.

[120] J.-Y. Park *et al.*, 'COMPLEMENTATION OF HYPERSENSITIVITY TO DNA INTERSTRAND CROSSLINKING AGENTS DEMONSTRATES THAT XRCC2 IS A FANCONI ANEMIA GENE', *J. Med. Genet.*, vol. 53, no. 10, pp. 672–680, Oct. 2016, doi: 10.1136/jmedgenet-2016-103847.

[121] S. Nath and G. Nagaraju, 'FANCJ helicase promotes DNA end resection by facilitating CtIP recruitment to DNA double-strand breaks', *PLoS Genet.*, vol. 16, no. 4, p. e1008701, Apr. 2020, doi: 10.1371/journal.pgen.1008701.

[122] K. Knies *et al.*, 'Biallelic mutations in the ubiquitin ligase RFWD3 cause Fanconi anemia', *J. Clin. Invest.*, vol. 127, no. 8, pp. 3013–3027, doi: 10.1172/JCI92069.

[123] M. Sebesta, P. Burkovics, L. Haracska, and L. Krejci, 'Reconstitution of DNA repair synthesis in vitro and the role of polymerase and helicase activities', *DNA Repair*, vol. 10, no. 6, pp. 567–576, Jun. 2011, doi: 10.1016/j.dnarep.2011.03.003.

[124] S. Zhang, H. H. Chao, X. Wang, Z. Zhang, E. Y. C. Lee, and M. Y. W. T. Lee, 'Loss of the p12 subunit of DNA polymerase delta leads to a defect in HR and sensitization to PARP inhibitors', *DNA Repair*, vol. 73, pp. 64–70, Jan. 2019, doi: 10.1016/j.dnarep.2018.11.003.

[125] M. E. Moynahan and M. Jasin, 'Mitotic homologous recombination maintains genomic stability and suppresses tumorigenesis', *Nat. Rev. Mol. Cell Biol.*, vol. 11, no. 3, pp. 196–207, Mar. 2010, doi: 10.1038/nrm2851.

[126] G. Zapotoczny and J. Sekelsky, 'Human Cell Assays for Synthesis-Dependent Strand Annealing and Crossing over During Double-Strand Break Repair', *G3 GenesGenomesGenetics*, vol. 7, no. 4, pp. 1191–1199, Apr. 2017, doi: 10.1534/g3.116.037390.

[127] H. D. M. Wyatt and S. C. West, 'Holliday Junction Resolvases', *Cold Spring Harb. Perspect. Biol.*, vol. 6, no. 9, p. a023192, Sep. 2014, doi: 10.1101/cshperspect.a023192.

[128] H. H. Y. Chang *et al.*, 'Different DNA End Configurations Dictate Which NHEJ Components Are Most Important for Joining Efficiency', *J. Biol. Chem.*, vol. 291, no. 47, pp. 24377–24389, Nov. 2016, doi: 10.1074/jbc.M116.752329.

[129] A. Sfeir and L. S. Symington, 'Microhomology-Mediated End Joining: A Back-up Survival Mechanism or Dedicated Pathway?', *Trends Biochem. Sci.*, vol. 40, no. 11, pp. 701–714, Nov. 2015, doi: 10.1016/j.tibs.2015.08.006.

[130] I. Robert, F. Dantzer, and B. Reina-San-Martin, 'Parp1 facilitates alternative NHEJ, whereas Parp2 suppresses IgH/c-myc translocations during immunoglobulin class switch recombination', *J. Exp. Med.*, vol. 206, no. 5, pp. 1047–1056, May 2009, doi: 10.1084/jem.20082468.

[131] D. W. Wyatt *et al.*, 'Essential Roles for Polymerase θ-Mediated End Joining in the Repair of Chromosome Breaks', *Mol. Cell*, vol. 63, no. 4, pp. 662–673, Aug. 2016, doi: 10.1016/j.molcel.2016.06.020.

[132] T. Kent, P. A. Mateos-Gomez, A. Sfeir, and R. T. Pomerantz, 'Polymerase θ is a robust terminal transferase that oscillates between three different mechanisms during end-joining', *eLife*, vol. 5, p. e13740, Jun. 2016, doi: 10.7554/eLife.13740.

[133] Z. Zhu, W.-H. Chung, E. Y. Shim, S. E. Lee, and G. Ira, 'Sgs1 helicase and two nucleases Dna2 and Exo1 resect DNA double strand break ends', *Cell*, vol. 134, no. 6, pp. 981–994, Sep. 2008, doi: 10.1016/j.cell.2008.08.037.

[134] R. Bhargava, D. O. Onyango, and J. M. Stark, 'Regulation of Single-Strand Annealing and its Role in Genome Maintenance', *Trends Genet.*, vol. 32, no. 9, pp. 566–575, 2016, doi: 10.1016/j.tig.2016.06.007.

[135] L. H. Hartwell, P. Szankasi, C. J. Roberts, A. W. Murray, and S. H. Friend, 'Integrating genetic approaches into the discovery of anticancer drugs', *Science*, vol. 278, no. 5340, pp. 1064–1068, Nov. 1997, doi: 10.1126/science.278.5340.1064.

[136] N. J. O'Neil, M. L. Bailey, and P. Hieter, 'Synthetic lethality and cancer', *Nat. Rev. Genet.*, vol. 18, no. 10, pp. 613–623, Oct. 2017, doi: 10.1038/nrg.2017.47.

[137] N. Saleh-Gohari, H. E. Bryant, N. Schultz, K. M. Parker, T. N. Cassel, and T. Helleday, 'Spontaneous homologous recombination is induced by collapsed replication forks that are caused by endogenous DNA single-strand breaks', *Mol. Cell. Biol.*, vol. 25, no. 16, pp. 7158–7169, Aug. 2005, doi: 10.1128/MCB.25.16.7158-7169.2005.

[138] T. Lindahl, M. S. Satoh, G. G. Poirier, and A. Klungland, 'Post-translational modification of poly(ADP-ribose) polymerase induced by DNA strand breaks', *Trends Biochem. Sci.*, vol. 20, no. 10, pp. 405–411, Oct. 1995, doi: 10.1016/s0968-0004(00)89089-1.

[139] C. Dulaney, S. Marcrom, J. Stanley, and E. S. Yang, 'Poly(ADP-ribose) polymerase activity and inhibition in cancer', *Semin. Cell Dev. Biol.*, vol. 63, pp. 144–153, Mar. 2017, doi: 10.1016/j.semcdb.2017.01.007.

[140] W. Topatana *et al.*, 'Advances in synthetic lethality for cancer therapy: cellular mechanism and clinical translation', *J. Hematol. Oncol.J Hematol Oncol*, vol. 13, p. 118, Sep. 2020, doi: 10.1186/s13045-020-00956-5.

[141] H. E. Bryant *et al.*, 'Specific killing of BRCA2-deficient tumours with inhibitors of poly(ADP-ribose) polymerase', *Nature*, vol. 434, no. 7035, pp. 913–917, Apr. 2005, doi: 10.1038/nature03443.

[142] M. S. Satoh and T. Lindahl, 'Role of poly(ADP-ribose) formation in DNA repair', *Nature*, vol. 356, no. 6367, pp. 356–358, Mar. 1992, doi: 10.1038/356356a0.

[143] B. Norquist *et al.*, 'Secondary somatic mutations restoring BRCA1/2 predict chemotherapy resistance in hereditary ovarian carcinomas', *J. Clin. Oncol. Off. J. Am. Soc. Clin. Oncol.*, vol. 29, no. 22, pp. 3008–3015, Aug. 2011, doi: 10.1200/JCO.2010.34.2980.

[144] P. Murthy and F. Muggia, 'PARP inhibitors: clinical development, emerging differences, and the current therapeutic issues', *Cancer Drug Resist.*, vol. 2, no. 3, pp. 665–679, Sep. 2019, doi: 10.20517/cdr.2019.002.

[145] S. F. Bunting *et al.*, '53BP1 inhibits homologous recombination in Brca1-deficient cells by blocking resection of DNA breaks', *Cell*, vol. 141, no. 2, pp. 243–254, Apr. 2010, doi: 10.1016/j.cell.2010.03.012.

[146] R. M. Hurley *et al.*, '53BP1 as a Potential Predictor of Response in PARP Inhibitor-Treated Homologous Recombination-Deficient Ovarian Cancer', *Gynecol. Oncol.*, vol. 153, no. 1, pp. 127–134, Apr. 2019, doi: 10.1016/j.ygyno.2019.01.015.

[147] A. Ray Chaudhuri *et al.*, 'Replication fork stability confers chemoresistance in BRCA-deficient cells', *Nature*, vol. 535, no. 7612, pp. 382–387, Jul. 2016, doi: 10.1038/nature18325.

[148] M. S. van der Heijden, C. J. Yeo, R. H. Hruban, and S. E. Kern, 'Fanconi Anemia Gene Mutations in Young-onset Pancreatic Cancer', *Cancer Res.*, vol. 63, no. 10, pp. 2585–2588, May 2003.

[149] C. D. Rogers *et al.*, 'The Genetics of FANCC and FANCG in Familial Pancreatic Cancer', *Cancer Biol. Ther.*, vol. 3, no. 2, pp. 167–169, Feb. 2004, doi: 10.4161/cbt.3.2.609.

[150] C. J. Hess *et al.*, 'Hypermethylation of the FANCC and FANCL promoter regions in sporadic acute leukaemia', *Anal. Cell. Pathol.*, vol. 30, no. 4, pp. 299–306, Jan. 2008, doi: 10.3233/CLO-2008-0426.

[151] M. F. Sharp, R. Bythell-Douglas, A. J. Deans, and W. Crismani, 'The Fanconi anemia ubiquitin E3 ligase complex as an anti-cancer target', *Mol. Cell*, vol. 81, no. 11, pp. 2278–2289, Jun. 2021, doi: 10.1016/j.molcel.2021.04.023.

[152] R. D. Kennedy *et al.*, 'Fanconi anemia pathway–deficient tumor cells are hypersensitive to inhibition of ataxia telangiectasia mutated', *J. Clin. Invest.*, vol. 117, no. 5, pp. 1440–1449, May 2007, doi: 10.1172/JCI31245.

[153] K. Yamamoto *et al.*, 'Upregulated ATM gene expression and activated DNA crosslink-induced damage response checkpoint in Fanconi anemia: implications for carcinogenesis', *Mol. Med. Camb. Mass*, vol. 14, no. 3–4, pp. 167–174, Apr. 2008, doi: 10.2119/2007-00122.Yamamoto.

[154] C. A. Lovejoy and D. Cortez, 'Common mechanisms of PIKK regulation', *DNA Repair*, vol. 8, no. 9, pp. 1004–1008, Sep. 2009, doi: 10.1016/j.dnarep.2009.04.006.

[155] H. Lempiäinen and T. D. Halazonetis, 'Emerging common themes in regulation of PIKKs and PI3Ks', *EMBO J.*, vol. 28, no. 20, pp. 3067–3073, Oct. 2009, doi: 10.1038/emboj.2009.281.

[156] Y. Shiloh and Y. Ziv, 'The ATM protein kinase: regulating the cellular response to genotoxic stress, and more', *Nat. Rev. Mol. Cell Biol.*, vol. 14, no. 4, pp. 197–210, Apr. 2013, doi: 10.1038/nrm3546.

[157] H. Kim and A. D. D'Andrea, 'Regulation of DNA cross-link repair by the Fanconi anemia/BRCA pathway', *Genes Dev.*, vol. 26, no. 13, pp. 1393–1408, Jan. 2012, doi: 10.1101/gad.195248.112.

[158] K.-K. Chan *et al.*, 'SIK2 kinase synthetic lethality is driven by spindle assembly defects in FANCA-deficient cells', *Mol. Oncol.*, 2021, doi: 10.1002/1878-0261.13027.

[159] C. C. Chen, R. D. Kennedy, S. Sidi, A. T. Look, and A. D'Andrea, 'CHK1 inhibition as a strategy for targeting fanconi anemia (FA) DNA repair pathway deficient tumors', *Mol. Cancer*, vol. 8, no. 1, p. 24, Apr. 2009, doi: 10.1186/1476-4598-8-24.

[160] M. Aarts *et al.*, 'Functional genetic screen identifies increased sensitivity to WEE1 inhibition in cells with defects in Fanconi Anaemia and HR pathways', *Mol. Cancer Ther.*, vol. 14, no. 4, pp. 865–876, Apr. 2015, doi: 10.1158/1535-7163.MCT-14-0845.

[161] F. Langevin, G. P. Crossan, I. V. Rosado, M. J. Arends, and K. J. Patel, 'Fancd2 counteracts the toxic effects of naturally produced aldehydes in mice', *Nature*, vol. 475, no. 7354, pp. 53–58, Jul. 2011, doi: 10.1038/nature10192.

[162] A. Hira *et al.*, 'Variant ALDH2 is associated with accelerated progression of bone marrow failure in Japanese Fanconi anemia patients', *Blood*, vol. 122, no. 18, pp. 3206–3209, Oct. 2013, doi: 10.1182/blood-2013-06-507962.

[163] M. Yabe *et al.*, 'Associations of complementation group, ALDH2 genotype, and clonal abnormalities with hematological outcome in Japanese patients with Fanconi anemia', *Ann. Hematol.*, vol. 98, no. 2, pp. 271–280, Feb. 2019, doi: 10.1007/s00277-018-3517-0.

[164] Z. Yang *et al.*, 'Transcriptional Silencing of ALDH2 Confers a Dependency on Fanconi Anemia Proteins in Acute Myeloid Leukemia', *Cancer Discov.*, vol. 11, no. 9, pp. 2300–2315, Sep. 2021, doi: 10.1158/2159-8290.CD-20-1542.

[165] R. Wang *et al.*, 'DNA polymerase $ıota$ compensates for Fanconi anemia pathway deficiency by countering DNA replication stress', *Proc. Natl. Acad. Sci.*, vol. 117, no. 52, pp. 33436–33445, Dec. 2020, doi: 10.1073/PNAS.2008821117.

[166] R. Ceccaldi *et al.*, 'Homologous-recombination-deficient tumours are dependent on Pol$þeta$ -mediated repair', *Nature*, vol. 518, no. 7538, pp. 258–262, Feb. 2015, doi: 10.1038/NATURE14184.

[167] K. E. Mengwasser *et al.*, 'Genetic Screens Reveal FEN1 and APEX2 as BRCA2 Synthetic Lethal Targets', *Mol. Cell*, vol. 73, no. 5, pp. 885-899.e6, Mar. 2019, doi: 10.1016/j.molcel.2018.12.008.

[168] R. Hromas *et al.*, 'The endonuclease EEPD1 mediates synthetic lethality in RAD52-depleted BRCA1 mutant breast cancer cells', *Breast Cancer Res. 2017 191*, vol. 19, no. 1, pp. 1–14, Nov. 2017, doi: 10.1186/S13058-017-0912-8.

[169] P. Pace, G. Mosedale, M. R. Hodskinson, I. V. Rosado, M. Sivasubramaniam, and K. J. Patel, 'Ku70 corrupts DNA repair in the absence of the Fanconi anemia pathway', *Science*, vol. 329, no. 5988, pp. 219–223, Jul. 2010, doi: 10.1126/science.1192277.

[170] A. Adamo *et al.*, 'Article Preventing Nonhomologous End Joining Suppresses DNA Repair Defects of Fanconi Anemia', *Mol. Cell*, vol. 39, no. 1, pp. 25–35, 2010, doi: 10.1016/j.molcel.2010.06.026.

[171] R. Barrangou *et al.*, 'CRISPR provides acquired resistance against viruses in prokaryotes', *Science*, vol. 315, no. 5819, pp. 1709–1712, Mar. 2007, doi: 10.1126/science.1138140.

[172] E. Charpentier and L. A. Marraffini, 'Harnessing CRISPR-Cas9 immunity for genetic engineering', *Curr. Opin. Microbiol.*, vol. 19, pp. 114–119, Jun. 2014, doi: 10.1016/j.mib.2014.07.001.

[173] K. S. Makarova *et al.*, 'Evolution and classification of the CRISPR-Cas systems', *Nat. Rev. Microbiol.*, vol. 9, no. 6, pp. 467–477, Jun. 2011, doi: 10.1038/nrmicro2577.

[174] M. Hryhorowicz, D. Lipiński, J. Zeyland, and R. Słomski, 'CRISPR/Cas9 Immune System as a Tool for Genome Engineering', *Arch. Immunol. Ther. Exp. (Warsz.)*, vol. 65, no. 3, pp. 233–240, 2017, doi: 10.1007/s00005-016-0427-5.

[175] S. A. Shah, S. Erdmann, F. J. M. Mojica, and R. A. Garrett, 'Protospacer recognition motifs: mixed identities and functional diversity', *RNA Biol.*, vol. 10, no. 5, pp. 891–899, May 2013, doi: 10.4161/rna.23764.

[176] F. J. M. Mojica, C. Díez-Villaseñor, J. García-Martínez, and C. Almendros, 'Short motif sequences determine the targets of the prokaryotic CRISPR defence system', *Microbiol. Read. Engl.*, vol. 155, no. Pt 3, pp. 733–740, Mar. 2009, doi: 10.1099/mic.0.023960-0.

[177] S. W. Cho, S. Kim, J. M. Kim, and J.-S. Kim, 'Targeted genome engineering in human cells with the Cas9 RNA-guided endonuclease', *Nat. Biotechnol.*, vol. 31, no. 3, pp. 230–232, Mar. 2013, doi: 10.1038/nbt.2507.

[178] M. Jinek, K. Chylinski, I. Fonfara, M. Hauer, J. A. Doudna, and E. Charpentier, 'A programmable dual-RNA-guided DNA endonuclease in adaptive bacterial immunity', *Science*, vol. 337, no. 6096, pp. 816–821, Aug. 2012, doi: 10.1126/science.1225829.

[179] J.-H. Zhang, P. Adikaram, M. Pandey, A. Genis, and W. F. Simonds, 'Optimization of genome editing through CRISPR-Cas9 engineering', *Bioengineered*, vol. 7, no. 3, pp. 166–174, Apr. 2016, doi: 10.1080/21655979.2016.1189039.

[180] D. C. Luther, Y. W. Lee, H. Nagaraj, F. Scaletti, and V. M. Rotello, 'Delivery approaches for CRISPR/Cas9 therapeutics in vivo: advances and challenges', *Expert Opin. Drug Deliv.*, vol. 15, no. 9, pp. 905–913, Sep. 2018, doi: 10.1080/17425247.2018.1517746.

[181] J. C. Oliveros *et al.*, 'Breaking-Cas—interactive design of guide RNAs for CRISPR-Cas experiments for ENSEMBL genomes', *Nucleic Acids Res.*, vol. 44, no. W1, pp. W267–W271, Jul. 2016, doi: 10.1093/nar/gkw407.

[182] D. Hamam, M. Abdouh, Z.-H. Gao, V. Arena, M. Arena, and G. O. Arena, 'Transfer of malignant trait to BRCA1 deficient human fibroblasts following exposure to serum of cancer patients', 2016, doi: 10.1186/s13046-016-0360-9.

[183] H. J. Van De Vrugt *et al.*, 'Embryonic Lethality after Combined Inactivation of Fancd2 and Mlh1 in Mice', *Pathobiol. Genet.*, 2009, doi: 10.1158/0008-5472.CAN-09-2452.

[184] M. Sabatella, A. Pines, J. Slyskova, W. Vermeulen, and H. Lans, 'ERCC1-XPF targeting to psoralen-DNA crosslinks depends on XPA and FANCD2', *Cell. Mol. Life Sci. CMLS*, vol. 77, no. 10, pp. 2005–2016, May 2020, doi: 10.1007/s00018-019-03264-5.

[185] C. S. Annealing *et al.*, 'Short Article FANCA Promotes DNA Double-Strand Break Repair FANCA Promotes DNA Double-Strand Break Repair by Catalyzing Single-Strand Annealing and Strand Exchange', *Mol. Cell*, vol. 71, no. 4, pp. 621-628.e4, 2018, doi: 10.1016/j.molcel.2018.06.030.

[186] J. C. Exell *et al.*, 'Cellularly active N-hydroxyurea Fen1 inhibitors block substrate entry to the active site', *Nat. Chem. Biol.*, vol. 12, 2016, doi: 10.1038/nCHeMBIO.2148.

[187] L. Qian, F. Yuan, P. Rodriguez-Tello, S. Padgaonkar, and Y. Zhang, 'Human Fanconi Anemia Complementation Group A Protein Stimulates the 5' Flap Endonuclease Activity of FEN1', *PLoS ONE*, vol. 8, no. 12, p. e82666, Dec. 2013, doi: 10.1371/journal.pone.0082666.

[188] J.-S. Diana *et al.*, 'A new step in understanding stem cell mobilization in patients with Fanconi anemia: A bridge to gene therapy', *Transfusion (Paris)*, vol. 62, no. 1, pp. 165–172, Jan. 2022, doi: 10.1111/trf.16721.

[189] P. Río *et al.*, 'Successful engraftment of gene-corrected hematopoietic stem cells in non-conditioned patients with Fanconi anemia', *Nat. Med.*, vol. 25, no. 9, pp. 1396–1401, Sep. 2019, doi: 10.1038/s41591-019-0550-z.

7 Annex

Annex 1: CCA of Patient ATM KO fibroblasts with siRNA against FANCA or FANCD2

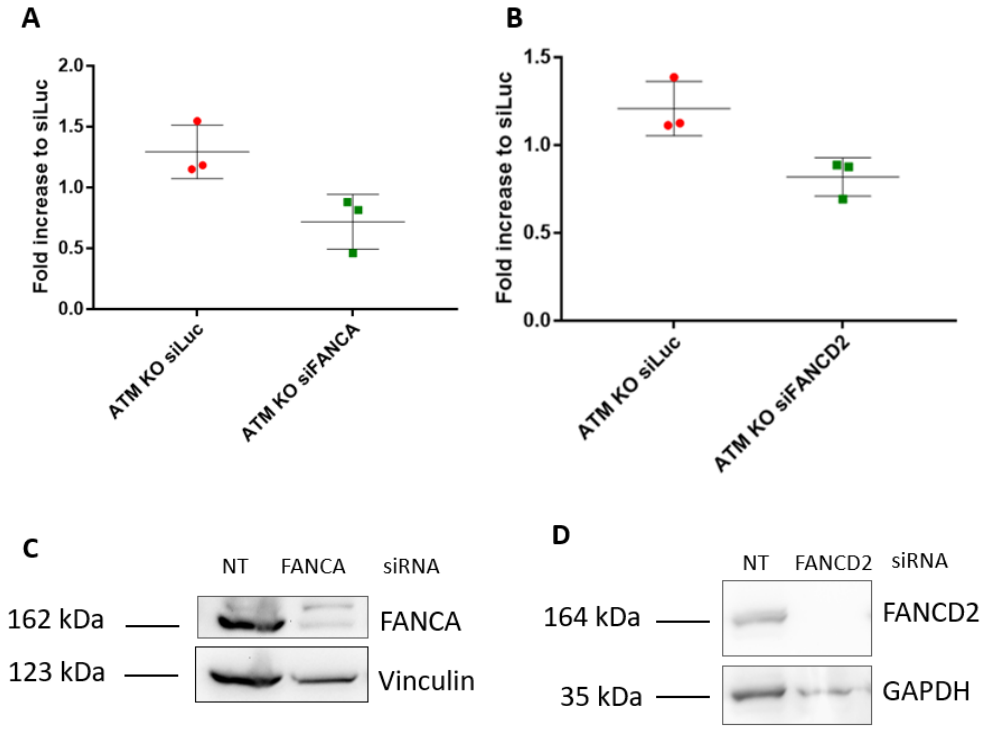

Annex 1: Proof of principle of the CCA as reversed experiment in ATM KO cells for synthetic lethality with FANCA and FANCD2, A: ***CCA of ATM KO tRFP siLuc vs ATM KO GFP siFANCA****: ATM KO tRFP siLuc vs ATM KO GFP siFANCA fold increase to ATM KO tRFP siLuc vs ATM KO GFP siLuc, B:* ***CCA of ATM KO tRFP siLuc vs ATM KO GFP siFANCD2:*** *: ATM KO tRFP siLuc vs ATM KO GFP siFANCD2 fold increase to ATM KO tRFP siLuc vs ATM KO GFP siLuc, C and D:* ***WB control of FANCA or FANCD2 expression after siRNA silencing:*** *7.5 PAA gel antibodies against either FANCA or FAND2 and loading control Vinculin or GAPDH*

Annex 2: CCA of HEK BRCA2 KO cells with Olaparib treatment or shFEN1 treatment

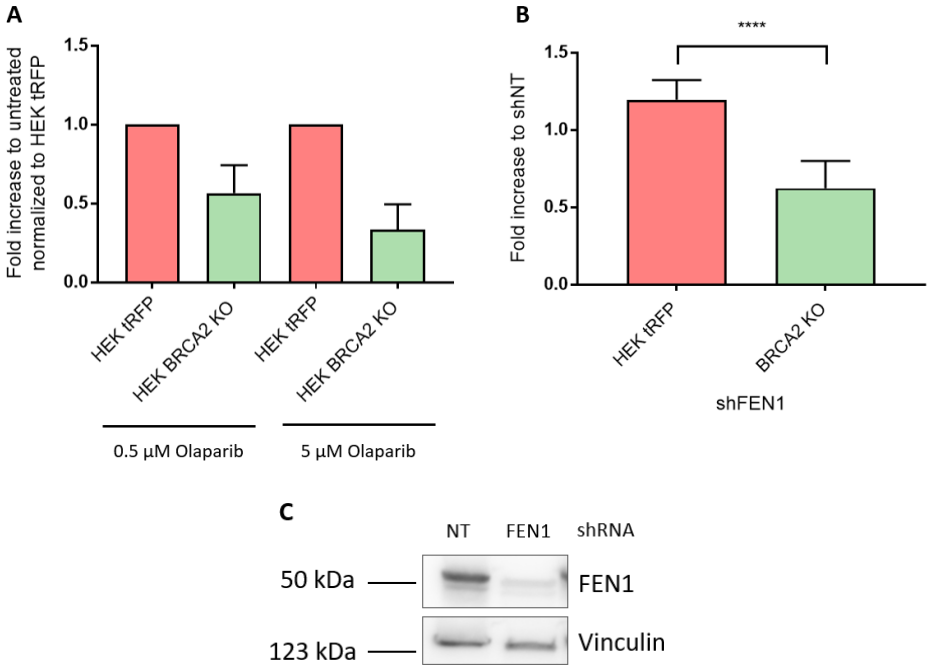

Annex 2: Proof of principle of the CCA in HEKC BRCA2 KO cells with shFEN1 and Olaparib treatment, A: ***CCA of HEK tRFP vs HEK BRCA2 KO GFP with Olaparib treatment:*** *CCA measured at day five, different concentrations of Olaparib and ratio of HKE tRFP vs HEK BRCA2 KO GFP of three independent experiments plotted as fold increase to untreated control, normalized to HEK tRFP, error bars show SD, B****: CCA of HEK tRFP vs HEK BRCA2 KO GFP with shFEN1 treatment:*** *measurement at day nine, plotted six independent experiments as fold increase to shNT, error bars show SD and the significance is calculated with the unpaired student t test, C:* ***WB of FEN1 expression in for CCA:*** *10 % PAA gel with antibody against FEN1 and loading control Vinculin, HEK tRFP vs HEK BRCA2 KO GFP treated with shRNA; Left Pocket: HEK tRFP vs HEK BRCA2 KO GFP treated with shN;, Right Pocket: HEK tRFP vs HEK BRCA2 KO GFP treated with shFEN1*

Annex 3: CCA of HeLa XPF KO tRFP vs HeLa XPF KO GFP treated with shRNA for FANCA

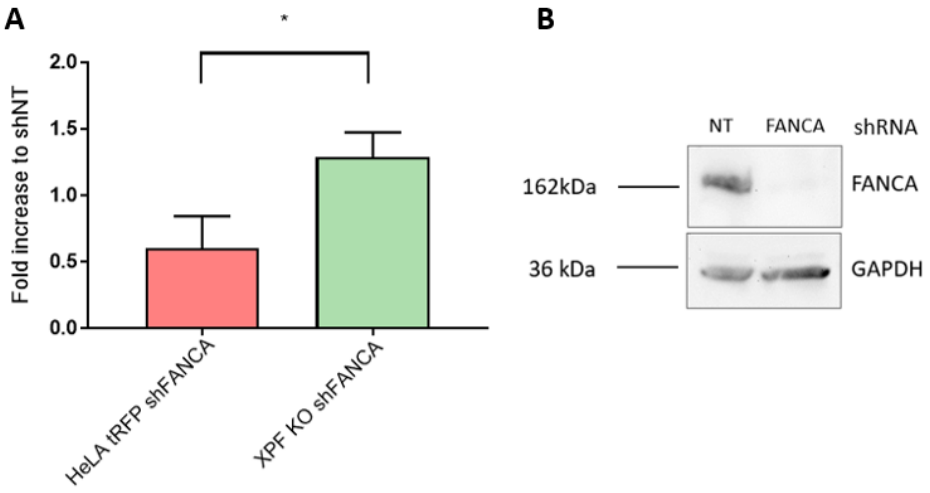

Annex 3: Confirmation of synthetic viability in HeLa cell line between XPF KO and FANCA, A: ***CCA of HeLa tRFP vs HeLa XPF KO GPF treated with shFANCA:*** *plotted is the fold increase of four independent experiments error bars show SD and significance was tested with unpaired Mann-Whitney, B:* ***WB control of FANCA expression after shRNA treatment:*** *7.5 % PAA gel with antibody against FANCA and loading control GAPDH*